

**ISTANBUL TECHNICAL UNIVERSITY ★ INSTITUTE OF SCIENCE AND TECHNOLOGY**

**EFFECT OF PLASTOMER ADDITION ON POLYPROPYLENE / GLASS  
FIBER COMPOUND ON PHYSICAL AND MECHANICAL PROPERTIES**

**M.Sc. Thesis by  
Deniz ERDİNÇ**

**Department : Polymer Science and Technology**

**Programme : Polymer Science and Technology**

**JUNE 2010**



**EFFECT OF PLASTOMER ADDITION ON POLYPROPYLENE / GLASS  
FIBER COMPOUND ON PHYSICAL AND MECHANICAL PROPERTIES**

**M.Sc. Thesis by  
Deniz ERDİNÇ  
515081009**

**Date of submission : 07 May 2010  
Date of defence examination: 07 June 2010**

**Supervisor (Chairman) : Prof. Dr. I.Ersin SERHATLI (ITU)  
Members of the Examining Committee : Prof. Dr. Hulusi ÖZKUL (ITU)  
Prof. Dr. Atilla GÜNGÖR (MU)**

**JUNE 2010**





**İSTANBUL TEKNİK ÜNİVERSİTESİ ★ FEN BİLİMLERİ ENSTİTÜSÜ**

**PP / CAM ELYAF BİLEŞİMİNE PLASTOMER İLAVESİNİN MEKANİK VE  
FİZİKSEL ÖZELLİKLERE ETKİSİ**

**YÜKSEK LİSANS TEZİ  
Deniz ERDİNÇ  
515081009**

**Tezin Enstitüye Verildiği Tarih : 07 Mayıs 2010**

**Tezin Savunulduğu Tarih : 07 Haziran 2010**

**Tez Danışmanı : Prof. Dr. I.Ersin SERHATLI (İTÜ)  
Diğer Jüri Üyeleri : Prof. Dr. Hulusi ÖZKUL (İTÜ)  
Prof. Dr. Atilla GÜNGÖR (MÜ)**

**HAZİRAN 2010**



## **FOREWORD**

I would like to thank my supervisor, Prof. Dr. I. Ersin SERHATLI, for the technical guidance, encouragement and advice he has provided throughout my time as his student. I have been extremely lucky to have a supervisor who cared so much about my work, and who responded to my questions and queries so promptly.

I would like to express my thanks to Arçelik A.S. for invaluable support in the name of Cemil INAN and Fatih ÖZKADI.

I sincerely thank to Dr. Osman G. ERSOY, for his invaluable help and support and I extend my thanks to all members of the Material Technologies Department in the name of Sibel ODABAŞ.

My very special thanks are to Mehmet Ali ORAL, Deniz TAŞKIN, Fatih KOTAN, Aylin MET, Eren DALGAKIRAN, Hamza SANCAKLI, Turgay GÖNÜL, Seda Cekli for their contribution in this thesis in almost every possible way.

I would like to thank my family Hasibe ERDİNÇ, Doğa ERDİNÇ and friends for their support throughout the duration of this project. I would especially like to thank Levent VURAL.

JUNE 2010

DENİZ ERDİNÇ  
Metallurgical & Material Engineer



## TABLE OF CONTENTS

	<u>Page</u>
<b>ABBREVIATIONS.....</b>	<b>ix</b>
<b>LIST OF TABLES.....</b>	<b>xii</b>
<b>LIST OF FIGURES.....</b>	<b>xiv</b>
<b>SUMMARY.....</b>	<b>xvii</b>
<b>ÖZET.....</b>	<b>xix</b>
<b>1. INTRODUCTION.....</b>	<b>1</b>
<b>2. OBJECTIVE OF STUDY.....</b>	<b>3</b>
<b>3. POLYMERIC COMPOSITES.....</b>	<b>5</b>
3.1 Fiber Reinforcements .....	6
3.1.1 Effect of fiber orientation and concentration .....	7
3.1.2 Effect of fiber length.....	11
3.2 The Matrix Phase of Composite.....	12
<b>4. CONCEPT OF E-PLASTOMER.....</b>	<b>15</b>
4.1 Metallocene Catalyst .....	15
4.2 Toughening Mechanism of PP.....	16
<b>5. INTERACTIVE RELATION BETWEEN REINFORCEMENT AND MATRIX IN POLYMER COMPOSITES.....</b>	<b>19</b>
5.1 Adhesion Between The Reinforcing Material and Polymer .....	19
5.1.1 Chemical adhesion.....	20
5.1.2 Diffusive adhesion.....	20
5.1.3 Thermodynamic absorption (wetting) .....	21
5.1.4 Mechanical adhesion .....	22
<b>6. FRACTURE AND TOUGHNESS OF COMPOSITES.....</b>	<b>23</b>
6.1 Introduction.....	23
6.2 Principles of Fracture Mechanics .....	24
6.2.1 Stress concentration.....	24
6.2.2 Fracture toughness.....	25
6.3 Crack Extension in Composites .....	26
6.3.1 Matrix effects .....	26
6.3.2 Fibre effects.....	26
<b>7. EXPERIMENTAL WORK .....</b>	<b>27</b>
7.1 Materials .....	27
7.2 Compounding Recipes.....	28
7.3 Compounding with Twin Screw Extruder and Test Specimen Preparation by Injection Molding .....	29
7.3.1 Twin screw extruder.....	29
7.3.2 Extruder screw desing and temperature profile .....	32
7.3.3 Compounding procedure.....	33
7.3.4 Injection molding process.....	33
7.4 Measurement of Density.....	37
7.5 Ash Content.....	37

7.6 Melt Flow Rate .....	38
7.7 Morphology Investigation .....	39
7.8 Measurement of Tensile Properties.....	39
7.9 Determination of Flexural Properties.....	41
7.10 Determination of Weld Line Factor.....	43
7.11 Determination of Izod Impact Strength.....	43
7.12 Determination of Vicat Softening Temperature and Heat Deflection temperature .....	44
<b>8. RESULTS AND DISCUSSION.....</b>	<b>45</b>
8.1 The Effect of Glass Fiber on The Properties Polypropylene.....	45
8.1.1 Measurement of density .....	45
8.1.2 Determination of melt flow index.....	45
8.1.3 Morphology investigation .....	46
8.1.4 Tensile properties.....	47
8.1.5 Flexural properties .....	48
8.1.6 Impact properties .....	48
8.1.7 Heat deflection temperature - Vicat softening temperature.....	49
8.2 The Effect of Compatibilizer Mah-g-PP on GFR-PP composite.....	50
8.2.1 Measurement of density .....	50
8.2.2 Determination of ash content.....	52
8.2.3 Determination of melt flow index.....	53
8.2.4 Morphology investigation .....	54
8.2.5 Tensile properties.....	55
8.2.6 Flexural properties .....	58
8.2.7 Impact properties .....	59
8.2.8 Heat deflection temperature - Vicat softening temperature.....	61
8.3 The Effect of Plastomer Additon on 2% Mah-g-PP Compatiblized GFR-PP composite.....	64
8.3.1 Measurement of density .....	65
8.3.2 Determination of melt flow index.....	66
8.3.3 Determination of ash content.....	67
8.3.4 Morphology investigation .....	68
8.3.5 Tensile properties.....	74
8.3.6 Flexural properties .....	77
8.3.7 Impact properties .....	78
8.3.8 Heat distortion temperature - Vicat softening temperature .....	79
<b>9. CONCLUSION.....</b>	<b>83</b>
<b>REFERENCES.....</b>	<b>85</b>
<b>CURRICULUM VITA .....</b>	<b>87</b>

## ABBREVIATIONS

<b>AVR</b>	: Average
<b>EPDM</b>	: Ethylene propylene diene monomer
<b>EPR</b>	: Ethylene propylene rubber
<b>FRP</b>	: Fiber reinforced polymer
<b>F1</b>	: Feeder 1
<b>F2</b>	: Feeder 2
<b>GF</b>	: Glass fiber
<b>GFR</b>	: Glass fiber reinforced
<b>HDT</b>	: Heat deflection temperature
<b>IPP</b>	: Isotactic polypropylene
<b>LLPE</b>	: Linear low-density polyethylene
<b>MA</b>	: Maleic anhydride
<b>Mah-g-PP</b>	: Maleic anhydride grafted polypropylene
<b>MAX</b>	: Maximum
<b>MFI</b>	: Melt flow index
<b>MIN</b>	: Minumum
<b>PA</b>	: Polyamide
<b>PP</b>	: Polypropylene
<b>PS</b>	: Polystyrene
<b>SD</b>	: Standart deviation
<b>SFRP</b>	: Short-fiber reinforced polymer
<b>STD</b>	: Standart deviation







## LIST OF TABLES

	<u>Page</u>
<b>Table 3.1:</b> Reinforcement efficiency of fiber-reinforced composites for several fiber orientations and at various directions of stress application.....	10
<b>Table 3.2:</b> Commonly used reinforcing fibres .....	11
<b>Table 6.1:</b> Room temperature yield strength and plane strain fracture toughness data for some polymers .....	25
<b>Table 7.1:</b> Physical properties of Borealis HE 125 MO .....	27
<b>Table 7.2:</b> Properties of Owens Corning DS 2100 – 13 P .....	27
<b>Table 7.3:</b> Physical properties of the Polybond 3200.....	27
<b>Table 7.4:</b> General properties of Dex Plastomer Exact 0210.....	28
<b>Table 7.5:</b> Compounding recipe according to % Mah-g-PP content.....	28
<b>Table 7.6:</b> Compounding recipe according to % plastomer content .....	29
<b>Table 7.7:</b> Properties of PRISM TSE24 IIC extruder.....	30
<b>Table 7.8:</b> The Arburg 320C injection machine’s specifications.....	35
<b>Table 8.1:</b> Result of density measurement of neat PP and 30% GFR-PP.....	45
<b>Table 8.2:</b> Melt flow index results of neat PP and 30% GFR-PP .....	46
<b>Table 8.3:</b> Tensile properties of neat PP and 30% GFR-PP (Normal Test Specimen).....	47
<b>Table 8.4:</b> Tensile properties of neat PP and 30% GFR-PP (Weld line Test Specimen) .....	47
<b>Table 8.5:</b> Flexural properties of neat PP and 30% GFR-PP.....	48
<b>Table 8.6:</b> Izod notched impact properties of neat PP and 30% GFR-PP .....	49
<b>Table 8.7:</b> Vicat (A-B) softening temperatures of neat PP and 30% GFR-PP.....	50
<b>Table 8.8:</b> Heat deflection temperatures (A-B) of neat PP and 30% GFR-PP.....	50
<b>Table 8.9:</b> Density of 30% GFR-PP according to % Mah-g-PP content .....	51
<b>Table 8.10:</b> Ash content measurements of composites in terms of % Mah-g-PP in 30 % GFR-PP.....	52
<b>Table 8.11:</b> MFI values of 30 % GFR-PP according to % Mah-g-PP content .....	53
<b>Table 8.12:</b> Tensile properties of 30% GFR-PP according to % Mah-g-PP content (Normal Test Specimen).....	55
<b>Table 8.13:</b> Tensile properties of 30% GFR-PP according to % Mah-g-PP content (Weld line Test Specimen) .....	56
<b>Table 8.14:</b> Flexural properties of 30% GFR-PP according to % Mah-g-PP content .....	58
<b>Table 8.15:</b> Notched Izod impact properties of 30% GFR-PP according to % Mah-g-PP content .....	60
<b>Table 8.16:</b> Heat deflection temperature (A) of 30% GFR-PP according to % Mah-g-PP content .....	61
<b>Table 8.17:</b> Heat deflection temperature (B) of 30% GFR-PP according to % Mah-g-PP content .....	62

<b>Table 8.18:</b> Vicat softening temperature (A) of 30% GFR-PP according to % Mah-g-PP content.....	63
<b>Table 8.19:</b> Vicat softening temperature (B) of 30% GFR-PP according to % Mah-g-PP content.....	64
<b>Table 8.20:</b> Density of 2% Mah-g-PP compatibilized GFR-PP according to % plastomer content.....	65
<b>Table 8.21:</b> MFI values of 2% Mah-g-PP compatibilized GFR-PP according to % plastomer content.....	66
<b>Table 8.22:</b> Ash content measurements of composites in terms of % plastomer in 2% Mah-g-PP compatibilized 30% GFR-PP .....	67
<b>Table 8.23:</b> Lengths of some selected fibers .....	72
<b>Table 8.24:</b> Diameters of some selected fibers.....	73
<b>Table 8.25:</b> Tensile properties of 2% Mah-g-PP + 30% GFR-PP according to plastomer content (Normal test specimen).....	74
<b>Table 8.26:</b> Tensile properties of 2% Mah-g-PP + 30% GFR-PP according to plastomer content (Weld line test specimen) .....	76
<b>Table 8.27:</b> Flexural values of 2% Mah-g-PP + 30% GFR-PP according to plastomer content.....	77
<b>Table 8.28:</b> Notched Izod impact properties of 2% Mah-g-PP + 30% GFR-PP according to plastomer content .....	78
<b>Table 8.29:</b> HDT A values of 2% Mah-g-PP + 30% GFR-PP according to plastomer content.....	79
<b>Table 8.30:</b> HDT B values of 2% Mah-g-PP + 30% GFR-PP according to plastomer content.....	80
<b>Table 8.31:</b> Vicat A values of 2% Mah-g-PP + 30% GFR-PP according to plastomer content.....	81
<b>Table 8.32:</b> Vicat B values of 2% Mah-g-PP + 30% GFR-PP according to plastomer content.....	81

## LIST OF FIGURES

	<u>Page</u>
<b>Figure 3.1:</b> Formation of a composite material using fibers and resin.....	5
<b>Figure 3.2:</b> (a) Continuous and aligned (b) Discontinuous and randomly oriented....	7
<b>Figure 3.3:</b> Effect of fiber orientation on the tensile strength of E-glass fiber-reinforced epoxy composites. (Brooks/Cole ©2003).....	10
<b>Figure 3.4:</b> The deformation pattern in the matrix surrounding a fiber that is subjected to an applied tensile load.....	11
<b>Figure 4.1:</b> General chemical structure of a metallocene compound, where M is some metal cation.....	16
<b>Figure 5.1:</b> Chemically coupled reinforcement.....	20
<b>Figure 5.2:</b> Diffusive adhesion depends on time, temperature and pressure. ....	21
<b>Figure 5.3:</b> Contact angle of a liquid droplet wetted to a rigid solid surface.....	21
<b>Figure 5.4:</b> Mechanical adhesion model a) a Good wetting of surface b) Moderate wetting of surface (Kulhestra A.K., C.Vasile, 2002.).....	22
<b>Figure 6.1:</b> Two different fracture profile.....	23
<b>Figure 6.2:</b> The geometry of surface and internal cracks. (William D. 2003).....	24
<b>Figure 7.1:</b> PRISM TSE24 IIC extruder.....	30
<b>Figure 7.2:</b> Prism Twin Screw Extruder Barrels and Screws .....	31
<b>Figure 7.3:</b> Prism granulating unit.....	32
<b>Figure 7.4:</b> Schematic representation of the barrel and screw configurations as well as the barrel temperature profile.....	32
<b>Figure 7.5:</b> Arburg 320 C injection molding machine .....	34
<b>Figure 7.6:</b> Injection molding machine and process parameter .....	34
<b>Figure 7.7:</b> Mold for tensile specimens according to the ISO R 527 (ISO 527, 1993) .....	35
<b>Figure 7.8:</b> Mold for tensile specimens (weld line) according to the ISO R 527 (ISO 527, 1993) .....	36
<b>Figure 7.9:</b> Mold for Flexural and Impact test specimens according to the ISO 178 (ISO 187, 2001) .....	36
<b>Figure 7.10:</b> Illustration of melt flow index machine.....	39
<b>Figure 7.11:</b> Tensile test illustration.....	40
<b>Figure 7.12:</b> Considered points in the stress-strain graph of specimens .....	41
<b>Figure 7.13:</b> Flexural test illustration .....	42
<b>Figure 8.1:</b> SEM micrograph of neat PP.....	46
<b>Figure 8.2:</b> SEM micrograph of 30 % GFR-PP .....	46
<b>Figure 8.3:</b> Density of 30% GFR-PP according to % Mah-g-PP content.....	51
<b>Figure 8.4:</b> Ash content measurements of composites in terms of % Mah-g-PP in 30 % GFR-PP.....	52
<b>Figure 8.5:</b> MFI values of 30 % GFR-PP according to % Mah-g-PP content.....	54
<b>Figure 8.6:</b> SEM micrograph of 30 % GFR-PP .....	54
<b>Figure 8.7:</b> SEM micrograph of 2% Mah-g-PP + 30 % GFR-PP .....	55

<b>Figure 8.8:</b> Tensile stress of 30% GFR-PP according to % Mah-g-PP content (Normal Test Specimen).....	56
<b>Figure 8.9:</b> Strain at yield of 30% GFR-PP according to % Mah-g-PP content (Normal Test Specimen).....	56
<b>Figure 8.10:</b> Tensile stress of 30% GFR-PP according to % Mah-g-PP content (Weld line Test Specimen).....	57
<b>Figure 8.11:</b> Strain at yield of 30% GFR-PP according to % Mah-g-PP content (Weld line Test Specimen).....	57
<b>Figure 8.12:</b> Flexural stress values of 30% GFR-PP according to % Mah-g-PP content.....	59
<b>Figure 8.13:</b> Flexural modulus values of 30% GFR-PP according to % Mah-g-PP content.....	59
<b>Figure 8.14:</b> Notched Izod impact properties of 30% GFR-PP according to % Mah-g-PP content.....	60
<b>Figure 8.15:</b> Heat deflection temperature (A) of 30% GFR-PP according to % Mah-g-PP content.....	62
<b>Figure 8.16:</b> Heat deflection temperature (B) of 30% GFR-PP according to % Mah-g-PP content.....	63
<b>Figure 8.17:</b> Vicat softening temperature (A) of 30% GFR-PP according to % Mah-g-PP content.....	63
<b>Figure 8.18:</b> Vicat softening temperature (B) of 30% GFR-PP according to % Mah-g-PP content.....	64
<b>Figure 8.20:</b> Density values of 2% Mah-g-PP compatibilized GFR-PP according to % plastomer content .....	65
<b>Figure 8.21:</b> MFI values of 2% Mah-g-PP compatibilized GFR-PP according to % plastomer content .....	66
<b>Figure 8.22:</b> % Ash content measurements of composites in terms of % plastomer in 2% Mah-g-PP compatibilized 30% GFR-PP .....	67
<b>Figure 8.23:</b> SEM micrograph of 2% Mah-g-PP compatibilized 30% GFR-PP .....	68
<b>Figure 8.24:</b> SEM micrograph of 2% plastomer + 2% Mah-g-PP compatibilized 30% GFR-PP .....	69
<b>Figure 8.25:</b> SEM micrograph of 4% plastomer + 2% Mah-g-PP compatibilized 30% GFR-PP .....	69
<b>Figure 8.26:</b> SEM micrograph of 6% plastomer + 2% Mah-g-PP compatibilized 30% GFR-PP .....	70
<b>Figure 8.27:</b> SEM micrograph of 8% plastomer + 2% Mah-g-PP compatibilized 30% GFR-PP .....	70
<b>Figure 8.28:</b> SEM micrograph of 10% plastomer + 2% Mah-g-PP compatibilized 30% GFR-PP .....	71
<b>Figure 8.29:</b> Lengths of some selected fibers.....	71
<b>Figure 8.30:</b> Diameters of some selected fibers .....	72
<b>Figure 8.31:</b> Lengths of some selected fibers.....	73
<b>Figure 8.32:</b> Diameters of some selected fibers .....	73
<b>Figure 8.33:</b> Tensile stress properties of 2% Mah-g-PP + 30% GFR-PP according to plastomer content (Normal test specimen).....	75
<b>Figure 8.34:</b> Strain values of 2% Mah-g-PP + 30% GFR-PP according to plastomer content (Normal test specimen).....	75
<b>Figure 8.35:</b> Tensile stress of 2% Mah-g-PP + 30% GFR-PP according to plastomer content (Weld line test specimen) .....	76

<b>Figure 8.36:</b> Strain values of 2% Mah-g-PP + 30% GFR-PP according to plastomer content (Weld line test specimen).....	76
<b>Figure 8.37:</b> Flexural stress of 2% Mah-g-PP + 30% GFR-PP according to plastomer content .....	77
<b>Figure 8.38:</b> Modulus values of 2% Mah-g-PP + 30% GFR-PP according to plastomer content .....	78
<b>Figure 8.39:</b> Notched Izod impact propeties of 2% Mah-g-PP + 30% GFR-PP according to plastomer content .....	79
<b>Figure 8.40:</b> HDT A values of 2% Mah-g-PP + 30% GFR-PP according to plastomer content .....	80
<b>Figure 8.41:</b> HDT B values of 2% Mah-g-PP + 30% GFR-PP according to plastomer content .....	80
<b>Figure 8.42:</b> Vicat A values of 2% Mah-g-PP + 30% GFR-PP according to plastomer content .....	81
<b>Figure 8.43:</b> Vicat B values of 2% Mah-g-PP + 30% GFR-PP according to plastomer content .....	82

## **EFFECT OF PLASTOMER ADDITION ON POLYPROPYLENE / GLASS FIBER COMPOUND ON PHYSICAL AND MECHANICAL PROPERTIES**

### **SUMMARY**

Polymeric composites have a long-standing reputation in the production of high performance structures and components. With the emerging trend of replacement of conventional materials with modified polymeric materials in the engineering application, the area of polymer composite research is spreading widely.

Fibre reinforced polymer (FRP) composites are used in almost every type of advanced engineering structure. Composites are the most versatile materials due to their good rigidity, low density, relatively high modulus, high impact strength, and high thermal properties.

Because of these outstanding properties, polymeric composites products are widely used in the demanding high technology markets of the aerospace, defence, white goods and medical industries.

One of the most important design characteristic for composite materials is impact strength. Impact strength is the ability of a material to resist shock loading. The impact failure mechanism of the glass fiber-reinforced polypropylene increases with addition of glass fiber. The most important thing during creating polymeric composites with reinforcement is the polymer - reinforcing material interaction. The impact properties can be improved by the increasing interaction between the matrix – reinforcing material interface. Another method of enhancing the impact resistance properties of the structure is achieved by adding to the elastomeric phase.

The aim of this thesis is to investigate the effects of plastomer addition to polypropylene / glass fiber compound on impact strength properties.

In this study, to increase the impact resistance of the material was used in two different stages.

Firstly, the commercial way to improve the impact strength properties of thermoplastics is through reinforcing polypropylene with fibers such as glass fibers. Enhancement in properties of glass fiber reinforced polypropylene has been achieved by virtue of the addition of the coupling agent that makes a strong interfacial bond between the matrix and the glass fiber.

Second way to improve the impact strength properties of glass fiber reinforced polypropylene have been achieved by the addition of the plastomer. Impact energy is absorbed during fracture when a propagating crack meets a plastomer domain and fracture energy is dispersed by deformation of the plastomeric material.

30 % glass fiber reinforced homopolymer polypropylene composites were prepared in a twin screw co-rotating extruder and by the injection molding tensile, impact, flexural test specimens were produced also glass fiber particles distribution were investigated by SEM from fracture surface. Produced composite's mechanical and physical properties such as tensile properties, flexural properties, Izod impact resistance, density, vicat softening point, hardness and thermal properties were examined according to the ISO or ASTM standards. Comparison of reinforced and neat PP test results showed that, by the addition of glass fibers in to the PP matrix increased density, tensile strength, flexural strength, impact strength and modulus value but it drastically reduced melt flow index and % elongation caused by incompatible polypropylene / glass fiber matrix. In order to improve polypropylene glass fiber interface interactions, maleic anhydride grafted polypropylene was chosen. After premixing of Mah-g-PP with polypropylene varying from 1 to 6 %, 30% glass fiber reinforced polypropylene composites were prepared by the twin screw co-rotating extruder and injection molded test specimens were subjected to the mechanical and physical test.

Test results can explain as; the addition of Mah-g-PP into the polypropylene - glass fiber matrix caused the interface interaction as seen in SEM micrographs and an improvement in interface interaction so tensile strength, flexural strength, impact strength, melt flow rate (up to 2%), HDT and vicat softening temperature values were increased.

2% Mah-g-PP + 30% glass fiber reinforced polypropylene which has the best strength of compatibilized formulas have been selected for adding plastomer. After an amount of plastomer varying from 2 to 10% was added to 2% Mah-g-PP + 30% GFR-PP and GFR-PP composites were prepared by the twin screw co-rotating extruder and injection molded test specimens were subjected to the mechanical and physical test.

Test results can explain as; the addition of plastomer varying from 2 to 10% into 2% Mah-g-PP + 30% glass fiber reinforced polypropylene caused improvement in density, % elongation, impact strength were increased, but it drastically reduced yield strength, flexural strength, modulus and melt flow rate.



## **CAM ELYAF POLİPROPİLEN BİLEŞİMİNE PLASTOMER İLAVESİNİN FİZİKSEL VE MEKANİK ÖZELLİKLERE ETKİSİ**

### **ÖZET**

Polimerik Kompozitler yüksek performanslı yapı ve bileşenlerinin üretiminde uzun zamandır üne sahiptir. Mühendislik uygulamalarında geleneksel malzemelerin yerine modifiye edilmiş polimerik malzemenin kullanılması ile polimerik kompozitlerin araştırma alanları genişlemektedir.

İleri Mühendislik yapılarının hemen her çeşidinde elyaf takviyeli polimer kompozitler kullanılmaktadır. Kompozit malzemeler düşük yoğunluk, nispeten yüksek rijitlik, yüksek modül, yüksek darbe dayanımı ve yüksek termal özellikleri nedeniyle çok yönlü malzemelerdir.

Bu üstün özelliklerinden dolayı polimerik kompozitler havacılık, savunma, beyaz eşya, tıp endüstrisi ve yüksek teknoloji pazarlarında kullanılmaktadır.

Kompozit malzemelerinin en önemli tasarım karakteristiklerinden biri darbe dayanımıdır. Darbe dayanımı bir malzemenin şok bir yüklemeye karşı dayanabilme gücü olarak tanımlanır. Homopolimer polipropilene cam elyaf takviyesi ile darbe dayanımı özellikleri arttırılabilmektedir.

Polimerik kompozit oluşturulurken en önemli etkenlerden birisi olarak polimer - takviye malzemesi etkileşimi kabul edilmektedir. Polimer ile takviye malzemesi arasındaki etkileşimin arttırılması ile darbe dayanımı özellikler geliştirilebilmektedir. Yapının darbe direnci özelliklerini geliştirmenin bir diğer yöntemi ise elastomerik faz ekleyerek elde edilmektedir.

Bu çalışmanın amacı; cam elyaf polipropilen bileşimine plastomer ilavesinin darbe dayanımına etkilerinin incelenmesidir.

Bu çalışmada; malzemenin darbe direncini arttırma işlemi iki farklı aşamada gerçekleştirilmiştir.

Termoplastiklerin darbe dayanımını arttırmak için bileşime cam elyaf ilavesi en geleneksel yollardan biridir. Uyumlaştırıcı ilavesi ile polimer matris ve cam elyaf ara yüzeyinde güçlü bir bağ oluşturularak cam elyaf takviyeli polipropilenin özellikleri arttırılmıştır.

Cam elyaf takviyeli polipropilenin darbe dayanımı özelliklerini arttırmanın ikinci yolu ise yapıya plastomer eklemesi sayesinde elde edilmiştir. Darbe dayanımının artışı, kırılma süresince ilerleyen çatlağın plastomer fazı ile karşılaştığında darbe enerjisinin absorblanması ve kırılma enerjisinin dağıtılması ile gerçekleşmektedir.

Cam elyaf ile polipropilen arasında uyumlaştırıcı ajan olarak maleik anhidrit aşılınmış polipropilen (Mah-g-PP) seçilmiştir. Mah-g-PP ile homopolimer PP mekanik karıştırma işleminden sonra çift vidalı ekstrüder ile farklı oranlarda (%1-6) Mah-g-PP içeren %30 cam elyaf takviyeli polipropilen kompozitler üretilmiş ve enjeksiyon işlemi sonrası mekanik ve fiziksel özellikleri incelenmiştir. Elde edilen test sonuçlarında yapıya ilave edilen Mah-g-PP ile akma dayanımı, darbe dayanımı, eğme dayanımı ve HDT – Vicat değerlerinde artış gözlenmiş olup bu artışın nedeni olarak ile SEM incelemesinde ise cam elyafların yüzeyi ile polipropilen arasında bir ara yüzey oluştuğu gözlenmiştir.

Uyumlaştırıcı ajan ilaveli formülasyonlarda en iyi mekanik değerlere sahip olan %2 maleik anhidrit aşılınmış %30 cam elyaf takviyeli polipropilen, plastomer ilavesi için seçilmiştir. Plastomer, Mah-g-PP ile homopolimer PP'nin mekanik karıştırma işleminden sonra çift vidalı ekstrüder ile farklı oranlarda (%2-10) plastomer içeren %30 cam elyaf takviyeli polipropilen kompozitler üretilmiş ve enjeksiyon işlemi sonrası mekanik ve fiziksel özellikleri incelenmiştir. Elde edilen test sonuçlarında yapıya ilave edilen plastomer ile yoğunluk, yüzde uzama ve darbe dayanımı değerlerinde artış gözlenmiştir. Buna karşın akma dayanımı, eriyik akış indeksi, eğme dayanımında azalma gözlenmiştir.

## 1. INTRODUCTION

A composite material is made by combining two or more materials to give a unique combination of properties. Fiber-reinforced composite materials differ from the above materials in that the constituent materials are different at the molecular level and are mechanically separable. In bulk form, the constituent materials work together but remain in their original forms. The final properties of composite materials are better than constituent material properties. (Mazumdar, 2002,1.a)

The matrix phase of fiber composites serves several functions. First, it binds the fibers together and acts as the medium by which an externally applied stress is transmitted and distributed to the fibers. The second function of the matrix is to protect the individual fiber from surface damage because of mechanical abrasion or chemical reactions with the environment. (Callister, Jr., 1985,1.a)

Polymers are used as matrix materials for polymeric matrix composites. Polymers are known as substances consisting of molecules characterized by the repetition (neglecting ends, branch junctions and other minor irregularities) of one or more types of monomeric units (ASTM C 177-D 1600). Polymers contain thousands to millions of atoms in a molecule, which is large; they are also called macromolecules. Polymers are prepared by joining a large number of small molecules called monomers. Monomers are generally simple organic molecules containing a double bond or a minimum of two active functional groups. The presence of the double bond or active functional groups act as the driving force to add one monomer molecule upon the other repeatedly to make a polymer molecule. This process of transformation of monomer molecules to a polymer molecule is known as polymerization. (Chanda and Roy, 2009)

Fiber is used as a reinforcing agent for many polymeric materials. The plastic resins are strong in compressive loading and relatively weak in tensile strength, the fibers are very strong in tension but have no strength against compression. By combining the two materials, Fiber reinforced polymer (FRP) becomes a material that resists both compressive and tensile forces well. The two materials may be used uniformly.

## **2. OBJECTIVE OF STUDY**

The main objective of the present work is to study the effects of plastomer addition on polypropylene / glass fiber compound on physical and mechanical properties.

At the same time, to investigate the effects of glass fiber (GF) addition on polypropylene matrix and the effects of polypropylene glass fiber interface improvements by using maleic anhydrite grafted PP on physical and mechanical properties of glass fiber reinforced polypropylene composite.



### 3. POLYMERIC COMPOSITES

Plastics have become the most common engineering materials over the past decade. The production of plastics on a volume basis has exceeded steel production. Due to their lightweight, easy processability, and corrosion resistance, plastics are widely used for automobile parts, aerospace components, and consumer goods.

A composite material is made by combining two or more materials to give a unique combination of properties (Figure 3.1). Composite materials have been utilized to solve technological problems for a long time but only in the 1960's did these materials start capturing the attention of industries with the introduction of polymeric-based composites. (Mazumdar, 2002, 1.a)

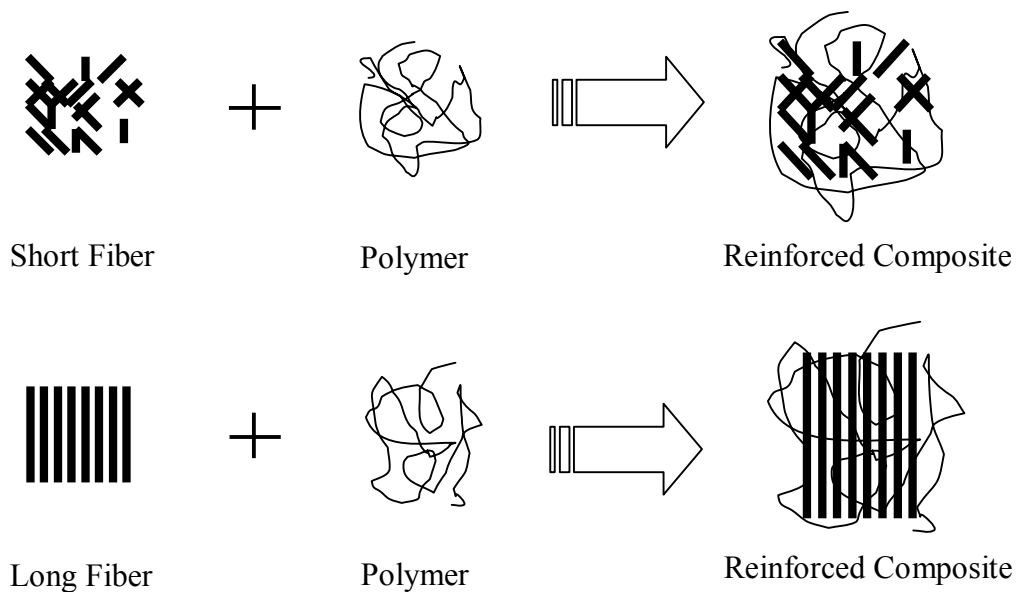


**Figure 3.1:** Formation of a composite material using fibers and resin.

Short-fiber reinforced polymer (SFRP) composites are very attractive because of their ease of fabrication, economy and superior mechanical properties. Extrusion compounding and injection molding processes are frequently employed to make SFRP composites. In general, high fiber content is required in order to achieve a high performance SFRP composite. Therefore, the effect of fiber content on the mechanical properties of SFRP composites is of particular interest and significance. It is often observed that the increase in fiber content leads to the increase in the strength and modulus in the toughness if the matrix has a low toughness.

However, for injection molded SFRP composites, fiber breakage takes place during processing. Fiber breakage results from fiber–polymer interaction, fiber–fiber interaction, and fiber contact with surfaces of processing equipment. Due to the increased fiber–fiber interaction and fiber-equipment wall contact, fiber length decreases with increasing fiber content and this reduction in fiber length then reduces fiber reinforcing efficiency. This is at least partially the reason why the addition of short fibers to a polymer matrix does not lead to a significant increase or brings about a decrease in composite strength and modulus and toughness. (Fu and others, 2000)

### **3.1 Fiber Reinforcements**

Fibre reinforced polymer (FRP) composites are used in almost every type of advanced engineering structure, with their usage ranging from aircraft, helicopters and spacecraft through to boats, ships and offshore platforms and to automobiles, sports goods, chemical processing equipment and civil infrastructure such as bridges and buildings. (Tong and others, 2002)

The main functions of the fibers in a composite are:

- To carry the load. In a structural composite, 70 to 90% of the load is carried by fibers.
- To provide stiffness, strength, thermal stability, and other structural properties in the composites.
- To provide electrical conductivity or insulation, depending on the type of fiber used. (Mazumdar, 2002, 1.b)



### 3.1.1 Effect of fiber orientation and concentration

Concentration and orientation of the fibers influence on the strength and other properties of the polymeric composites. Two cases are possible for fibers in matrix. First one is parallel alignment of the fibers in a single direction (Figure 3.2.a), and as a totally random alignment (Figure 3.2.b)

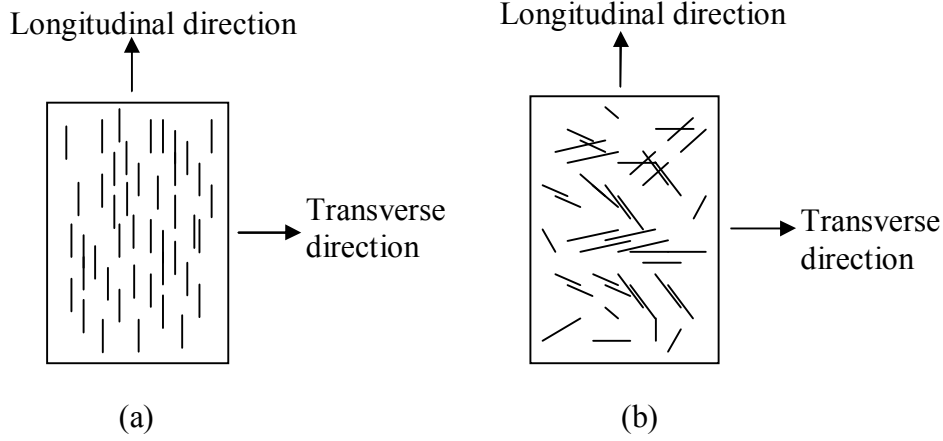


**Figure 3.2:** (a) Continuous and aligned (b) Discontinuous and randomly oriented

The properties of composites are highly anisotropic. Properties of fiber-reinforced composites depend on the direction.

In this case, if the force is applied to the longitudinal for continuous and oriented fiber;

Assume, the fiber-matrix interfacial bond is very good and deformation of both matrix and fibers is the same (isostrain). Under these conditions;

Total load sustained by the composite  $F_c$  is equal to the loads carried by the matrix phase  $F_m$  and the fiber phase  $F_f$ .

$$F_c = F_m + F_f \quad (3.1)$$

From definition of stress or  $F = \sigma \cdot A$

$$\sigma_c \cdot A_c = \sigma_m \cdot A_m + \sigma_f \cdot A_f \quad (3.2)$$

Then, dividing through by the total cross sectional area of the composite  $A_c$

$$\sigma_c = \sigma_m \cdot \frac{A_m}{A_c} + \sigma_f \cdot \frac{A_f}{A_c} \quad (3.3)$$

The area fractions of matrix:  $\frac{A_m}{A_c}$

The area fractions of fiber:  $\frac{A_f}{A_c}$

If the composite, matrix and fiber phase lengths are equal;

The volume fractions of matrix:  $V_m = \frac{A_m}{A_c}$

The volume fractions of fiber:  $V_f = \frac{A_f}{A_c}$

$$\sigma_c = \sigma_m \cdot V_m + \sigma_f \cdot V_f \quad (3.4)$$

The previous assumption of an iso strain state means that:  $\varepsilon_c = \varepsilon_m = \varepsilon_f$

When each term in equation upper stage is divided by its respective strain,

$$\frac{\sigma_c}{\varepsilon_c} = \frac{\sigma_m}{\varepsilon_m} \cdot V_m + \frac{\sigma_f}{\varepsilon_f} \cdot V_f \quad (3.5)$$

If the composite, matrix and fiber deformations are all elastic, E-modul can be obtained for **continous and oriented composite**. (eq.3.6)

$$E_c = E_m \cdot V_m + E_f \cdot V_f \text{ or } E_c = E_m \cdot (1 - V_f) + E_f \cdot V_f \quad (3.6)$$

\* The composite consists of only matrix and fiber phases;  $V_m + V_f = 1$

If the force is applied to the transverse for continous and oriented fiber;

The load is applied at a 90° angle to the direction of fiber as shown in Figure 3.2.a. For this situation the stress  $\sigma$  to which the composite as well as both phases are exposed is the same,  $\sigma = \sigma_c = \sigma_m = \sigma_f$ , this is termed isostress state. The deformation of composite  $\varepsilon_c$  is

$$\varepsilon_c = \varepsilon_m.V_m + \varepsilon_f.V_f \quad (3.7)$$

But, since  $\varepsilon = \frac{\sigma}{E}$ , then

$$\frac{\sigma}{E_c} = \frac{\sigma}{E_m}.V_m + \frac{\sigma}{E_f}.V_f \quad (3.8)$$

Dividing through by  $\sigma$ , E-Modul can be obtained (eq.3.9).

$$\frac{1}{E_c} = \frac{V_m}{E_m} + \frac{V_f}{E_f} \text{ or } E_c = \frac{E_m.E_f}{V_m.E_f + V_f.E_m} \quad (3.9)$$

If the fiber orientation is random, short and discontinuous fibers are used, equation (eq.3.9) may be utilized in the previous one (eq.3.10), as follows;

$$E_c = KE_f.V_f + E_m.V_m \quad (3.10)$$

In this formula, K (eq.3.10) is a fiber efficiency parameter (Table 3.1), which depends on  $V_f$  and the  $\frac{E_f}{E_m}$  ratio.

Fiber orientation is the most important part for reinforced composites. Effect of fiber orientation on tensile strength is given in Figure 3.3. Commonly used fiber types are listed Table 3.2.

**Table 3.1:** Reinforcement efficiency of fiber-reinforced composites for several fiber orientations and at various directions of stress application

Fiber Orientation	Stress Direction	Reinforcement Efficiency
All fibers parallel	Parallel to fibers	1
	perpendicular to fibers	0
Fibers in two directions, in proportions $a_1$ and $a_2$	Parallel to direction of $a_1$ fiber	$a_1$
	Parallel to direction of $a_2$ fiber	$a_2$
Fibers randomly and uniformly distributed within a specific plane	Any direction in the plane of the fibers	$3/8$
Fibers randomly and uniformly distributed within three dimensions in space	Any direction	$1/5$

Source: H.Krenchel, 1964

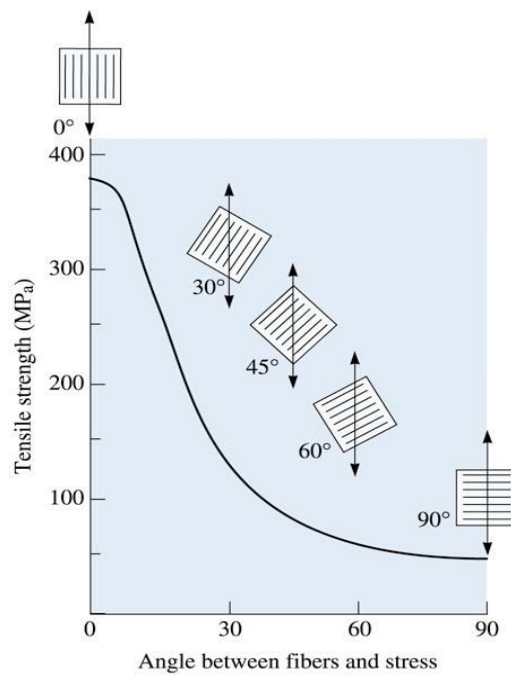


**Figure 3.3:** Effect of fiber orientation on the tensile strength of E-glass fiber reinforced epoxy composites. (Brooks/Cole ©2003)

**Table 3.2:** Commonly used reinforcing fibres

Fibre/grade	Density (g/cm <sup>3</sup> )	Tensile Strength(MPa)	Flexural Modulus (GPa)	Specific Modulus ( $E/\rho$ )
Carbon HT	1.8	3500	160-270	90-150
Carbon IM	1.8	5300	270-325	150-180
Carbon HM	1.8	3500	325-440	180-240
Carbon UHM	2.0	2000	440+	200+
Aramid LM	1.45	3600	60	40
Aramid HM	1.45	3100	120	80
Aramid UHM	1.47	3400	180	120
E-glass	2.5	2400	69	27
R-glass	2.5	3450	86	34
Quartz glass	2.2	3700	69	31
Aluminium	2.8	400	72	26
Titanium	4.5	930	110	24
Steel (bulk)	7.8	620	207	26
Steel (extruded)	7.8	2410	207	26
Steel (stainless)	7.9	1450	197	25

Source: Murpy j.2001,

### 3.1.2 Effect of fiber length

The overall strength of a fiber-reinforced composite depends not only on the tensile strength of the fibers, but in addition, on the degree to which an applied load is transmitted to the fibers. The extent of this load transmittance is a function of fiber length, as already mentioned, the magnitude of the fiber - matrix interfacial bond. Under an applied stress, this fiber-matrix bond ceases at the fiber ends, yielding a matrix deformation pattern as shown schematically in Figure 3.4 (Callister, Jr., 1985, 1.b)

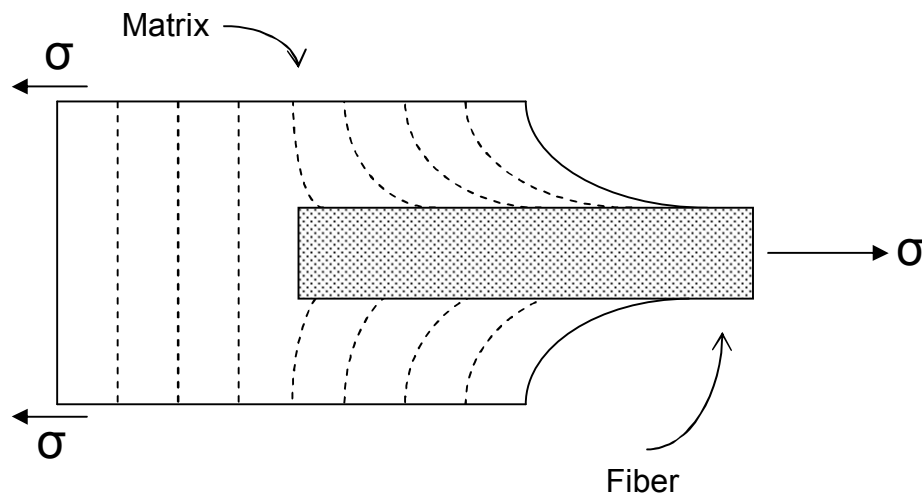


**Figure 3.4:** The deformation pattern in the matrix surrounding a fiber that is subjected to an applied tensile load

The critical fiber length that is necessary for effective strengthening of the composite material is dependent on fiber diameter, its ultimate strength, and the interfacial fiber-matrix bond strength.

$$l_c = \frac{\sigma_f \cdot d}{\tau_c} \quad (3.11)$$

$l_c$  = critical length

$\sigma_f$  = tensile stress of the fiber

$d$  = diameter of the fiber

$\tau_c$  = shear strength of the bond between the matrix and the fiber

### 3.2 The Matrix Phase of Composite

The purpose of the matrix is to bind the reinforcements together by virtue of its cohesive and adhesive characteristics, to transfer load to reinforcements, and to protect the reinforcements from environments and handling.

The matrix also provides a solid form to the composite, which aids handling during manufacture and is typically required in a finished part. This is particularly necessary in discontinuously reinforced composites, because the reinforcements are not of sufficient length to provide a handleable form. Because the reinforcements are typically stronger and stiffer, the matrix is often the “weak link” in the composite, from a structural perspective. As a continuous phase, the matrix therefore controls the transverse properties, interlaminar strength, and elevated-temperature strength of the composite. However, the matrix allows the strength of the reinforcements to be used to their full potential by providing effective load transfer from external forces to the reinforcement. (ASM Handbook, 2001)

The important functions of a matrix material include the following:

- The matrix material binds the fibers together and transfers the load to the fibers. It provides rigidity and shape to the structure.
- The matrix isolates the fibers so that individual fibers can act separately. This stops or slows the propagation of a crack.

- The matrix provides a good surface finish quality and aids in the production of net-shape or near-net-shape parts.
- The matrix provides protection to reinforcing fibers against chemical attack and mechanical damage (wear).
- Depending on the matrix material selected, performance characteristics such as ductility, impact strength, etc. are also influenced. A ductile matrix will increase the toughness of the structure. For higher toughness requirements, thermoplastic-based composites are selected.
- The failure mode is strongly affected by the type of matrix material used in the composite as well as its compatibility with the fiber. (Mazumdar, 2002, 1.b)





#### **4. CONCEPT OF E-PLASTOMER**

Plastomer, a nomenclature constructed from the synthesis of the words plastic and elastomer, illustrates a family of polymers, which are softer (lower flexural modulus) than the common engineering thermoplastics such as polyamides (PA), polypropylenes (PP), or polystyrenes (PS).

Plastomers are ethylenelalpha-olefin copolymers with compositions and properties spanning the range between plastics such as LLDPE and elastomers such as EPR and EPDM. These plastomers are produced by using metallocene catalysts that permit tighter control of molecular weight, crystallinity and comonomer concentrations. Comonomer content typically ranges from about 10 wt% to about 30 wt%. Density ranges from about 0.860 to about 0.910 g/cm<sup>3</sup> (Dani,K.2000,1.a).

The common, current usage of this term is restricted by two limitations. First, plastomers are polyolefins where the inherent crystallinity of a homopolymer of the predominant incorporated monomer (polyethylene or isotactic polypropylene [iPP]) is reduced by the incorporation of a minority of another monomer (e.g., octene in the case of polyethylene, ethylene for iPP), which leads to amorphous segments along the polymer chain. The minor comonomer is selected to distort and, in the limit, not incorporate into the crystalline lattice of the predominant monomer. Second, the most common designators for plastomers are copolymers, which are intermolecularly and intramolecularly uniform in composition. This requires their synthesis to be with a single-site polymerization in a uniformly back-mixed polymerization process. These functional limitations on the definition of plastomers eliminates copolymers such as styrene–butadiene copolymers since they are not polyolefins or compositionally broad polyolefins such as those made with Ziegler–Natta process by incorporation of a minority of ethylene into iPP (random copolymers)(Bhowmick,K.,2008).

##### **4.1 Metallocene Catalyst**

A metallocene is a coordination compound consisting of a transition metal ion, such as zirconium or titanium, with one or two cyclopentadienyl ligands (Figure 4.1).

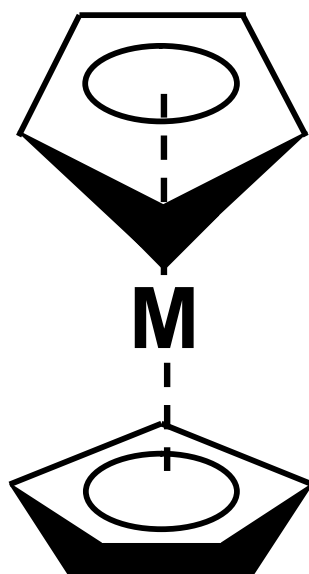


**Figure 4.1:** General chemical structure of a metallocene compound, where M is some metal cation

The ligands are frequently joined by a short "bridge", which constrains the shape of the complex to "clam shell" geometry. The discovery that opened the door to commercial success was that substitution of the cyclopentadienyl rings allows the metallocene to produce highmolecular - weight polymers. The length and structure of the bridge and the nature of cyclopentyl ring substitution are critical factors that control the activity and selectivity of the catalyst, the structure, and sometimes the stereochemistry of the polymer product. (Dani, K.2000, 1.b)

#### **4.2 Toughening Mechanism of PP**

The morphology of the rubber phase has a strong influence on physical properties of impact modified polymer blends. In many cases, the function of the rubber phase in impact modified polymer blends is to initiate cavitation upon impact. This is the major energy absorption and polymer toughening mechanism. High impact behavior in polymer blends is achieved through the control of both the fine rubber dispersion and the blend morphology. Deformation and breakup of the rubber phase is particularly important in order to achieve the desirable morphology for high impact performance in TPOs.

Metallocene catalyzed plastomers exhibit very desirable viscoelastic properties for PP impact modification applications. This is attributed to the long chain branching structure inherent in these plastomers. The higher shear-thinning characteristic of plastomers allows for easy deformation of the plastomer in the PP matrix and the high polymer melt elasticity facilitates breakup of the elongated polymer into small droplets. (Dani, K.2000, 1.c)



## **5. INTERACTIVE RELATION BETWEEN REINFORCEMENT AND MATRIX IN POLYMER COMPOSITES**

An increase in the mechanical properties of reinforced composites can explain with the interaction between reinforcement and polymer matrix. Usually, a high interfacial bonding will impart high properties to a polymer composite, such as, tensile strength, high modulus and hardness as well as resistance to tear, fatigue, cracking, and corrosion.

When the polymeric composites are face up to a force on it that force is transmitted to the filler or reinforcing materials by interface. In case of having poor or none interface interaction between filler and polymeric materials, polymeric composites mechanical properties are affected in a bad way, actually with poor or none interface interaction composites tensile strength are decreased.(Oral,M.A.,2007,1.a)

### **5.1 Adhesion Between The Reinforcing Material and Polymer**

Interaction between the reinforcing material and the polymer is the most important point when the subject is mechanical properties of a polymer composite. There are five kinds of adhesion mechanisms used for explaining the adhesion between polymer and reinforcing material;

- a) Chemical adhesion
- b) Diffusive adhesion
- c) Thermodynamic absorption
- d) Mechanical adhesion
- e) Electrostatic adhesion

### 5.1.1 Chemical adhesion

Two materials may form a compound at the join. The strongest joins are where atoms of the two materials swap (ionic bonding) or share (covalent bonding) outer electrons. A weaker bond is formed if a Hydrogen atom in one molecule is attracted to an atom of Nitrogen, Oxygen, or Fluorine in another molecule, a phenomenon called Hydrogen bonding (Figure 5.1).

Chemical adhesion is the strongest adhesion type of all. Adhesives that are used in daily life works this way. Chemical adhesion can take place with ionic bonding, covalent bonding or the weakest of all; hydrogen bonding. Chemical adhesion is more resistant to water and temperature. As an example of this theory; silane coupled filler or reinforcing materials surface form primary bonds with the matrix. (Ahagon A. and Gent, 1975)

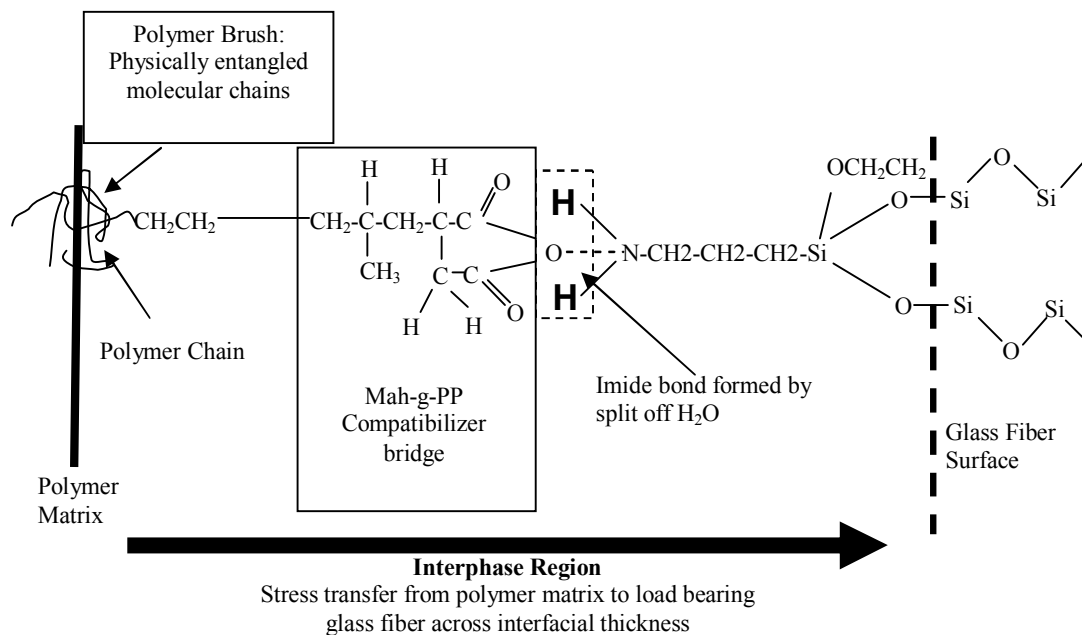


**Figure 5.1:** Chemically coupled reinforcement

### 5.1.2 Diffusive adhesion

Some materials may merge at the joint by diffusion (Figure 5.2). This may occur when the molecules of both materials are mobile and soluble in each other. This would be particularly effective with polymer chains where one end of the molecule diffuses into the other material.

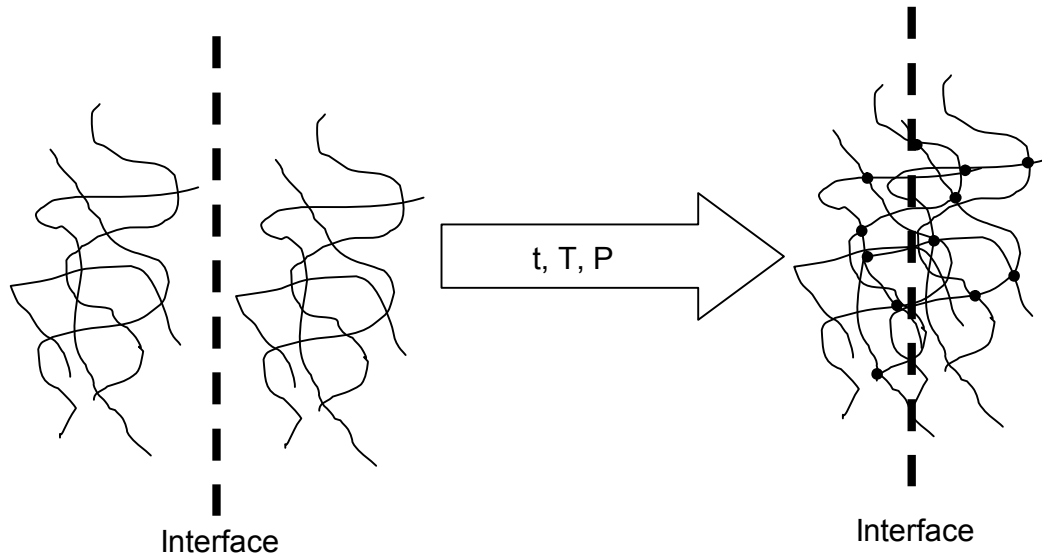


**Figure 5.2:** Diffusive adhesion depends on time, temperature and pressure.

### 5.1.3 Thermodynamic absorption (wetting)

Wetting is the ability of a liquid to maintain contact with a solid surface, resulting from intermolecular interactions when the two are brought together. A force balance between adhesive and cohesive forces determines the degree of wetting (wettability) (Figure 5.3).

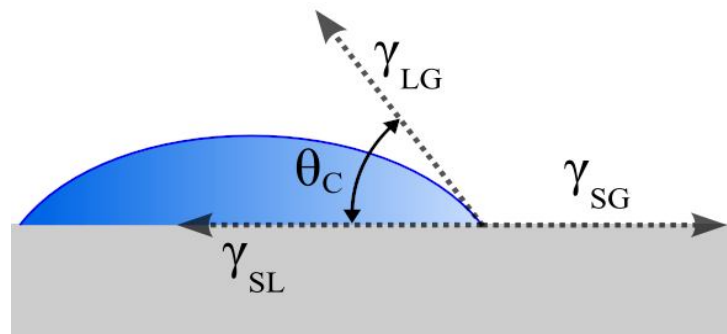


**Figure 5.3:** Contact angle of a liquid droplet wetted to a rigid solid surface.

In Young equation, contact angle is estimated and measured by drop deposited on a solid surface. Young's equation;

$$\gamma_s = \gamma_{SL} + \gamma_L \cos \theta \quad (5.1)$$

$\gamma_s$  = free surface energy of solid

$\gamma_L$  = free surface energy of solid

$\gamma_{SL}$  = solid/liquid interfacial energy

$\theta$  = contact angle

#### 5.1.4 Mechanical adhesion

The adhesion that exists between surfaces in which the adhesive secures the adherends by means of interlocking forces (Figure 5.4).

The theory of mechanical adhesion can be explained as penetration of the adhesive polymeric material in the rough surface of filler. This mechanical adhesion can be improved by increasing the porosity and surface roughness of fillers or reinforcing materials.(Kotan,F.,2008)

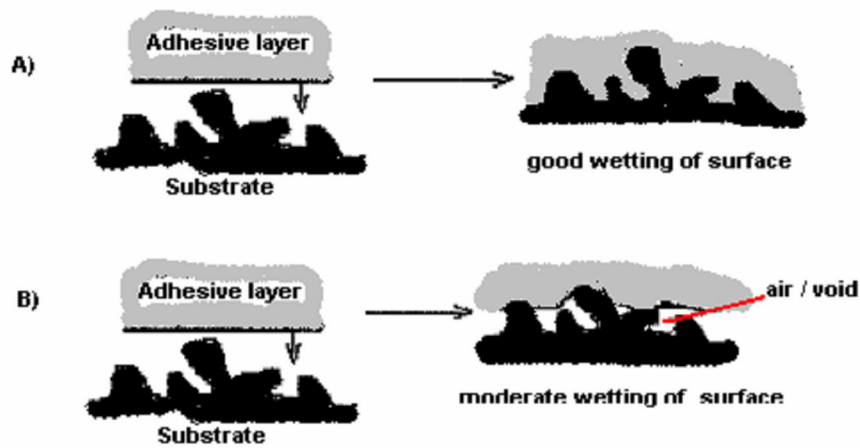


**Figure 5.4:** Mechanical adhesion model a) a Good wetting of surface b) Moderate wetting of surface (Kulhestra A.K., C.Vasile, 2002.)



## 6. FRACTURE AND TOUGHNESS OF COMPOSITES

### 6.1 Introduction

Generally reinforced plastics consists of brittle fibres, such as glass fiber, carbon fiber, etc., in a weak brittle polymer matrix such as epoxy, polyester resin etc. For composite materials, two models are possible: ductile and brittle (Figure 6.1). It depends on the ability of a material to experience plastic deformation.

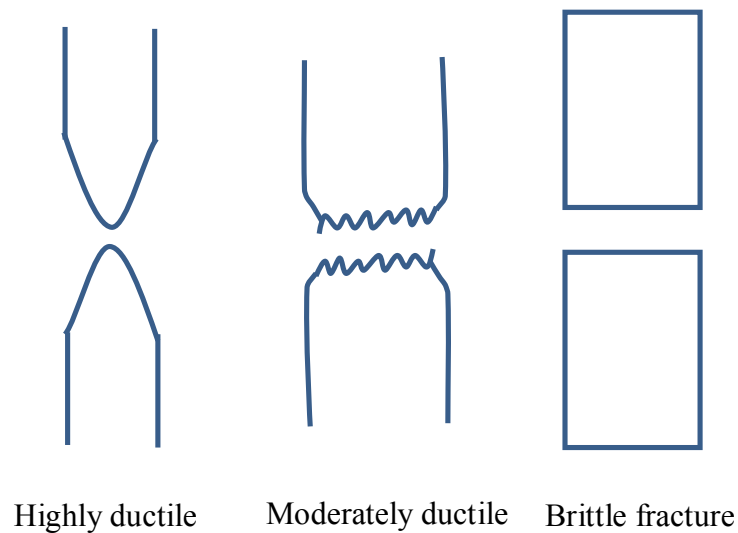


**Figure 6.1:** Two different fracture profile

During deformation, crack growth inhibited by the presence of interfaces both at the microstructural level between fibres and matrix in the composite materials. When the increase interfaces properties between fibers and matrix with compatibilizer, crack growth is harder than uncompatibilized composite.

Generally, composites fracture properties goes to brittle fracture from ductile fracture with increase of reinforcing material in composition.

## 6.2 Principles of Fracture Mechanics

### 6.2.1 Stress concentration

The measured fracture strengths for most brittle materials are significantly lower than those predicted by theoretical calculations based on atomic bonding energies.

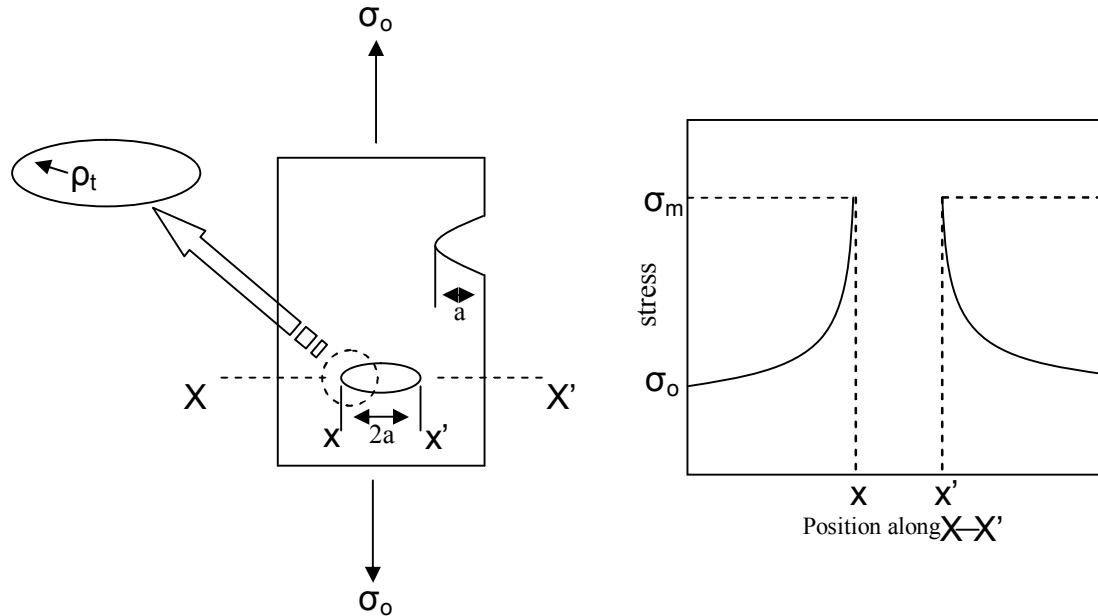


**Figure 6.2:** The geometry of surface and internal cracks. (William D. 2003)

A stress across a cross section containing an internal crack (Figure 6.2). As indicated by this profile, the magnitude of this localized stress diminishes with distance away from the crack tip. At positions far removed, the stress is just nominal stress  $\sigma_o$ , or the applied load divided by the specimen cross-sectional area. Due to their ability to amplify an applied stress in their locale, these flaws are sometimes called stress raisers. (William D. 2003)

If it is assumed that a crack is similar to an elliptical hole through a plate, and is oriented perpendicular to the applied stress, the maximum stress,  $\sigma_m$  occurs at the crack tip and may be approximated by (eq.6.1);

$$\sigma_m = 2\sigma_o \left( \frac{a}{\rho_t} \right)^{1/2} \quad (6.1)$$

$\rho_t$  = the radius of curvature of the crack tip

$a$  = the length of a surface crack

Sometimes the ratio  $\sigma_m / \sigma_0$  is denoted as the stress concentration factor  $K_t$

$$K_t = \frac{\sigma_m}{\sigma_0} = 2 \left( \frac{a}{\rho_t} \right)^{1/2} \quad (6.2)$$

Using principles of fracture mechanics it is possible to show that the critical stress  $\sigma_c$  (eq.6.3) required for crack propagation in a brittle material is described by the expression

$$\sigma_c = \left( \frac{2E\gamma_s}{a\pi} \right)^{1/2} \quad (6.3)$$

$E$ = modulus of elasticity

$\gamma_s$  = specific surface energy

$a$ = one half the length of an internal crack

### 6.2.2 Fracture toughness

Furthermore, using fracture mechanical principles an expression has been developed that relates this critical stress for crack propagation  $\sigma_c$  and crack length  $a$  as

$$K_c = Y\sigma_c \sqrt{\pi a} \quad (6.4)$$

In this expression  $K_c$  (eq.6.4) is the fracture toughness, a property that is a measure of a material's resistance to brittle fracture when a crack is present.  $Y$  is a dimensionless parameter or function that depends on both crack and specimen sizes and geometries, as well as the manner of load application. Fracture toughness data for some polymers are given Table 6.1.

**Table 6.1:** Room temperature yield strength and plane strain fracture toughness data for some polymers

Material	Yield Strength (MPa)	$K_{Ic}$ (MPa $\sqrt{m}$ )
Polystyrene (PS)	-	0,7 – 1,1
Polycarbonate (PC)	62,1	2,2

## 6.3 Crack Extension in Composites

### 6.3.1 Matrix effects

In practical fibre composites the proportion of fibre present will vary between about 10% (in dough moulding compounds. for example) and 70% (in high-performance composites), and crack resistance effects directly attributable to the matrix material may not be significant except perhaps in composites reinforced with relatively low volume fractions of short fibres. Three specific matrix effects might be listed.

a) The effective toughness of a "on-brittle matrix, such as a metal or thermoplastic will be reduced by the presence of a high  $V_f$  of rigid, brittle fibres or particles as a result of plastic constraint which leads triaxial tensile stress components in the matrix.

b) The effective toughness of a low-toughness, flexible matrix may be increased by the presence of a low  $V_f$  of rigid particles or fibres because a high overall stress level on the composite may then be required to generate a critical extent of crack opening in the 'stiffened' matrix

c) The effective toughness of a low-toughness matrix may be increased by the presence of fibres or particles because of the slowing of cracks in the neighbourhood of the filler. The toughness of certain brittle plastics, for example, shows a strong dependence on the crack speed, often linked to changes in the crack face roughness - the slower the crack, the rougher the crack face and the higher the associated work of fracture. (Harris B., 1986)

### 6.3.2 Fibre effects

Certain types of fibre, such as the drawn steel wires used for reinforcing concrete, or the polyester textile fibres used to reinforce rubber tyres or the aromatic polyamide fibres used in high performance laminates, may be classified as 'tough' because they are capable of extensive non-elastic deformation after yielding. (Harris B., 1986)

A bundle of such fibres possesses large fracture energy, and a substantial portion of this fracture energy can be transferred into a composite containing the bundle.

## 7. EXPERIMENTAL WORK

### 7.1 Materials

In this work, as a base polymer of the matrix; polypropylene (PP) is used, supplied from Borealis/Austria, grade HE125MO with the MFI value of 12 g/10min. The properties of homopolymer polypropylene are given in the Table 7.1.

**Table 7.1:** Physical properties of Borealis HE 125 MO

Properties	Typical Value	Test Method
Density	908 kg/m <sup>3</sup>	ISO 1183
Melt Flow Rate (230 °C/2,16 kg)	12 g/10min	ISO 1133
Tensile Modulus (1 mm/min)	1.550 MPa	ISO 527-2
Tensile Strain at Yield (50 mm/min)	9%	ISO 527-2
Tensile Stress at Yield (50 mm/min)	34,5 MPa	ISO 527-2
Heat Deflection Temperature (0,45 N/mm <sup>2</sup> )	88 °C	ISO 75-2
Charpy Impact Strength, notched (23 °C)	3,5 kJ/m <sup>2</sup>	ISO 179/1eA
Hardness, Rockwell (R-scale)	100	ISO 2039-2

Glass fiber was supplied from Owens corning, the grade of glass fiber was DS 2100-13P. The properties of glass fiber are given Table 7.2.

**Table 7.2:** Properties of Owens Corning DS 2100 – 13 P

Propeties	Value
Diameter	13 $\mu$ m
Fiber length	4mm
Solid content	0,6%
Moisture content	max 0,05%

Polymer modifier; Maleic Anhydride grafted polypropylene (Mah-g-PP) was supplied from Uniroyal Chemical, grade Polybond 3200 with 1% Maleic anhydride (MA) grafted. The physical properties of the material are given in The table 7.3.

**Table 7.3:** Physical properties of the Polybond 3200

Propeties	Value	Test Method
Appearance	Pellets	
Melt Flow Rate (190 °C/2,16 kg)	115 g/10min	ASTM D-1238
Density	908 g/cm <sup>3</sup>	ASTM D-792
Melting point	157 °C	DSC
Maleic Anhydride Level	1 weight %	

Plastomers was supplied from Dex plastomer, grade Exact 0210 with the MFI value of 10 g/10min. General properties of plastomer are given Table 7.4.

**Table 7.4:** General properties of Dex Plastomer Exact 0210

General properties	Units	Typical values	Method
Melt Flow Rate (2.16 kg/190°C)	dg/min	10.0	ISO 1133
Density (23°C)	kg/m <sup>3</sup>	902	ISO 1183
Shore D hardness	--	37	ISO 868
DSC peak melting point	°C	95	ASTM D3418
DSC heat of fusion	J/g	120	ASTM D3418
Vicat softening temperature. (at 10 N)	°C	77	ISO 306
Brittleness temperature	°C	< -73	ASTM D746
Moulded plaque properties			
Tensile strength at break	MPa	28	ISO 527-2
Elongation at break	%	1550	ISO 527-2
Flexural modulus	MPa	65	ISO 178
Notched Izod @ 23°C and @ -40 °C	J/m	No break	ASTM D256
Environmental stress crack resistance	hr	100	ASTM D1693

## 7.2 Compounding Recipes

In this study, two main group of recipes were studied. In the first group, the optimum compatibilizer ratio for 30 % fiber content was investigated. As shown in the Table 7.5. In the second group, effect of plastomer amount was investigated as shown in Table 7.6.

**Table 7.5:** Compounding recipe according to % Mah-g-PP content

Glass fiber (DS2100-13P)	Polypropylene (HE125MO)	Mah-g-PP (Polybond 3200)
%	%	%
30	70	0
30	69	1
30	68	2
30	67	3
30	66	4
30	65	5
30	64	6

**Table 7.6:** Compounding recipe according to % plastomer content

Glass fiber (DS2100-13P)	Polypropylene (HE125MO)	Mah-g-PP (Polybond 3200)	Plastomer (Exact 0210)
%			
30	68-a*	a*	2
30	66-a*	a*	4
30	64-a*	a*	6
30	62-a*	a*	8
30	60-a*	a*	10

\* Optimum amount of Mah-g-PP would be determined from the first group

### 7.3 Compounding with Twin Screw Extruder and Test Specimen Preparation by Injection Molding

#### 7.3.1 Twin screw extruder

Formulations of composites, containing polypropylene (PP), glass fiber (GF), compatibilizer and plastomer were prepared with twin-screw extruder. Co-rotating twin-screw extruder was used in this study. The twin-screw extruder that was used in this study is a PRISM TSE24 IIC, with the screw diameter 24mm and L/D ratio 28:1 (shaft length/screw diameter). Properties of the PRISM TSE24 IIC extruder is given in Table 7.7

Prism TSE 24 IIC extruder has seven temperature controlled barrel segments with length of 96 mm or 4D and a die with three-strand hole having diameter of 3 mm. The barrel temperatures are controlled by electrical resistances and water cooling channels. At the third, fifth, and seventh zone of barrels, thermocouples are mounted to measure melt temperature of polymeric materials. Parameters such as barrel temperatures, motor speed, shaft torque and melt temperature controlled by computer. PRISM TSE24 IIC extruder with K-Tron 3 gravimetric feeders is given Figure 7.1

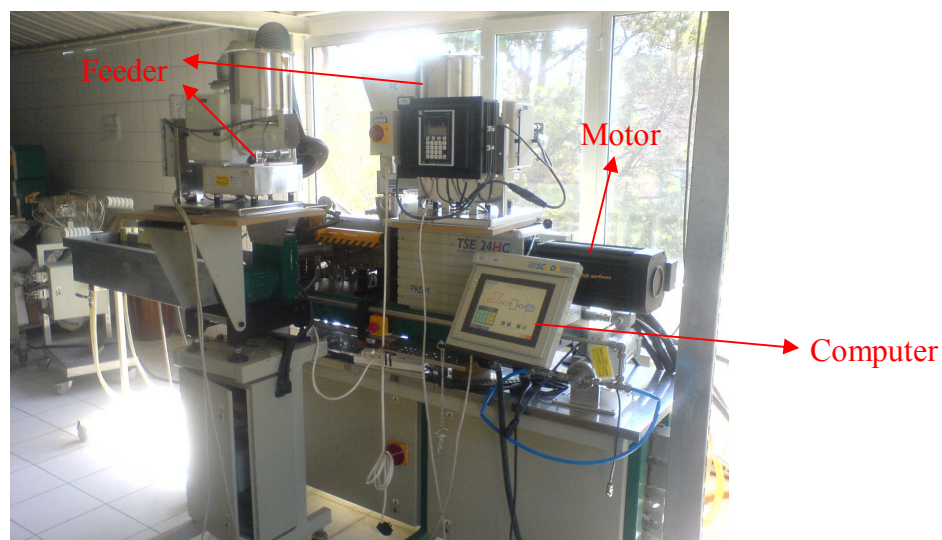


**Figure 7.1:** PRISM TSE24 IIC extruder

**Table 7.7:** Properties of PRISM TSE24 IIC extruder

	Units	PRISM TSE24
Screw diameter	Mm	24
Maximum screw speed	Rpm	1000
L/D (shaft length/screw diameter)	-	28:1
Channel depth	Mm	5.15
Screw diameter/channel depth	-	5.15
Screw/barrel clearance	Mm	0.2
Shaft center line distance	Mm	18.75
Shaft center line/radius ratio	-	1.5625
Total Area	cm <sup>2</sup>	8.5
Screw area	cm <sup>2</sup>	4.7
Free area	cm <sup>2</sup>	3.8
Total volume	cm <sup>3</sup>	511
Free volume	cm <sup>3</sup>	228
Barrel peripheral surface area	cm <sup>2</sup>	830
Surface area/total volume	m <sup>2</sup> /litre	0.14
Surface area/Free volume	m <sup>2</sup> /litre	0.31
Max. channel shear rate @ 1000 rpm	s <sup>-1</sup>	244
Max. power	kW	9
Max. torque/shaft	Nm	43
Max. torque/Free volume	Nm/ cm <sup>3</sup>	0.16



The first barrel is known as inlet zone and it was cooled down to prevent the messing-up of the polymers through the walls of barrel and screw. In the inlet zone, polymeric materials start conveying into other zones and by the effect of heat and work supplied by the shafts on the polymers, polymeric material starts to melt down. To remove the gases occurred during compounding; one degassing unit is connected to the Edwards rotary vacuum pump by hoses at sixth zone of barrel. The barrels finish with a three-strand hole die, so molten polymeric composite can pull out of the extruder and it can be cooled down into a water bath and solidified as spaghetti and then pelletizing by rotation blade.

As shown in Figure 7.2., the barrel can be split in the middle for easy screw removal and cleaning purpose. Electrical resistances and water-cooling channels controlled by thermo regulator are connected to each modular barrel zone to ensure that the set temperature is achieved. Thermocouples are assembled at the third, fifth, and seventh zone of barrel up to the internal surface for the purpose of the melt temperature measurement. The die with three-strand hole having diameter of 3 mm is mounted at the forward end of the extruder. Pressure sensor is connected to the die barrel to measure the melt pressure generated by movement of the screws. (Ersoy.O.G, 2003)

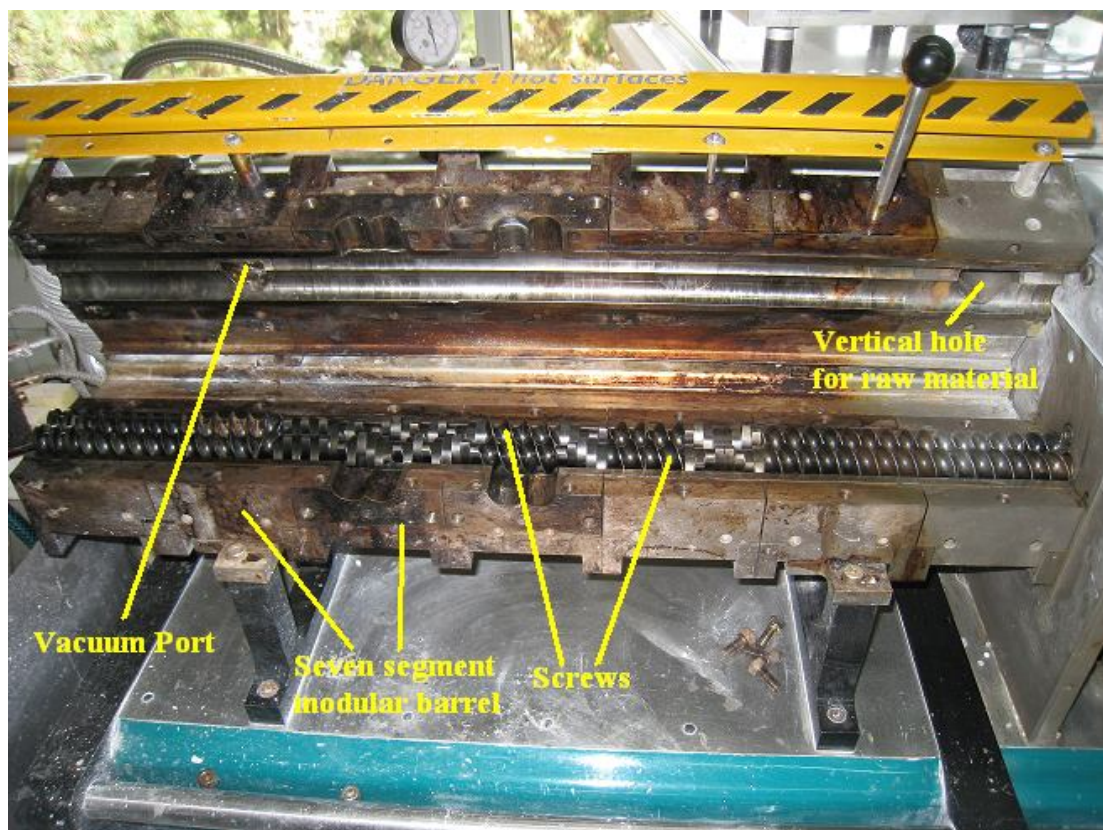


**Figure 7.2:** Prism Twin Screw Extruder Barrels and Screws

After mixing process in extruder, spaghetti like strands are cut into granules with the granulating unit shown in the Figure 7.3.



**Figure 7.3:** Prism granulating unit

### 7.3.2 Extruder screw desing and temperature profile

For the best melting and mixing of polymers special screw which segmented high shear, high residence time in the reaction zones, and venting close to the outlet of the extruder were selected as shown schematically in the Figure 7.4

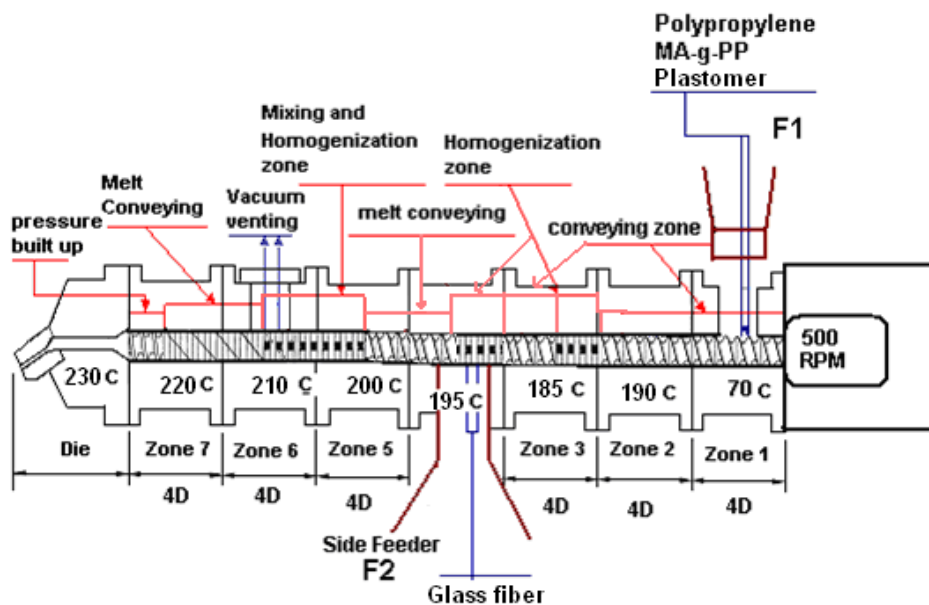


**Figure 7.4:** Schematic representation of the barrel and screw configurations as well as the barrel temperature profile

### **7.3.3 Compounding procedure**

For compatibilized formulations, compatibilizer material (Polybond 3200) is humidity sensitive material. It can lose efficiency with humidity. Loss of anhydride functionality may occur due to conversion to acid groups by reaction with atmospheric moisture. Therefore, compatibilizer was being dried in oven for three hours at 105°C to remove moisture.

Polypropylene and compatibilizer were premixed before feeding the Feeder 1 (F1). Feeder 2 (F2) feeds glass fiber, which was located at the side of extruder. Positions of the feeders are shown in Figure 7.4. The compounded materials were left the extruder as spaghettis, they were cooled down in water bath, and spaghetti like compound was cut into granules with the granulating units.

For plastomer addition formulations, plastomer, polypropylene and compatibilizer were premixed before loading into the feeder 1 (F1). Feeder 2 (F2) was used to feed glass fiber.

For uncompatibilized formulations, (F1) was used to feed only polypropylene, (F2) was used to feed only glass fiber. All feeders were calibrated previously.

### **7.3.4 Injection molding process**

Injection molding is a manufacturing process for producing parts from both thermoplastic and thermosetting plastic materials. Material was fed into a heated barrel, mixed, and forced into a mold cavity where it cools and hardens to the configuration of the mold cavity. (Robert H. Todd, 1994) After a product was designed, usually by an industrial designer or an engineer, molds are made by a moldmaker (or toolmaker) from metal, usually either steel or aluminium, and precision-machined to form the features of the desired part.

Injection molding machines are mainly divided into 3 parts. These are mold, clamping unit and injection unit. (Figure 7.5)



**Figure 7.5:** Arburg 320 C injection molding machine

For test specimen production, granules were loaded into a hopper on top of the injection machine. The granules feed into the cylinder by the reciprocating movement of the screw and heated until they melt. When the molten plastic was accumulated in front of the screw, injection process begins. The speed controlled forward movement of screw forces molten plastic into mold cavity and then holds the force for a while to minimize the shrinkage of molded part. After finishing injection and holding the pressure, the mold was kept closed to cool down the melted plastic and shape it. When the cooling was completed, mold opens and the ejectors force the molded-shaped parts out. (Oral, M.A., 2007, 1.b)

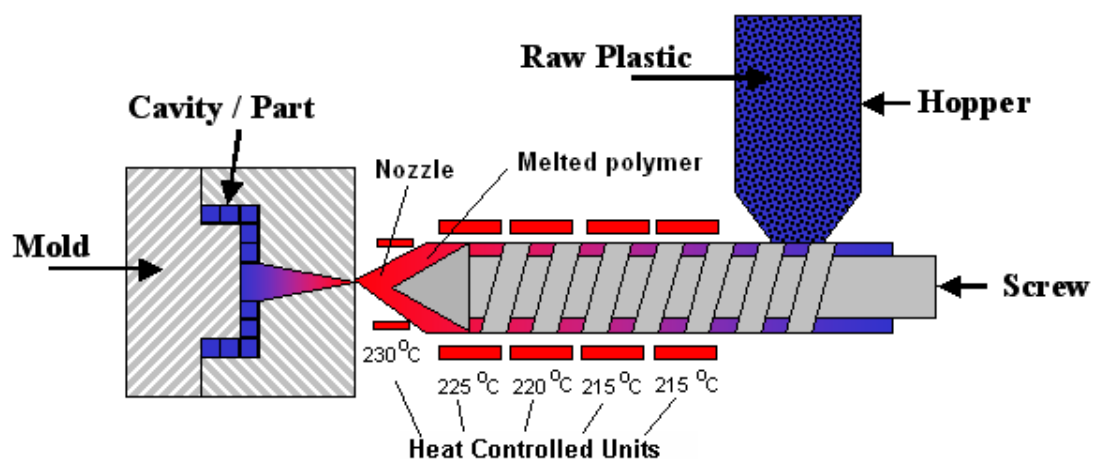


**Figure 7.6:** Injection molding machine and process parameter



Tensile, flexural, impact and HDT-vicat test specimens were produced by Arburg Allrounder 320C injection machine according to the ISO standards. The Arburg injection machine's specifications are given in Table 7.8 The molds for test specimens are shown in Figures 7.7.-7.8.-7.9. Mold temperature during the injection process was kept constant at 23°C with a water-cooling chiller.

**Table 7.8:** The Arburg 320C injection machine's specifications

Properties	Unit	Arburg Allrounder 320C
Screw diameter	mm	30
Max. injection pressure	bar	2000
Max. volumetric displacement	cm <sup>3</sup>	144
Hydraulic motor power	W	1500
Max. clamping force	tones	50
Max. screw speed	rpm	154
Screw back pressure	bar	350

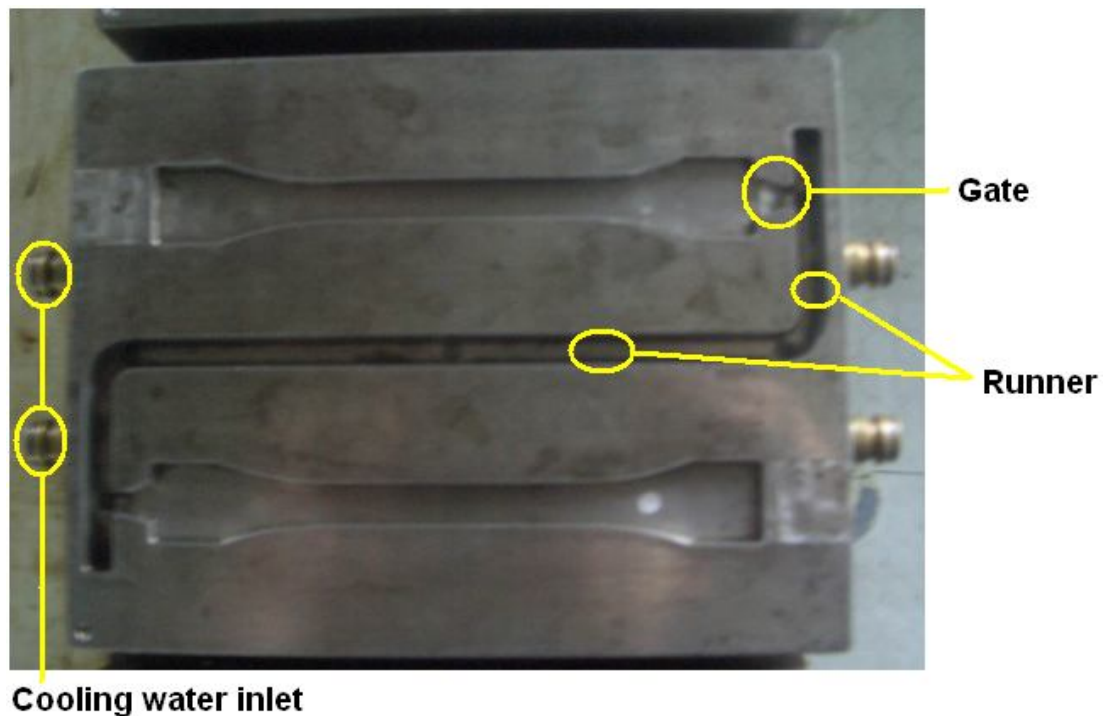


**Figure 7.7:** Mold for tensile specimens according to the ISO R 527 (ISO 527, 1993)

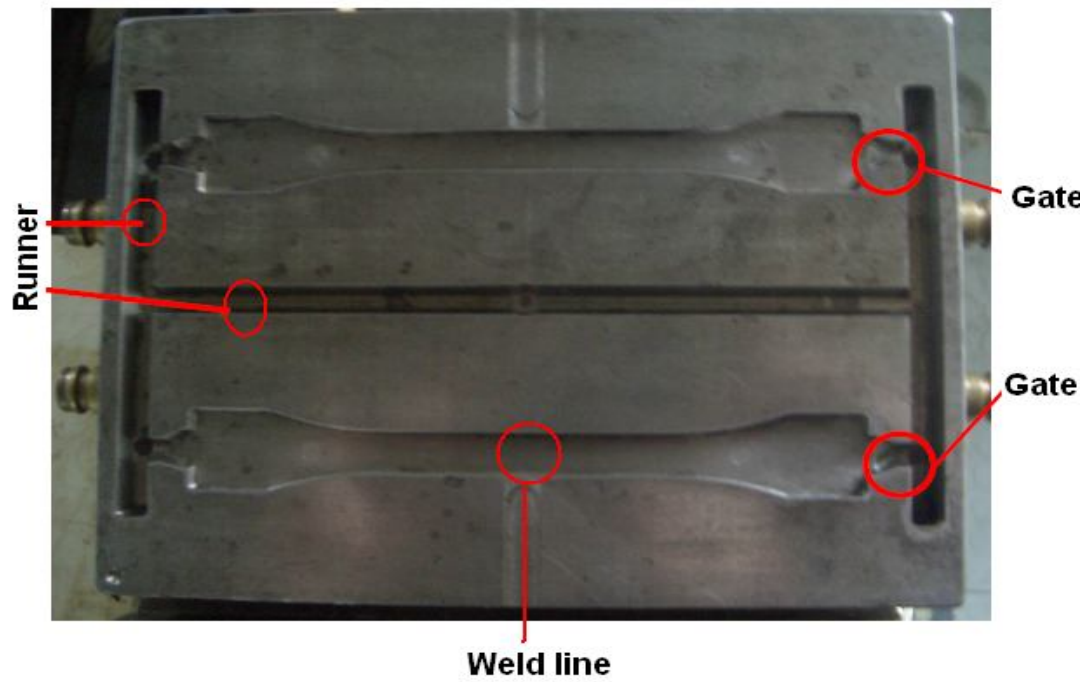


**Figure 7.8:** Mold for tensile specimens (weld line) according to the ISO R 527 (ISO 527, 1993)

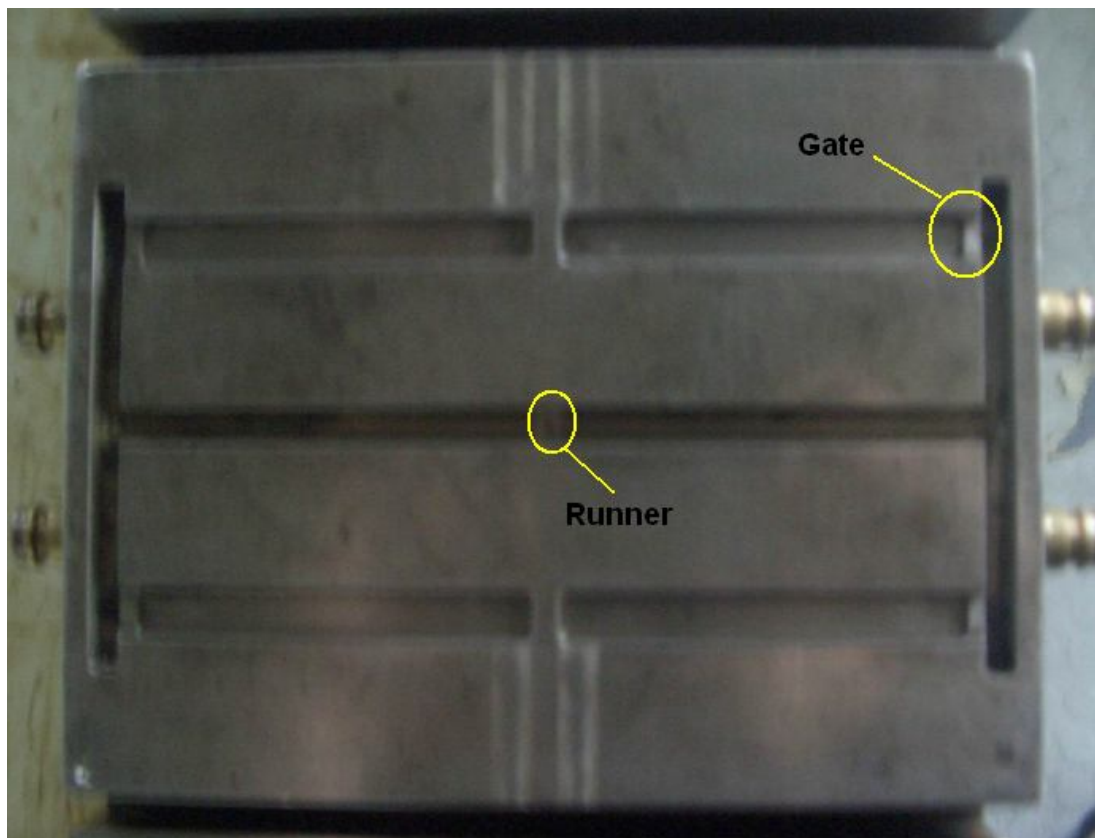


**Figure 7.9:** Mold for Flexural and Impact test specimens according to the ISO 178 (ISO 187, 2001)

## 7.4 Measurement of Density

Density is the mass per unit volume of a material. Specific gravity is a measure of the ratio of mass of a given volume of material at 23°C to the same volume of deionized water. Specific gravity and density are especially relevant because plastic is sold on a cost per pound basis and a lower density or specific gravity means more material per pound or varied part weight.

The density of specimens is measured according to the procedure described in ISO1183. (ISO 1183, 1999) Test specimens can be used with sheet, rod, tube and molded articles. The specimen is weighed in air then weighed when immersed in distilled water at 23°C using a sinker and wire to hold the specimen completely submerged as required. Density and specific gravity were calculated.

$$\text{Specific gravity} = \frac{a}{(a + w) - b} \quad (7.1)$$

a = mass of specimen in air.

b = mass of specimen and sinker (if used) in water.

w = mass of totally immersed sinker if used and partially immersed wire.

## 7.5 Ash Content

Determination of ash content of the reinforced polymeric composites were measured according to ISO 3451 Method A. (ISO 3451 Method A, 1981)

An Ash test was used to determine if a material was filled. The test will identify the total reinforcement content. It cannot identify individual percentages in multi-filled materials without additional test procedures being performed.

An Ash test involves taking a known amount of sample, placing the weighed sample into a dried / pre-weighed porcelain crucible, burning away the polymer in an air atmosphere at temperatures above 600°C, and weighing the crucible after it has been cooled to room temperature in a desiccator.

The Ash test result was expressed as % ash. A magnified optical examination of the ash residue was performed to determine if the ash is glass, mineral, or a combination of both. The total ash content equals the weight of the ash divided by the weight of the original sample multiplied by 100%.

Six grams of sample was typically used, which represents three crucibles each containing two grams of sample. Smaller sample weights can be tested but accuracy diminishes with smaller sample sizes. Typically, the average of three crucibles was reported.

## **7.6 Melt Flow Rate**

Melt flow index or MFI is a measure of the ease of flow of the melt of a thermoplastic polymer. It is defined as the mass of polymer, in grams, flowing in ten minutes through a capillary of a specific diameter and length by a pressure applied via prescribed alternative gravimetric weights for alternative prescribed temperatures. The method was described in the ISO 1133. (ISO 1133, 2005)

Melt flow rate is an indirect measure of molecular weight, with high melt flow rate corresponding to low molecular weight. At the same time, melt flow rate is a measure of the ability of the material's melt to flow under pressure. Melt flow rate is inversely proportional to viscosity of the melt at the conditions of the test, though it should be borne in mind that the viscosity for any such material depends on the applied force. Ratios between two melt flow rate values for one material at different gravimetric weights are often used as a measure for the broadness of the molecular weight distribution.

The test is very similar to an extrusion plastometer operating at a fixed temperature and under load. According to the polymer, load and temperature were predefined. (For example, PP - 2,16kg, 230°C) The testing device consists of heating cylinder, temperature control equipment, piston, die and the loading unit. (Figure7.10)



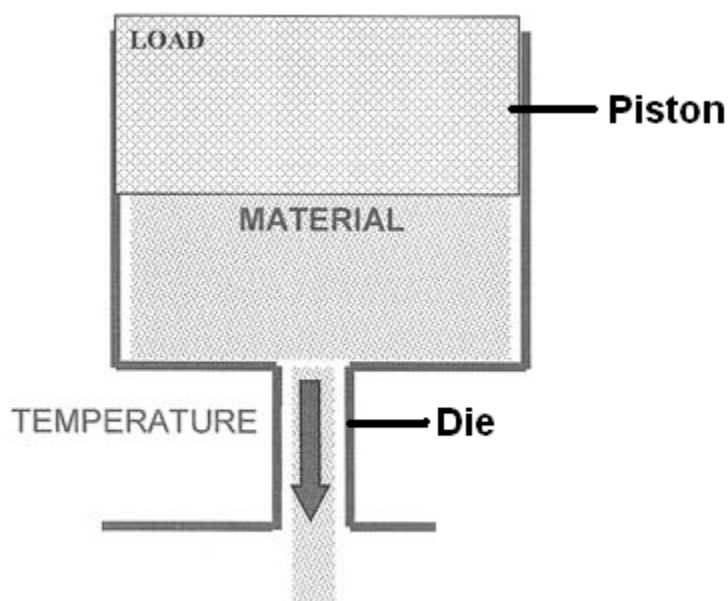


**Figure 7.10:** Illustration of melt flow index machine

### 7.7 Morphology Investigation

Examination of the morphology of the polymeric composite was done by a scanning electron microscope (Jeol JSM 6400). To investigate the interface between polymer and the reinforcing material dispersion in the matrix, injection molded test bars having dimensions of  $4 \pm 0.2$  mm,  $10 \pm 0.2$  mm,  $80 \pm 0.2$  mm were left in a desiccator for at least 48 hours to get rid of post crystallization or physical aging and any hydrolysis effect. Then 2 mm notched test samples were immersed in liquid nitrogen for 2 hours and it was broken with a sudden impact. Before the SEM investigation, to provide electro conductivity the fractured surfaces were coated with gold by sputter. Goldcoated fracture surfaces were investigated with different magnifying values.

### 7.8 Measurement of Tensile Properties

Zwick universal tensile testing machine Z020 equipped with 20 kN load cell as load indicator and a mechanical long stroke extensometer as extension indicator was used to measure tensile properties of samples. Tensile specimens, injection molded according to ISO / R 527 (ISO 527, 1993) without weld line (normal specimens) and specimens with weld line were used to measure tensile properties.

Test specimens were left in a heat controlled room for at least 48 hours to eliminate the effects of post crystallization or physical aging. Testing speed was set to 50 mm/min and gauge length ( $L_0$ ) was set to 70 mm as shown in the Figure 7.11

The test was performed at standard condition, i.e.,  $23 \pm 2^\circ\text{C}$  and 50 % humidity. A micrometer reading at least 0.02 mm did measurement of the thickness and width. After measurement, the specimen was fixed to self-aligning grips of the tensile test machine with 123 mm distance between grips. The extensometer was attached to the specimen over the parallel portion of it, beginning distance between the extensometer path was 70 mm and the machine was started. The loads and corresponding elongations were recorded at the time interval of 0.1 second.

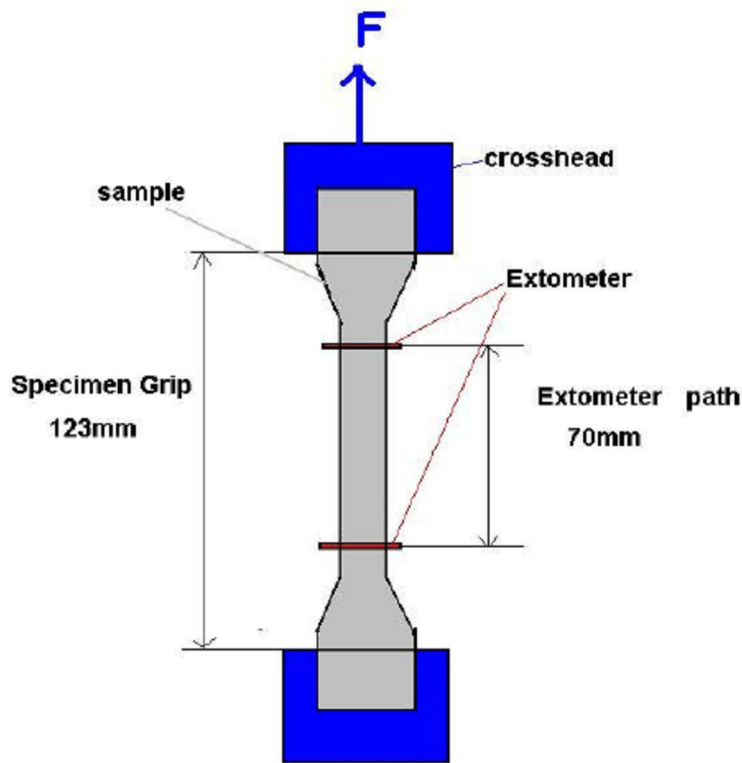


**Figure 7.11:** Tensile test illustration.

Following tensile properties were measured:

- Tensile stress or yield stress shown as  $\sigma_y$  (tensile load per unit area of original cross section within the narrow parallel portion). Tensile stress expressed in MPa means Newton per square millimeter ( $\text{N/mm}^2$ ) is the first top point on the load / extension curve at which an increase occurs in the elongation but without an increase in load.

- Tensile strain or percentage elongation at yield shown as  $\varepsilon_y$  (percent increase in the distance of extensometer path). Tensile strain is the percentage elongation corresponding to tensile stress point.
- Elastic modulus or Young modulus is calculated according to the stress values at %0.1 and %0.25 elongations by regression method.(Figure 7.12)

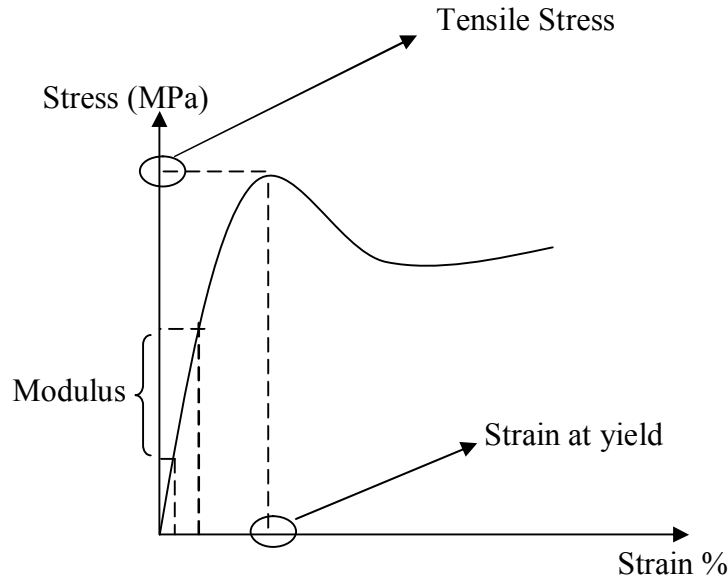


**Figure 7.12:** Considered points in the stress-strain graph of specimens

## 7.9 Determination of Flexural Properties

Flexural properties of the polymeric composites were examined by using Instron 4505 universal testing machine equipped with 10 KN load cell as load indicator and three point bending fixture. The test is performed at standard condition, i.e.,  $23 \pm 2^\circ\text{C}$  and 50 % humidity. ISO 178 (ISO 178, 2001) standard was followed to determine flexural properties. Similar to tensile test specimens, injection molded test bars having dimensions of  $40 \pm 2$  mm,  $10 \pm 0.5$  mm,  $80 \pm 0.5$  mm were left in a heat-controlled room for at least 48 hours to eliminate post crystallization or physical aging. Span of two lower arms of bending fixture was set to 60 mm. Testing speed was set to 5 mm/min and the extension was measured from travel of traverse of testing machine.

The thickness and width were measured by screw micrometer reading at least 0.02 mm. Then, the specimen was laid to lower arms of the bending fixture fixed to stationary testing machine base.

The third arm of the fixture fixed to movable traverse of testing machine was slowly contacted with test piece at mid-span and the machine was started. The loads and corresponding deformations were recorded at the time interval of 0.2 second. Following flexural properties are measured:

Flexural stress or flexural yield stress designated as  $\sigma_y$  was calculated as follows:

$$\sigma_f = (3 \times F \times L) / (2 \times b \times h^2) \quad (7.2)$$

- Where F is applied load in meganewtons (MN), L is the span length, b is the width and h is the thickness of specimen in meters. Flexural stress is express in megapascal (MPa) or newton per square millimeter (N/mm<sup>2</sup>).
- Flexural strain is the distance over which the top of specimen surface at midspan has deviated during flexure from its original position and is designated as  $\varepsilon_{fy}$ .
- Flexural modulus or apparent modulus of elasticity ( $E_b$ ) was calculated from initial linear portion of the load extension curve by using at least five values of the deflection and load.  $E_b$  was calculated as follows:

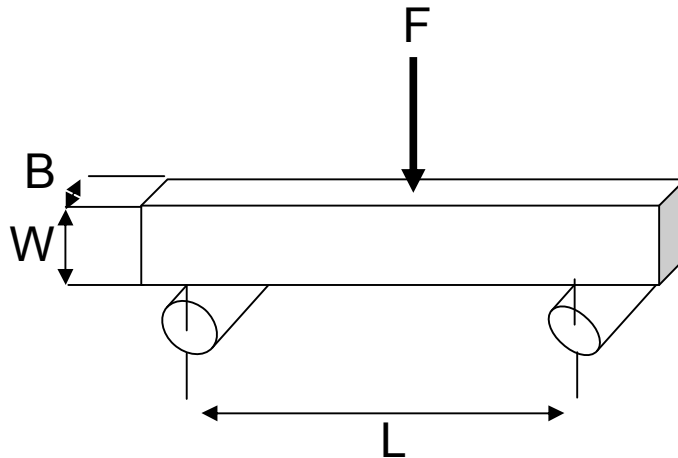


**Figure 7.13:** Flexural test illustration

where L is span length, b and h are the width and thickness of the specimen respectively, F is the load at a chosen point on the initial linear portion of the load deflection curve, Y is the deflection corresponding to load F, L, b, h and Y are in millimeter and F is in Newton, then  $E_b$  is in N/mm<sup>2</sup>.

### 7.10 Determination of Weld Line Factor

The effect of weld line on mechanical properties of molded material, the weld line factor ( $F_{wl}$ ) is defined as (Malguarnera, S.C. and Manisali, A., 1981)

$$F_{wl} = \frac{\text{Property value of specimen with weld line}}{\text{property value of specimen without weld line}} \quad (7.3)$$

Weld line factor was calculated for tensile yield strength, yield elongation.

### 7.11 Determination of Izod Impact Strength

According to ISO 180 standard (ISO 180, 2000) Izod impact strength of samples was determined. Similar to tensile test specimens, injection molded test bars having dimensions of  $4 \pm 0.2$  mm,  $10 \pm 0.2$  mm,  $80 \pm 0.2$  mm were left in a desiccator for at least 48 hours to get rid of post crystallization or physical aging and any hydrolysis effect.

The thickness and width were measured by screw micrometer reading at least 0.02 mm. Then, 2 mm notch with notch base radius  $0.25 \pm 0.05$  mm was machined at mid-span of specimen. The test specimen and the notch were defined in the ISO standard as type 1A. The testing machine is Cheast Impact Tester equipped with 2.75 J impact capacity pendulums. Blank test (i.e. without a specimen in place) was carried out to ensure the total friction losses. The specimen was placed into test machine grips in such a way that the notched surface was faced to the impact point. The pendulum was then released and the impact energy was recorded after making correction for frictional losses. The Izod impact strength, in kilojoules per square meter ( $\text{KJ/m}^2$ ), was calculated as follows:

$$\text{Izod Impact Strength} = A_k / (X \times Y_k) \times 10^3 \quad (7.4)$$

Where  $A_k$  is the impact energy, in joules, absorbed by the test specimens and it is corrected for frictional losses.  $X$  is the thickness, in millimeters, of specimen.  $Y_k$  is the difference of width and notch depth, in millimeters.

### **7.12 Determination of Vicat Softening Temperature and Heat Deflection temperature**

Vicat softening point or Vicat hardness is the determination of the softening point for materials that have no definite melting point. It was taken as the temperature at which the specimen was penetrated to a depth of 1 mm by a flat-ended needle with a 1 square mm circular or square cross-section. For the Vicat A test, a load of 9.81 N is used. For the Vicat B test, the load is 49.05 N.

The Heat Distortion Temperature was determined by the following the test procedure outlined in ISO 306. The test specimen was loaded in three-point bending in the edgewise direction. The outer fiber stress used for testing is either 0.455 MPa or 1.82 MPa, and the temperature was increased at 2 °C/min until the specimen deflects 0.32 mm.

## 8. RESULTS AND DISCUSSION

First objective of this study, to investigate the effects of compatibilizer on the glass fiber - polypropylene, Second objective of this study, to investigate the effect of plastomer on the optimum compatibilized glass fiber/polypropylene composite. All formulas were produced and tested as described in section 7.

### 8.1 The Effect of Glass Fiber on The Properties Polypropylene

#### 8.1.1 Measurement of density

Measurement of density was done as described in Section 7.4. Test results are given in Table 8.1

**Table 8.1:** Result of density measurement of neat PP and 30% GFR-PP.

% Glass fiber	Density g/cm <sup>3</sup>	Average Density g/cm <sup>3</sup>
0	0,9123	0,9112
	0,9020	
	0,9194	
30	1,0973	1,1004
	1,1033	
	1,1006	

With the addition of reinforcement material into the polymeric matrix, density value was increased as expected, since the glass fiber has higher density more than polypropylene.

#### 8.1.2 Determination of melt flow index

Determination of melt flow index was done as described in section 7.6. Melt flow index test results of neat PP and glass fiber reinforced PP are given in the Table 8.2. The viscosity of the glass fiber is higher, which results in the decrease in the melt-flow index of the glass-reinforced PP as the amount of glass fiber increases.

**Table 8.2:** Melt flow index results of neat PP and 30% GFR-PP

% Glass fiber	MFI (g/10min.)	Average MFI (g/10min.)
0	13,28	13,4667
	13,60	
	13,52	
30	11,47	11,53
	11,52	
	11,60	

### 8.1.3 Morphology investigation

Morphology investigation was done as described in section 7.7. SEM micrographs show that, during extrusion process, the glass fiber particles were well dispersed and there is no interaction between surface of the glass fiber and polypropylene. Glass fiber surfaces are very smooth because of no interaction between matrix and fiber.

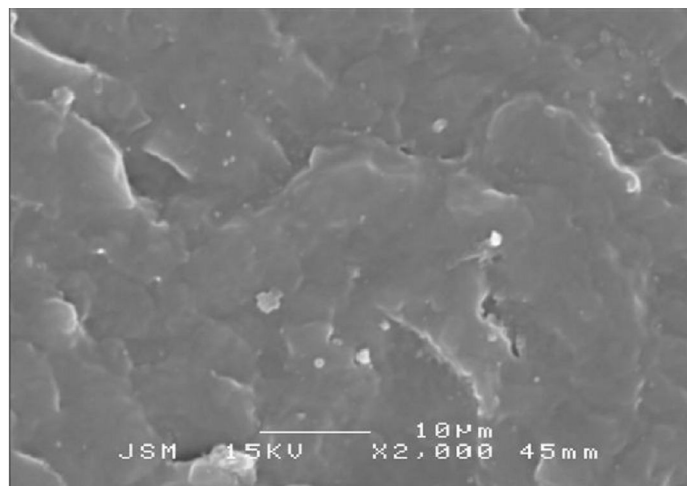


**Figure 8.1:** SEM micrograph of neat PP

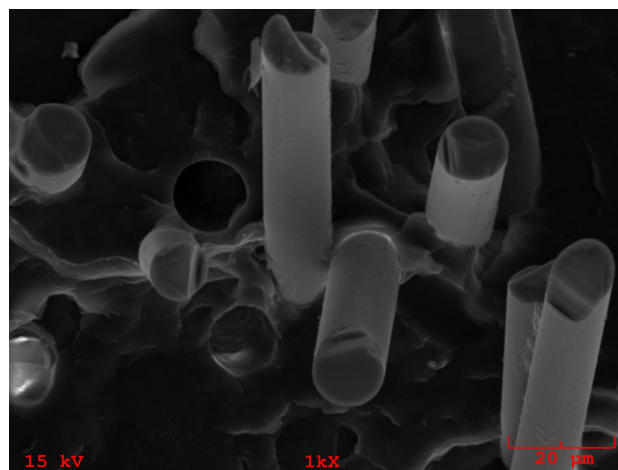


**Figure 8.2:** SEM micrograph of 30 % GFR-PP



### 8.1.4 Tensile properties

Measurement of tensile properties of composites was done as described in Section 7.8. In mechanical properties, tensile properties were increased with addition of the glass fiber, while elongation at break decreases. Because of stress transferred to the fiber by the matrix, therefore tensile properties were increased.

By addition of glass fiber, maximum stress increases by 205%, strain % decreases by 72%, E-modul increases by 385% for normal specimen, test results are given Table 8.3

**Table 8.3:** Tensile properties of neat PP and 30% GFR-PP (Normal Test Specimen)

Sample	Tensile Normal			Tensile Normal		
	Neat PP			30% Glass fiber reinforced PP		
	Max. Stress Mpa	Strain %	E-Modul Mpa	Max. Stress Mpa	Strain %	E-Modul Mpa
1	32,29	9,69	1536	68,68	2,67	5915
2	33,53	9,54	1640	68,27	2,60	6095
3	32,88	9,76	1578	68,43	2,60	5866
4	33,69	9,09	1506	68,21	2,64	6027
5	33,59	9,49	1501	68,26	2,61	5981
Avr.	33,20	9,51	1552	68,37	2,62	5977
Max.	33,69	9,76	1640	68,68	2,67	6095
Min.	32,29	9,09	1501	68,21	2,60	5866
SD	0,60	0,26	57,86	0,19	0,03	90,10

By addition of glass fiber, stress increases by 115%, strain % decreases by 73%, E-modul increases by 298% for weld line specimen, test results are given table 8.4

**Table 8.4:** Tensile properties of neat PP and 30% GFR-PP (Weld line Test Specimen)

Sample	Tensile Weld			Tensile Weld		
	Neat PP			30% Glass fiber reinforced PP		
	Max. Stress Mpa	Strain %	E-Modul Mpa	Max. Stress Mpa	Strain %	E-Modul Mpa
1	27,38	3,12	1552	29,98	0,79	4538
2	28,48	3,76	1557	30,76	0,83	4289
3	25,38	2,92	1532	30,47	0,78	4866
4	25,58	2,49	1543	30,13	0,77	4761
5	25,07	2,81	1527	30,43	0,79	4529
Avr.	26,38	3,02	1542	30,35	0,79	4597
Max.	28,48	3,76	1557	30,76	0,83	4866
Min.	25,07	2,49	1527	29,98	0,77	4289
SD	1,48	0,47	12,76	0,31	0,02	224,86

### 8.1.5 Flexural properties

Flexural test procedure is given in section 7.9 and the test results are given in Table 8.5, with the addition of glass fibers especially modulus and stress value were increased but strain values were decreased as seen in Table 8.5 Flexural strength is the ability of the material to withstand bending forces applied perpendicular to its longitudinal axes. Both flexural strength and flexural modulus of the glass-reinforced PP increase with the increase in the proportion of the glass fiber. Glass fibers act as a stress transfer agent and have a high capacity to bear load.

**Table 8.5:** Flexural properties of neat PP and 30% GFR-PP.

Sample	Flexural Properties			Flexural Properties		
	Neat PP			30% Glass fiber reinforced PP		
	Max. Stress Mpa	Displacement at yield (mm)	E-Modul Mpa	Max. Stress Mpa	Displacement at yield (mm)	E-Modul Mpa
1	40,41	11,43	1233	75,07	4,19	4799
2	40,32	11,74	1238	75,10	4,29	4702
3	40,12	10,89	1241	74,80	4,41	4544
4	40,4	11,50	1252	75,01	4,35	4746
5	40,03	11,14	1241	73,69	4,24	4552
Avr.	40,26	11,34	1241	74,73	4,30	4669
Max.	40,41	11,74	1252	75,10	4,41	4799
Min.	40,03	10,89	1233	73,69	4,19	4544
SD	0,17	0,33	6,96	0,60	0,09	115,36

By addition of glass fiber, maximum stress increases by 185%, displacement decreases by 62%, E-modul increases by 376% for flexural specimen, test results are given table 8.5

### 8.1.6 Impact properties

Izod notched impact test applied according to the procedure explained in section 7.11 and test results are given in Table 8.6

**Table 8.6:** Izod notched impact properties of neat PP and 30% GFR-PP

	Neat PP	30 % GFR PP
	Impact	Impact
	$\text{kJ/m}^2$	$\text{kJ/m}^2$
	4,28	6,21
	4,18	6,12
	4,26	5,87
	4,56	6,04
	4,09	5,82
	4,28	5,90
	4,18	5,87
	4,38	6,64
	4,26	6,13
	4,27	6,32
Avr.	4,27	6,09
Max.	4,56	6,64
Min.	4,09	5,82
SD	0,13	0,25

The impact properties of the polymeric materials are directly related to the overall toughness of the material. The impact resistance of the glass-reinforced PP increases with addition of glass fiber. This is because glass fibers have a higher capacity to absorb energy, and it results in less fiber breakage and a higher residual strength to the composite. Secondary, matrix cracking as a result of the initial fiber failure also reduces, which results in the increase of residual compressive strength of the composite.

#### 8.1.7 Heat deflection temperature - Vicat softening temperature

Glass fibers were directed during injection process. Load was applied to oriented fibers perpendicularly during test process and load was carried by fibers. Therefore, HDT and Vicat values increases by addition of glass fiber because of softening temperature of glass fiber is higher than polypropylene.

HDT - Vicat test applied according to the procedure explained in section 7.12 and test results are given in Table 8.7-8.8

**Table 8.7:** Vicat (A-B) softening temperatures of neat PP and 30% GFR-PP

	Vicat A (10N)	Vicat B (50N)	Vicat A (10N)	Vicat B (50N)
	30% GFR - PP		Neat PP	
	165,60	130,50	155,80	96,00
	166,50	136,30	154,00	95,40
Avr.	166,05	133,40	154,90	95,70
Max.	166,50	136,30	155,80	96,00
Min.	165,60	130,50	154,00	95,40
SD	0,64	4,10	1,27	0,42

**Table 8.8:** Heat deflection temperatures (A-B) of neat PP and 30% GFR-PP

	HDT A (1,8MPa)	HDT B (0,45MPa)	HDT A (1,8MPa)	HDT B (0,45MPa)
	30% GFR - PP		Neat PP	
	155,70	140,00	60,00	97,00
	155,80	138,10	60,40	98,80
Avr.	155,75	139,05	60,20	97,90
Max.	155,80	140,00	60,40	98,80
Min.	155,70	138,10	60,00	97,00
SD	0,07	1,34	0,28	1,27

## 8.2 The Effect of Compatibilizer Mah-g-PP on GFR-PP composite

The effect of a coupling agent on glass fiber-reinforced polypropylene has been studied and test results given section 8.2. Compatibilized compound formulations are given table 7.4.

### 8.2.1 Measurement of density

Measurement of density was done as described in section 7.4. Coupling agents show negligible effect on the specific gravity. Test results are given in Table 8.9

**Table 8.9:** Density of 30% GFR-PP according to % Mah-g-PP content

Mah-g-PP	Density	Avr. Density
%	g/cm <sup>3</sup>	g/cm <sup>3</sup>
0	1,100	1,10
	1,110	
	1,090	
1	1,091	1,09
	1,092	
	1,090	
2	1,089	1,09
	1,090	
	1,091	
3	1,098	1,10
	1,099	
	1,099	
4	1,100	1,10
	1,100	
	1,090	
5	1,090	1,09
	1,088	
	1,091	
6	1,100	1,10
	1,098	
	1,099	

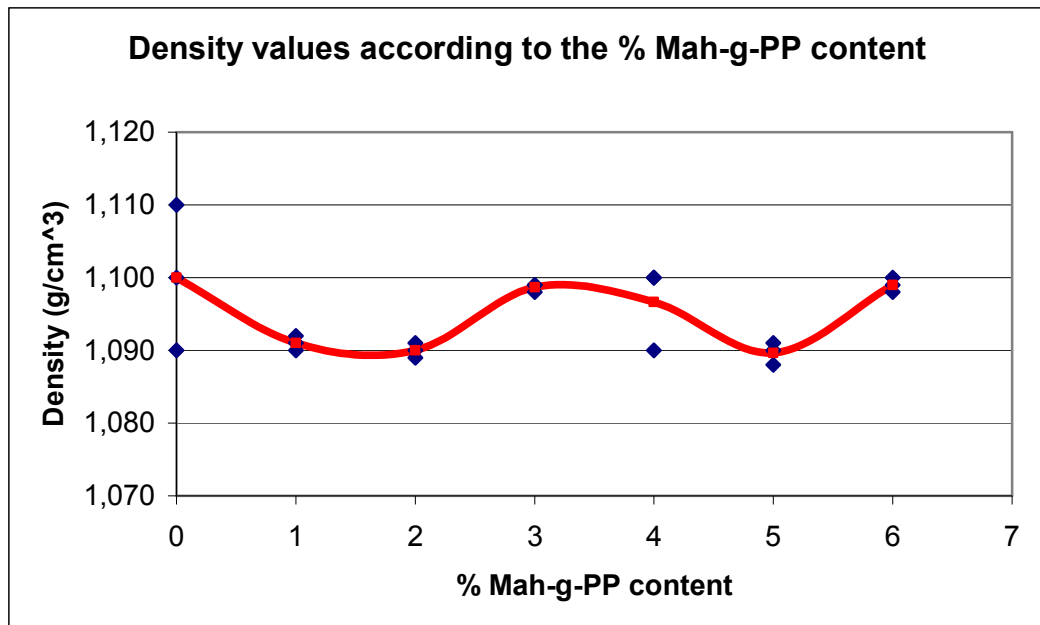


**Figure 8.3:** Density of 30% GFR-PP according to % Mah-g-PP content

### 8.2.2 Determination of ash content

The test samples taken during extrusion process (at the beginning, in the middle and at the end) were used to determine ash content and test was done as explained in section 7.5. Test results are given in Table 8.10. Ash content measurement results show that extrusion process was done.

**Table 8.10:** Ash content measurements of composites in terms of % Mah-g-PP in 30 % GFR-PP

% Mah-g-PP	% Ash	Avr. % Ash
0	28,044	30,959
	33,951	
	30,882	
1	30,137	30,035
	29,832	
	30,137	
2	30,317	30,332
	31,214	
	29,464	
3	27,928	29,171
	30,097	
	29,487	
4	28,814	29,458
	29,204	
	30,357	
5	29,310	29,935
	29,661	
	30,833	
6	28,000	29,395
	30,097	
	30,088	

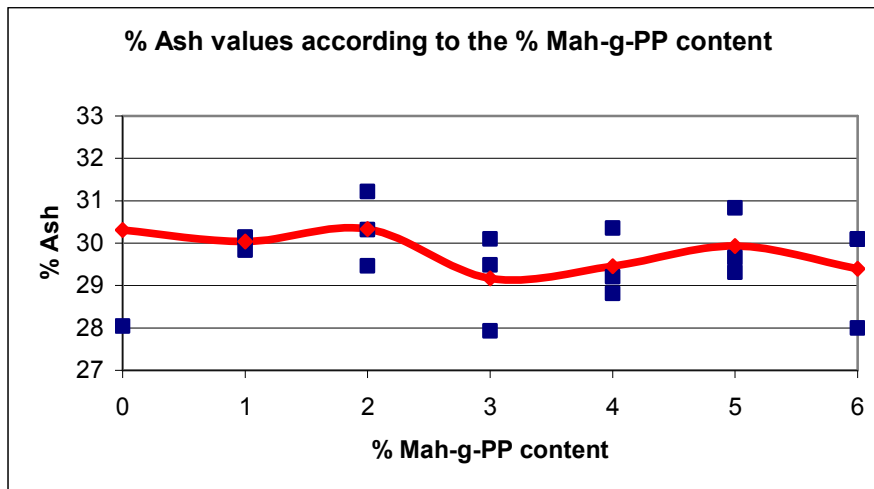


**Figure 8.4:** Ash content measurements of composites in terms of % Mah-g-PP in 30 % GFR-PP

### 8.2.3 Determination of melt flow index

Determination of MFI test was done as described in section 7.6. Melt flow index test results of neat PP and glass fiber reinforced PP are given in the Table 8.11

In the melt state of polymer, addition of the glass fiber particles cause to decrease the melt flow index value because of viscosity of the glass fiber is higher, which results in the decrease in the melt-flow index of the glass-reinforced PP as the amount of glass fiber increases. It is expected that addition of Mah-g-PP coat of the fiber surface with polymer; which can reduce surface energy of fiber. Depends on that increase in the MFI value of composites containing Mah-g-PP certain limit, i.e. 2 %.

**Table 8.11:** MFI values of 30 % GFR-PP according to % Mah-g-PP content

Mah-g-PP	MFI	Avr. MFI
%	g/10'	g/10'
0	11,47	11,530
	11,52	
	11,60	
1	17,88	18,240
	18,36	
	18,48	
2	16,90	16,927
	16,96	
	16,92	
3	14,24	14,160
	14,10	
	14,14	
4	13,98	14,087
	14,10	
	14,18	
5	13,94	14,053
	14,00	
	14,22	
6	13,12	13,960
	14,46	
	14,30	

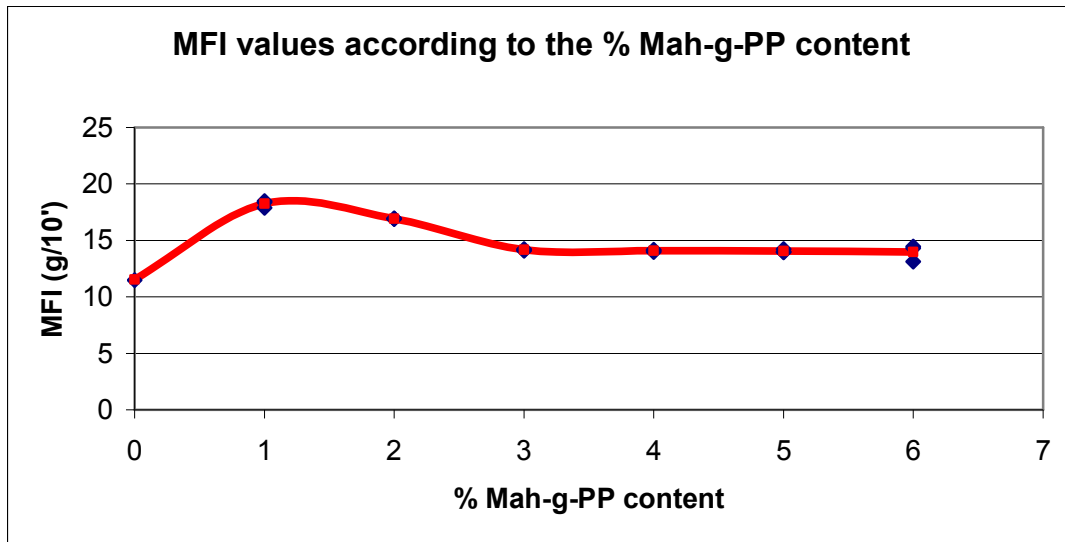


**Figure 8.5:** MFI values of 30 % GFR-PP according to % Mah-g-PP content

### 8.2.4 Morphology investigation

Morphology investigation was done as described in section 7.7. SEM micrographs show that, during extrusion process, the glass fiber were well dispersed and there was no interaction between glass fiber and polypropylene (Figure 8.6)

Glass fiber surfaces are not smooth because of interaction between matrix and fiber for compatibilized compound (Figure 8.7). The coupling agents increase the strength of the interfacial bond between glass fiber and polypropylene.

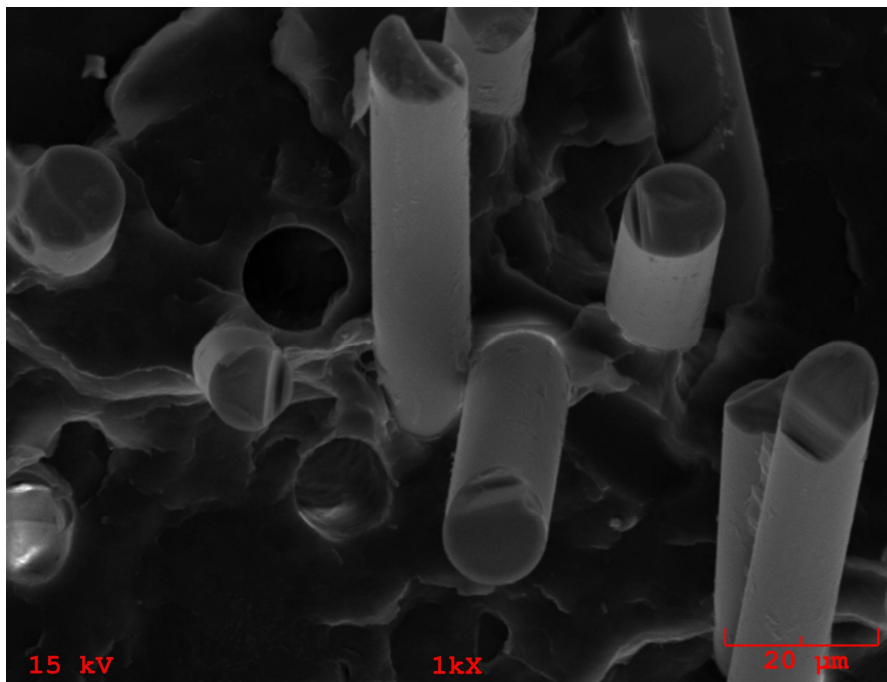


**Figure 8.6:** SEM micrograph of 30 % GFR-PP



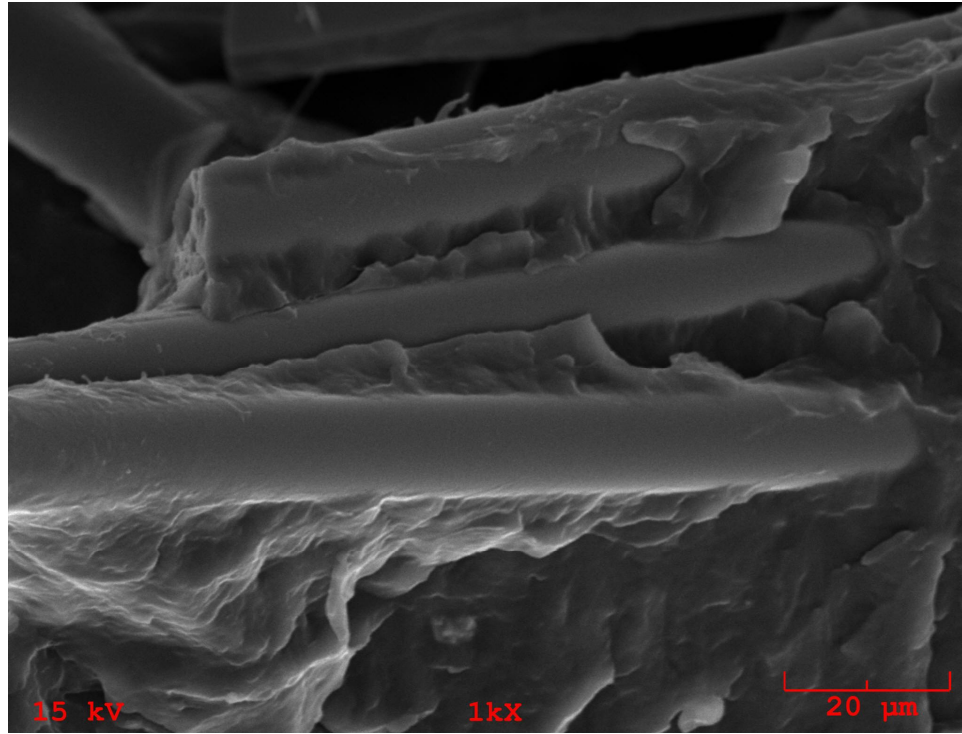


**Figure 8.7:** SEM micrograph of 2% Mah-g-PP + 30 % GFR-PP

### 8.2.5 Tensile properties

Measurement of tensile properties of composites was done as described in section 7.8. Normal and weld-line test specimens were used for tensile properties. Each test specimen results are given table 8.12 and 8.13

**Table 8.12:** Tensile properties of 30% GFR-PP according to % Mah-g-PP content (Normal Test Specimen)

Mah-g-PP	Tensile Stress		Strain at yield		E-Modul	
%	MPa	STD	%	STD	MPa	STD
0	68,37	0,19	2,62	0,03	5977	90,10
1	87,23	0,27	3,43	0,04	6760	116,95
2	87,93	0,30	3,50	0,03	6960	144,62
3	85,94	0,79	3,46	0,02	6762	109,14
4	85,56	0,38	3,40	0,03	6634	287,13
5	85,04	0,32	3,38	0,07	6356	286,66
6	84,03	0,23	3,37	0,03	6263	125,49

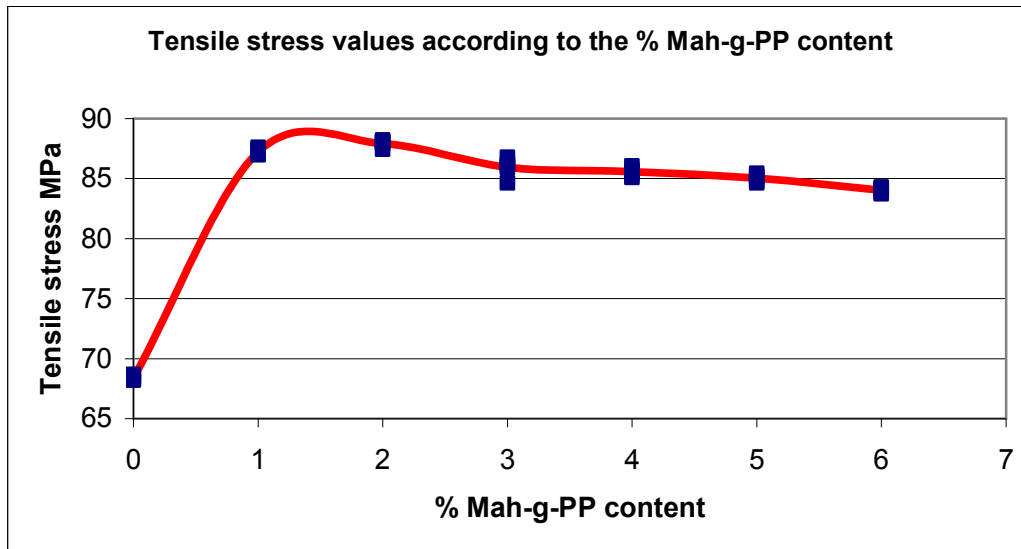


**Figure 8.8:** Tensile stress of 30% GFR-PP according to % Mah-g-PP content (Normal Test Specimen)

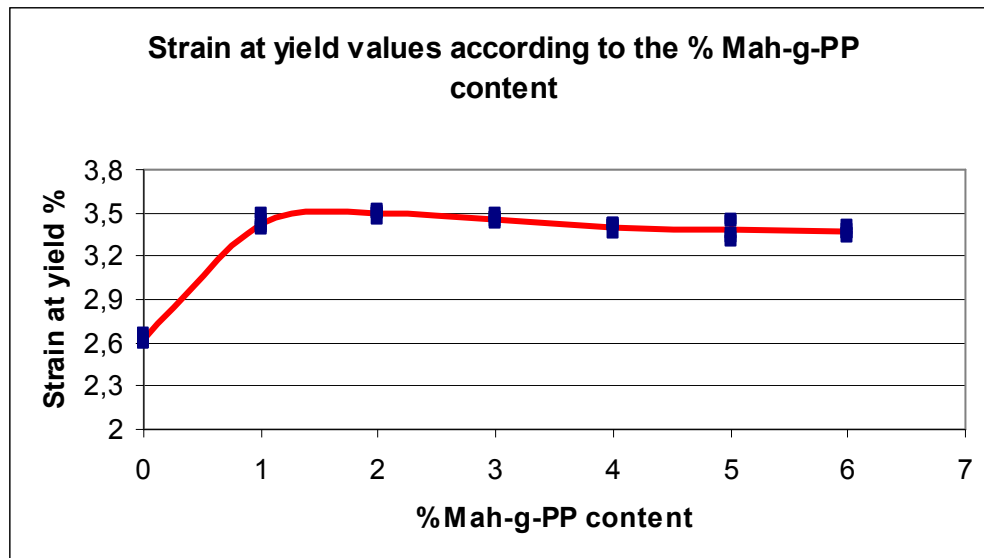


**Figure 8.9:** Strain at yield of 30% GFR-PP according to % Mah-g-PP content (Normal Test Specimen)

**Table 8.13:** Tensile properties of 30% GFR-PP according to % Mah-g-PP content (Weld line Test Specimen)

Mah-g-PP	Tensile Stress		Strain at yield		E-Modul	
%	MPa	STD	%	STD	MPa	STD
0	28,7	0,22	0,71	0,01	4669,04	87,79
1	36,15	0,37	0,92	0,02	4696,87	125,8
2	35,83	0,89	0,91	0,02	4768,06	231,14
3	35,77	0,23	0,94	0,01	4654,75	239,94
4	35,6	0,35	0,89	0,02	4803,07	150,26
5	34,83	0,19	0,9	0,01	4486,53	150,22
6	33,97	0,41	0,89	0,02	4471,51	208,41

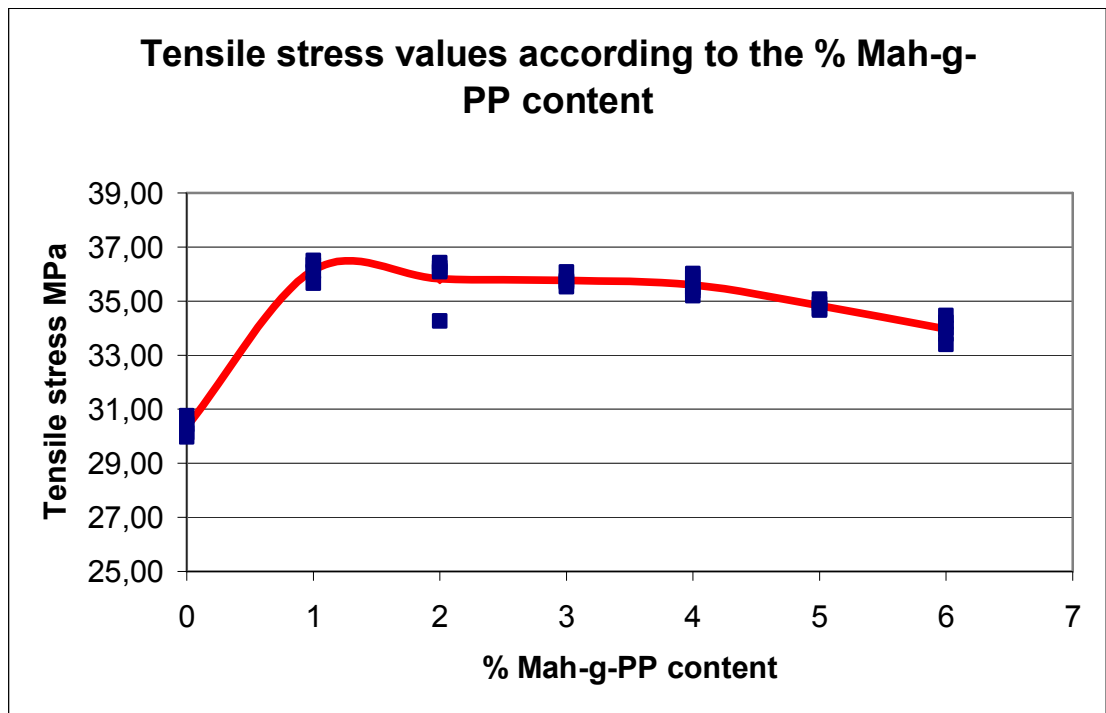


**Figure 8.10:** Tensile stress of 30% GFR-PP according to % Mah-g-PP content (Weld line Test Specimen)

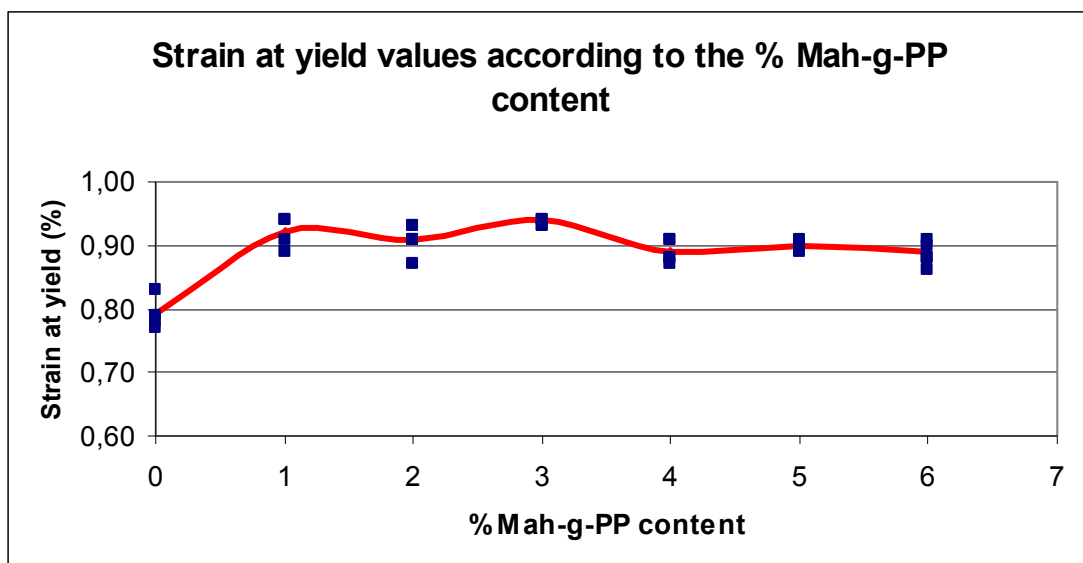


**Figure 8.11:** Strain at yield of 30% GFR-PP according to % Mah-g-PP content (Weld line Test Specimen)

Up to certain Mah-g-PP level (2%), increased Mah-g-PP concentrations caused increase in the tensile stress, E-Modul and strain. Addition of Mah-g-PP causes to increase filler matrix interaction by chemical or physical bond formation. Due to that chemical or physical interaction, applied force was transferred between those phases.

More than 2% Mah-g-PP loading tensile stress seems to be constant, while rapid increase in tensile stress was observed. The surface of reinforcement was thought to be coated with Mah-g-PP after certain level; excess Mah-g-PP could not coat the surface and act as a lubricant or plasticizer.

### 8.2.6 Flexural properties

In section 7.9 followed flexural test procedure is given and the test results are given Table 8.14. Up to certain Mah-g-PP level (2%), increased Mah-g-PP concentrations caused increase in the flexural stress, because, normally fiber pull away easily under flexural forces. However, fiber was stripped harder from matrix because of interaction between fiber and matrix with additon compatibilizer. It causes an increase on the flexrual properties until 2% level of Mah-g-PP. After this level, strength is decreased until 6% level of Mah-g-PP. After 2% level of Mah-g-PP could not coat the surface and act as a lubricant or plasticizer.

**Table 8.14:** Flexural properties of 30% GFR-PP according to % Mah-g-PP content

Mah-g-PP	Stress		Displacement		E-Modul	
%	MPa	STD	mm	STD	MPa	STD
0	74,730	0,600	4,300	0,090	4669	115,36
1	118,117	0,563	6,639	0,098	5030	33,033
2	119,924	0,975	6,476	0,158	5064	40,807
3	118,464	0,370	6,257	0,158	5036	32,500
4	117,862	0,200	6,364	0,112	5017	59,914
5	116,999	0,652	6,088	0,118	5002	145,125
6	114,025	1,222	6,115	0,252	4965	142,884

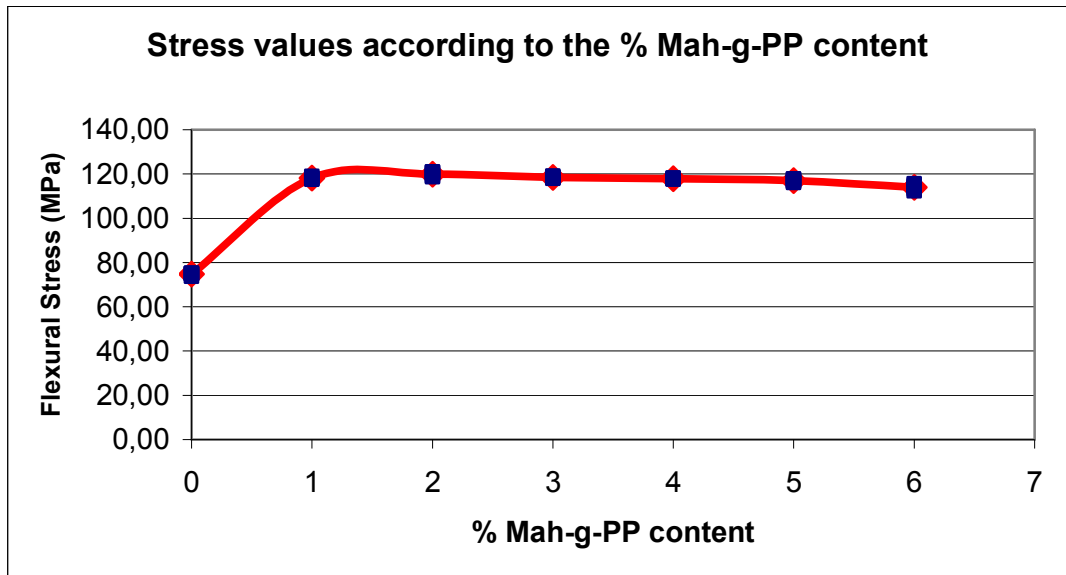


**Figure 8.12:** Flexural stress values of 30% GFR-PP according to % Mah-g-PP content

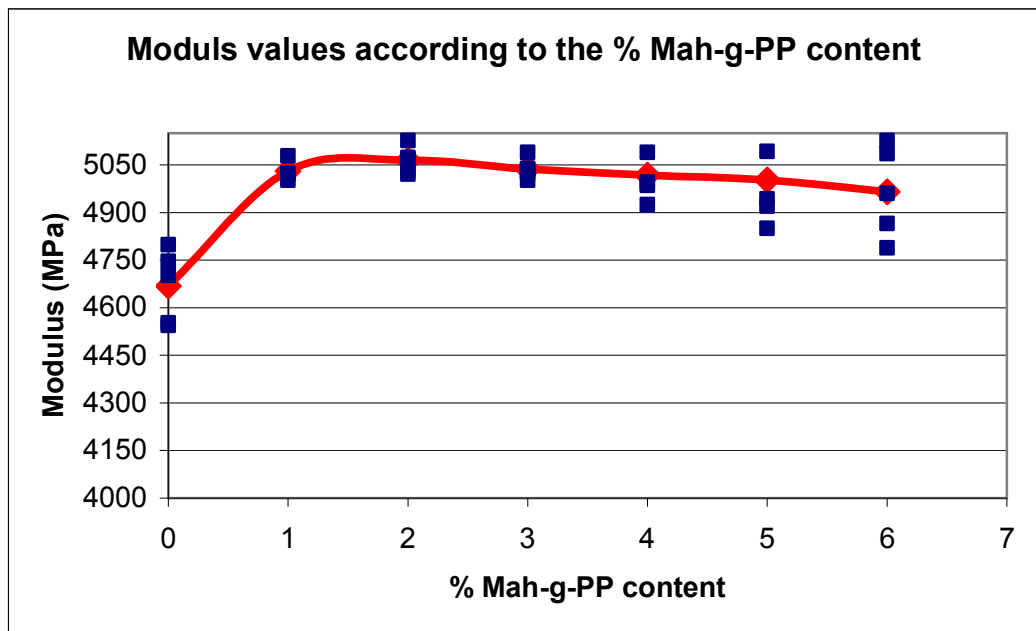


**Figure 8.13:** Flexural modulus values of 30% GFR-PP according to % Mah-g-PP content

### 8.2.7 Impact properties

Izod notched impact test applied according to the procedure explained in section 7.11 and test results are given in Table 8.15

**Table 8.15:** Notched Izod impact properties of 30% GFR-PP according to % Mah-g-PP content

% Mah-g-PP	0	1	2	3	4	5	6
	Impact						
	$\text{kJ/m}^2$	$\text{kJ/m}^2$	$\text{kJ/m}^2$	$\text{kJ/m}^2$	$\text{kJ/m}^2$	$\text{kJ/m}^2$	$\text{kJ/m}^2$
	6,21	9,85	10,93	10,61	10,64	9,50	9,39
	6,12	10,03	9,84	10,60	10,40	9,62	10,60
	5,87	10,23	11,65	10,35	9,97	9,61	9,57
	6,04	10,71	9,95	10,39	10,00	9,41	9,79
	5,82	11,29	10,21	10,12	10,53	10,49	9,86
	5,90	10,01	10,89	10,61	9,97	10,45	9,54
	5,87	10,03	10,93	10,60	10,55	10,30	9,58
	6,64	10,23	9,84	10,35	10,37	10,06	9,91
	6,13	10,71	11,65	10,39	10,15	9,63	9,94
	6,32	10,01	9,95	10,12	10,27	10,07	9,63
Avr.	6,63	10,31	10,58	10,42	10,29	9,91	9,78
Max.	7,73	11,29	11,65	10,61	10,64	10,49	10,60
Min.	6,23	9,85	9,84	10,12	9,97	9,41	9,39
SD	0,49	0,45	0,72	0,19	0,25	0,41	0,34

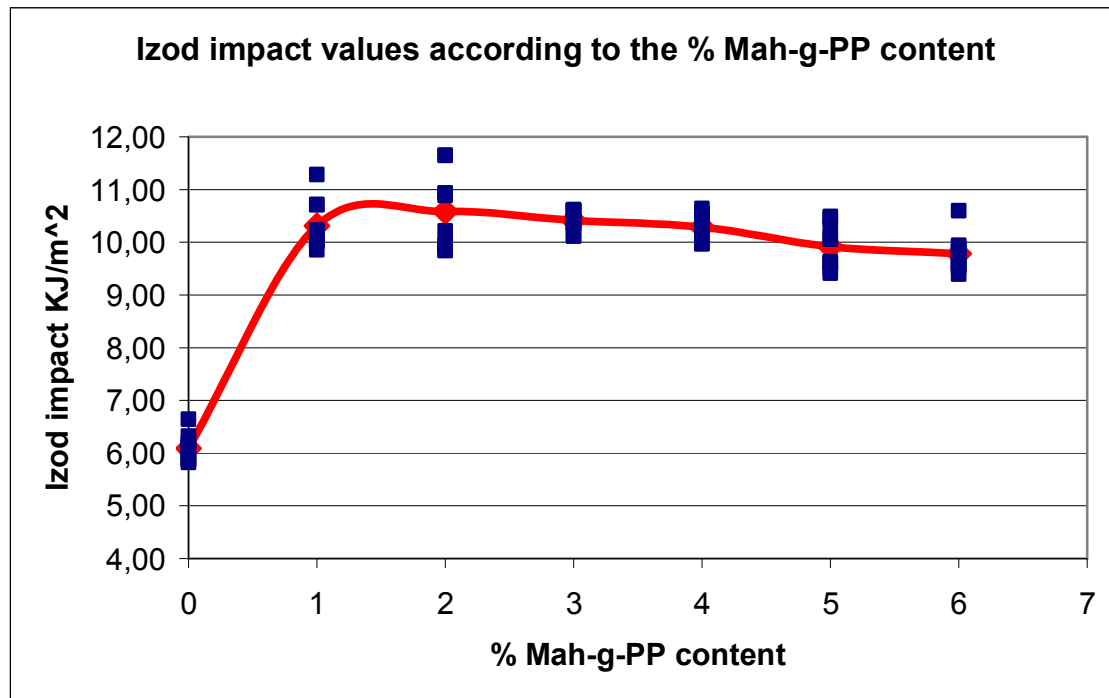


**Figure 8.14:** Notched Izod impact properties of 30% GFR-PP according to % Mah-g-PP content

The impact properties of the polymeric materials are directly related to the overall toughness of the material. Most polymers when subjected to the impact loading seem to undergo fracture. The impact failure mechanism of the glass-reinforced PP increases with addition of glass fiber. This is because glass fibers have a higher capacity to absorb energy, and it results in less fiber breakage and a higher residual strength to the composite. Coupling agents further increase the impact strength because they make the strong interfacial bonds, which have the higher ability to absorb energy.

Increase of impact strength up to 2% Mah-g-PP supported that increase in bond formation and restriction of chain mobility. Above 2% Mah-g-PP concentration, impact strength was decreasing because of above 2% level of Mah-g-PP could not coat the surface and act as a lubricant or plasticizer.

#### 8.2.8 Heat deflection temperature - Vicat softening temperature

The Vicat and HDT test results of glass fiber reinforced PP according to the Mah-g-PP concentrations are given in Table 8.16 and 8.17. The coupling agent further enhances the HDT because the adhesion between polypropylene and glass fiber increases. As shown in Figure 8.16 and 8.17 Vicat softening temperature was not affected very much. Only vicat (B) temperature was increased slightly with the presence of coupling agent.

**Table 8.16:** Heat deflection temperature (A) of 30% GFR-PP according to % Mah-g-PP content

% Mah-g-PP	HDT A (C°) (1,8MPa)						
	0	1	2	3	4	5	6
	140,10	143,40	143,90	143,70	142,20	144,00	141,10
	133,60	141,00	142,10	141,90	139,70	138,50	137,70
Avr.	136,85	142,20	143,00	142,80	140,95	141,25	139,40
Max.	140,10	143,40	143,90	143,70	142,20	144,00	141,10
Min.	133,60	141,00	142,10	141,90	139,70	138,50	137,70
SD	4,60	1,70	1,27	1,27	1,77	3,89	2,40

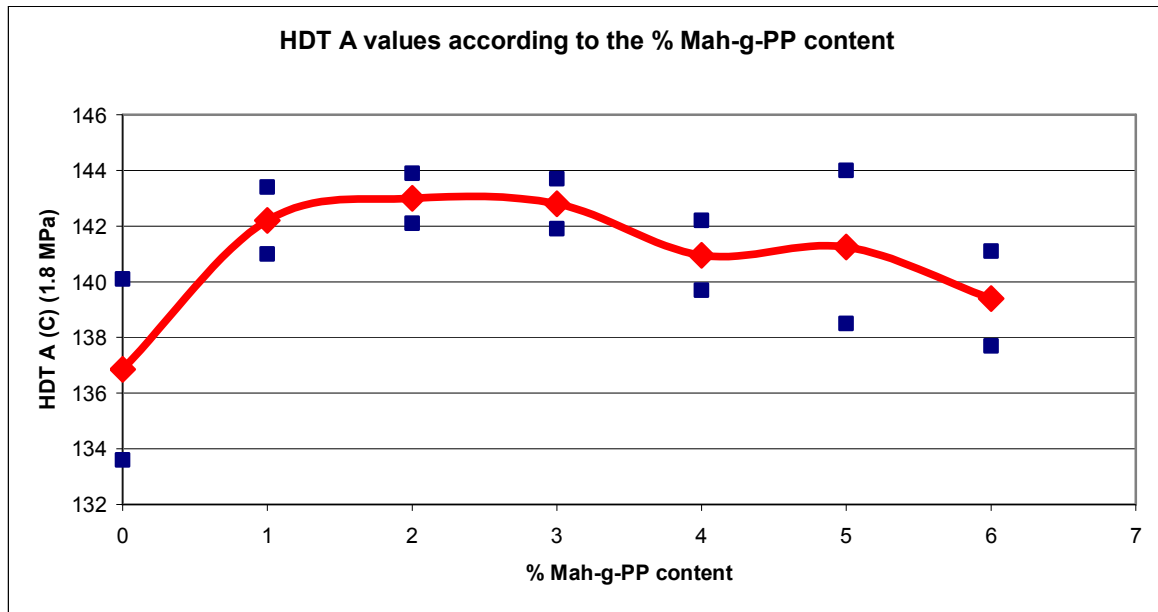


**Figure 8.15:** Heat deflection temperature (A) of 30% GFR-PP according to % Mah-g-PP content

**Table 8.17:** Heat deflection temperature (B) of 30% GFR-PP according to % Mah-g-PP content

% Mah-g-PP	HDT B (C°) (0,45MPa)						
	0	1	2	3	4	5	6
	140,00	158,60	159,90	159,60	160,30	158,90	159,20
	138,10	156,20	157,00	156,80	158,30	154,50	155,30
Avr.	139,05	157,40	158,45	158,20	159,30	156,70	157,25
Max.	140,00	158,60	159,90	159,60	160,30	158,90	159,20
Min.	138,10	156,20	157,00	156,80	158,30	154,50	155,30
SD	1,34	1,70	2,05	1,98	1,41	3,11	2,76



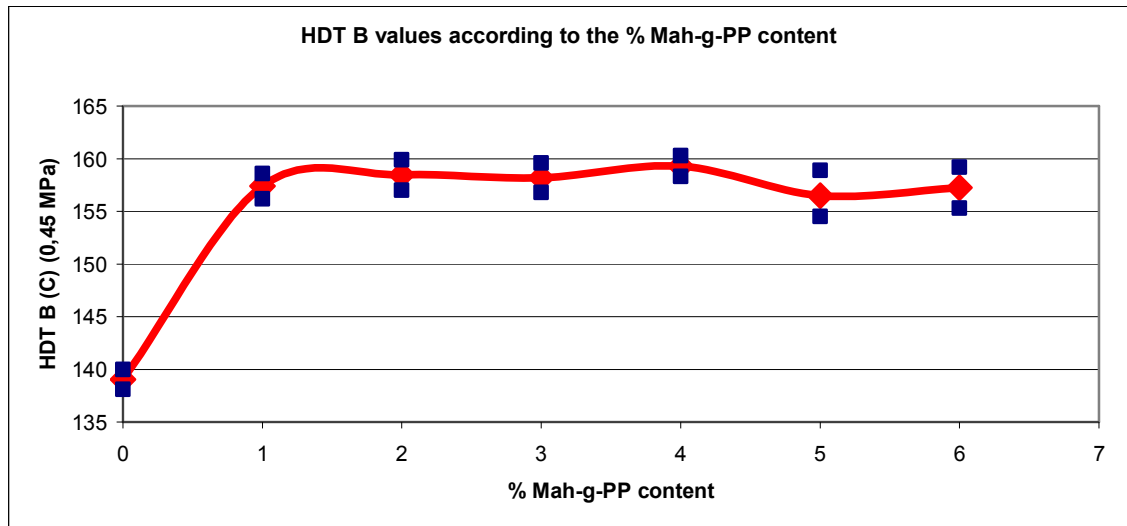


**Figure 8.16:** Heat deflection temperature (B) of 30% GFR-PP according to % Mah-g-PP content

**Table 8.18:** Vicat softening temperature (A) of 30% GFR-PP according to % Mah-g-PP content

% Mah-g-PP	Vicat A (C°) (10N)						
	0	1	2	3	4	5	6
	165,60	166,50	164,50	163,90	166,60	165,60	166,30
	166,50	166,50	164,20	164,90	167,30	165,70	167,20
Avr.	166,05	166,50	164,35	164,40	166,95	165,65	166,75
Max.	166,50	166,50	164,50	164,90	167,30	165,70	167,20
Min.	165,60	166,50	164,20	163,90	166,60	165,60	166,30
SD	0,64	0,00	0,21	0,71	0,49	0,07	0,64

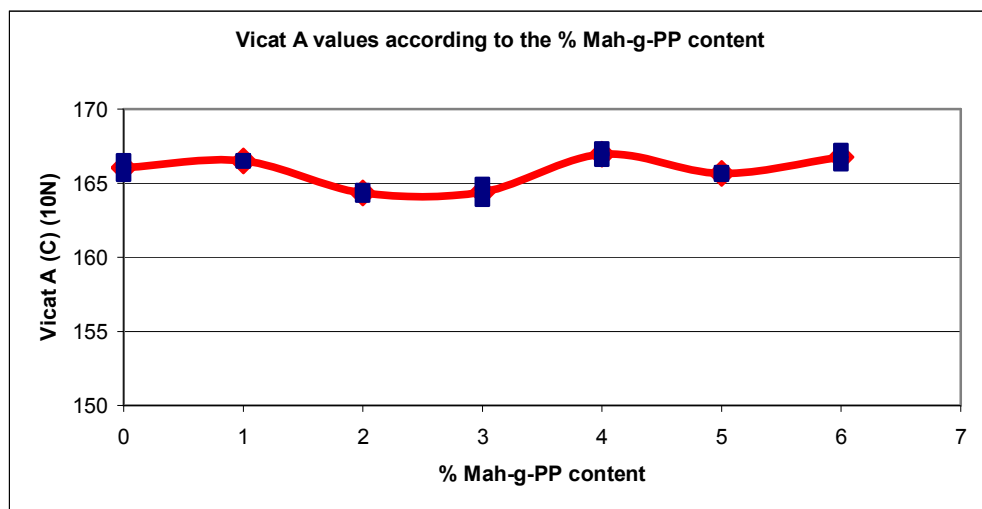


**Figure 8.17:** Vicat softening temperature (A) of 30% GFR-PP according to % Mah-g-PP content

**Table 8.19:** Vicat softening temperature (B) of 30% GFR-PP according to % Mah-g-PP content

% Mah-g-PP	Vicat B (C°) (50N)						
	0	1	2	3	4	5	6
	130,50	136,80	135,30	138,10	138,30	138,10	144,10
	136,30	143,50	142,60	139,40	142,00	138,90	140,20
Avr.	133,40	140,15	138,95	138,75	140,15	138,50	142,15
Max.	136,30	143,50	142,60	139,40	142,00	138,90	144,10
Min.	130,50	136,80	135,30	138,10	138,30	138,10	140,20
SD	4,10	4,74	5,16	0,92	2,62	0,57	2,76

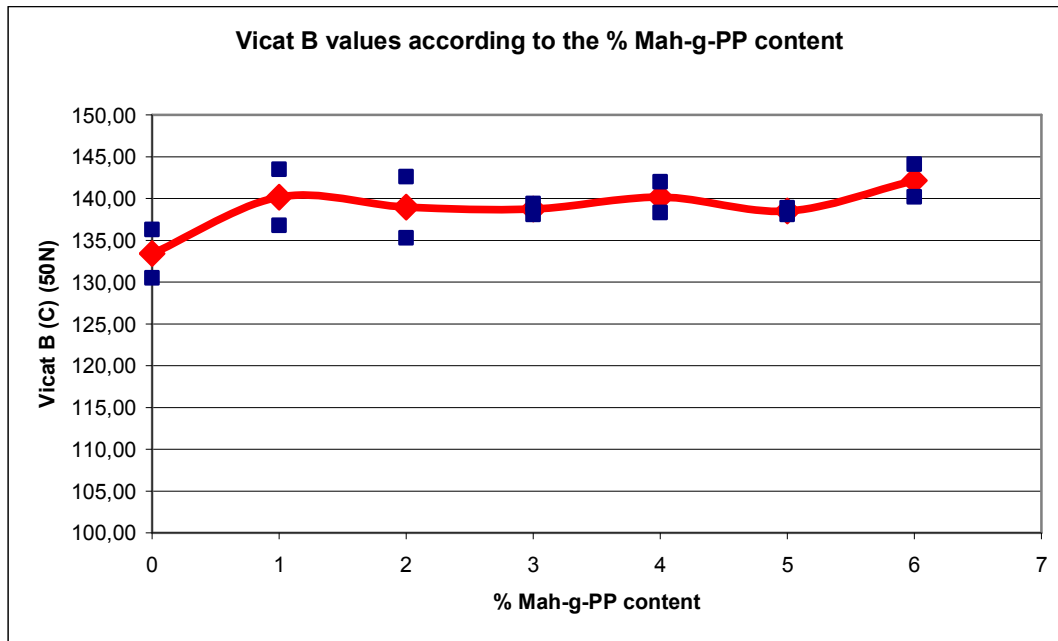


**Figure 8.18:** Vicat softening temperature (B) of 30% GFR-PP according to % Mah-g-PP content

### 8.3 The Effect of Plastomer Additon on 2% Mah-g-PP Compatibilized GFR-PP Composite

2% Mah-g-PP compatibilized 30% GFR-PP with the best mechanical properties was found in the previous section.

The purpose of the second section is 2% Mah-g-PP compatibilized 30% GFR polypropylene by the addition of different ratios plastomer to increase the toughness of the material. Compound formulations are given table 7.5.

### 8.3.1 Measurement of density

Measurement of density was done as described in section 7.4. Plastomer show slightly increasing effect on the specific gravity. Test results are given in Table 8.20.

**Table 8.20:** Density of 2% Mah-g-PP compatibilized GFR-PP according to % plastomer content

Plastomer	Density	Avr. Density
%	g/cm <sup>3</sup>	g/cm <sup>3</sup>
0	1,089	1,090
	1,090	
	1,091	
2	1,116	1,114
	1,113	
	1,114	
4	1,121	1,118
	1,115	
	1,118	
6	1,120	1,116
	1,112	
	1,116	
8	1,117	1,118
	1,119	
	1,118	
10	1,118	1,118
	1,117	
	1,118	

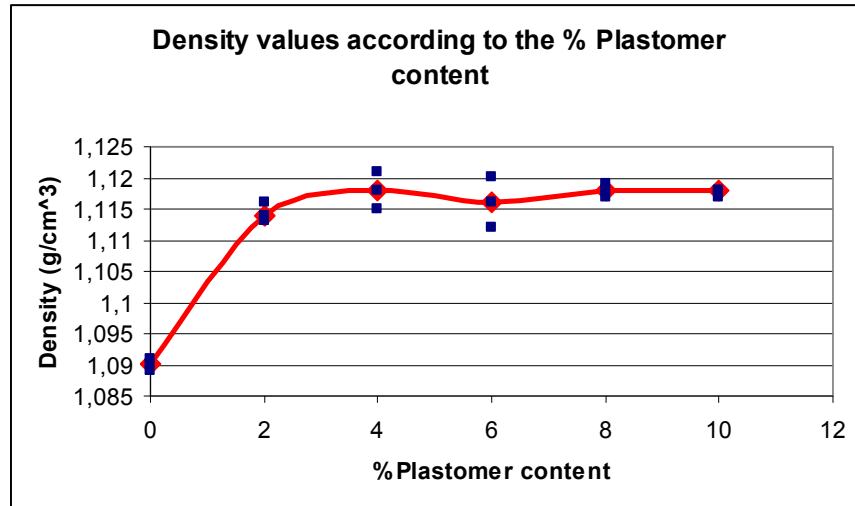


**Figure 8.20:** Density values of 2% Mah-g-PP compatibilized GFR-PP according to % plastomer content

### 8.3.2 Determination of melt flow index

Determination of MFI test was done as described in section 7.6. Melt flow index test results of neat PP and glass fiber reinforced PP are given in the Table 8.21. The plastomer resins have low melt index (i.e., high molecular weight), which provides melt strength in the compound as is seen in Figure 8.21.

**Table 8.21:** MFI values of 2% Mah-g-PP compatibilized GFR-PP according to % plastomer content

Plastomer	MFI	Avr. MFI
%	g/10'	g/10'
0	16,90	16,927
	16,96	
	16,92	
2	17,26	17,100
	16,98	
	17,06	
4	16,76	16,607
	16,48	
	16,58	
6	14,84	15,107
	15,24	
	15,24	
8	15,00	15,053
	15,12	
	15,04	
10	14,80	14,867
	14,80	
	15,00	

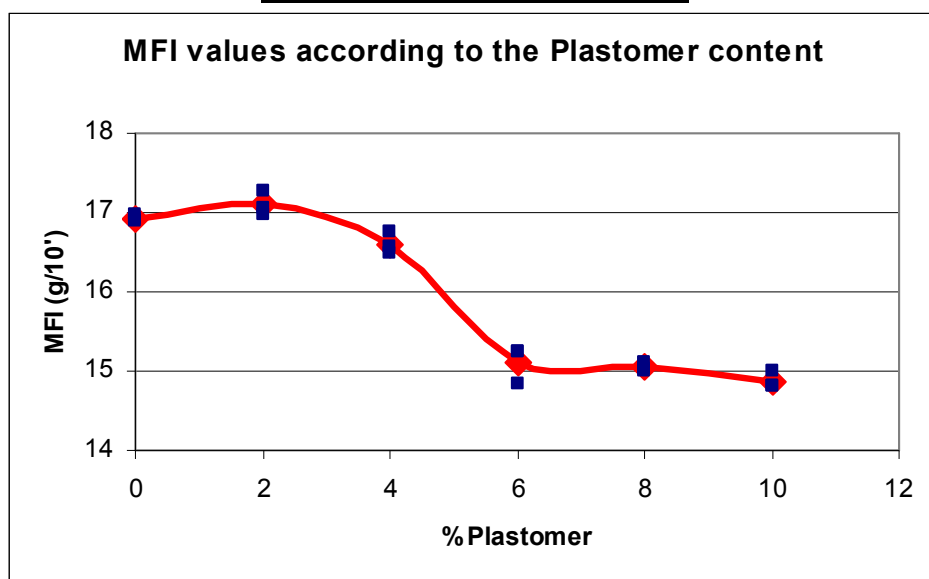


**Figure 8.21:** MFI values of 2% Mah-g-PP compatibilized GFR-PP according to % plastomer content

### 8.3.3 Determination of ash content

The test samples taken during extrusion process (at the beginning, in the middle and at the end) were used to determine ash content and test was done as explained in section 7.5. Test results are given in Table 8.22. Ash content measurement results show that extrusion process was done.

**Table 8.22:** Ash content measurements of composites in terms of % plastomer in 2% Mah-g-PP compatibilized 30% GFR-PP

Plastomer	% Ash	Avr. % Ash
%	%	%
0	30,317	30,332
	31,214	
	29,464	
2	30,898	29,408
	28,725	
	28,600	
4	29,971	29,899
	30,056	
	29,670	
6	29,496	29,531
	29,956	
	29,141	
8	29,585	29,289
	29,735	
	28,548	
10	29,314	29,817
	30,001	
	30,135	

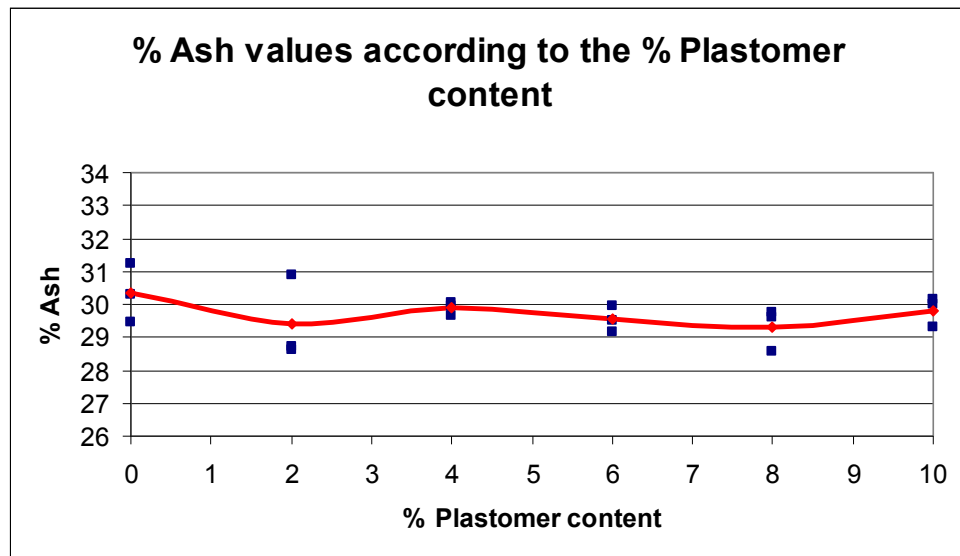


**Figure 8.22:** % Ash content measurements of composites in terms of % plastomer in 2% Mah-g-PP compatibilized 30% GFR-PP

### 8.3.4 Morphology investigation

Investigation of morphology was done as described in section 7.7. SEM micrographs show that, during extrusion process, the glass fiber particles were well dispersed. Glass fiber surfaces are not smooth because of interaction between matrix and fiber for compatibilized compound. The coupling agents increase the strength of the interfacial bond between glass fiber and polypropylene. Plastomeric phase images can't be selected because of completely mixed with polypropylene.

SEM micrographs are given Figure 8.23 – 8.28

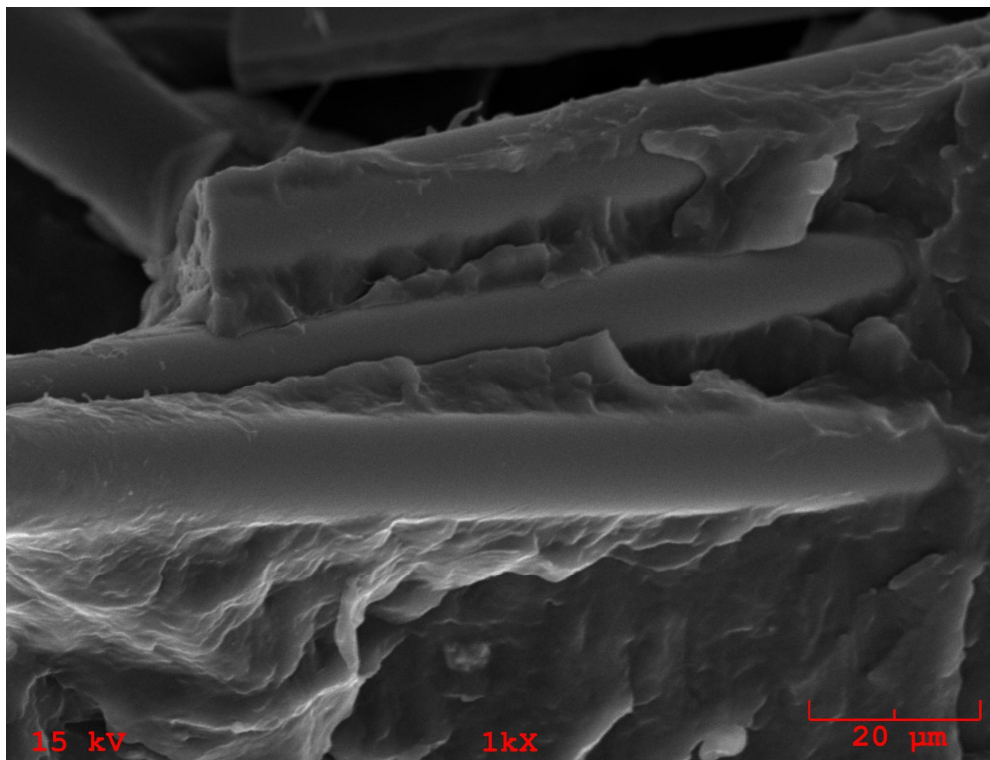


**Figure 8.23:** SEM micrograph of 2% Mah-g-PP compatibilized 30% GFR-PP

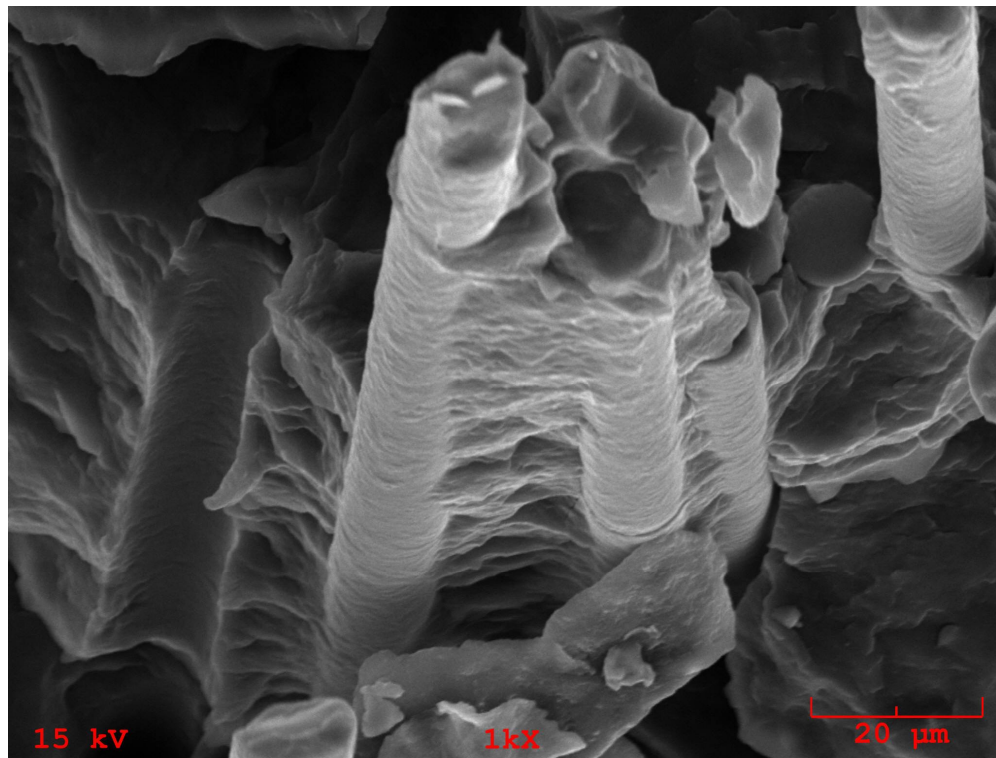


**Figure 8.24:** SEM micrograph of 2% plastomer + 2% Mah-g-PP compatibilized 30% GFR-PP

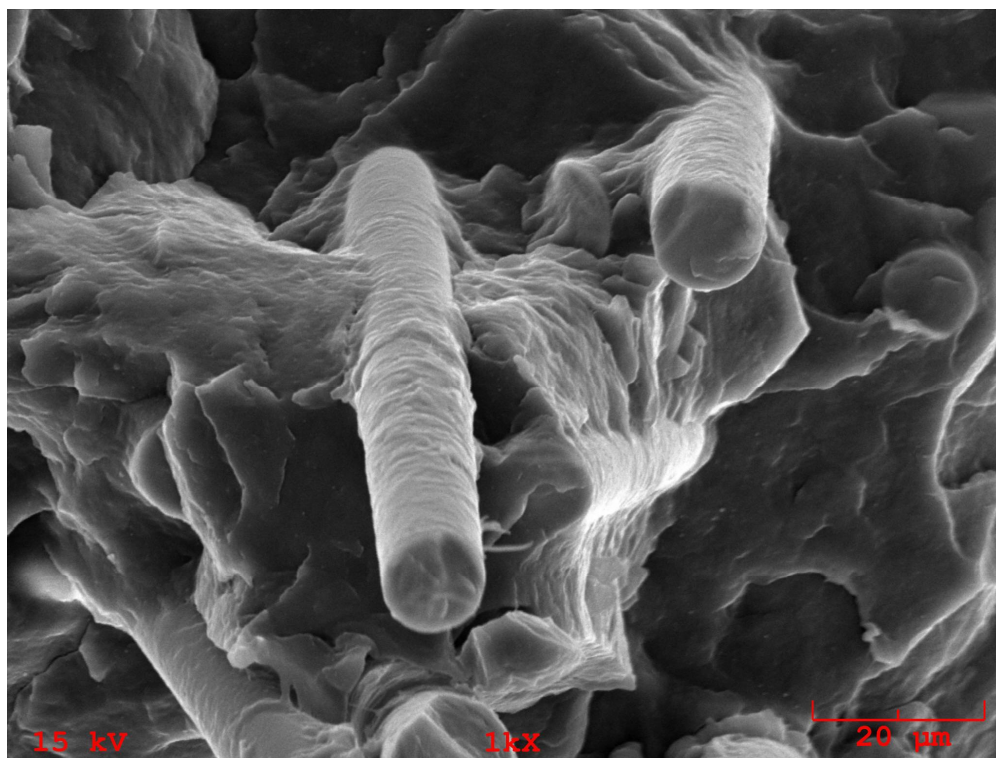


**Figure 8.25:** SEM micrograph of 4% plastomer + 2% Mah-g-PP compatibilized 30% GFR-PP



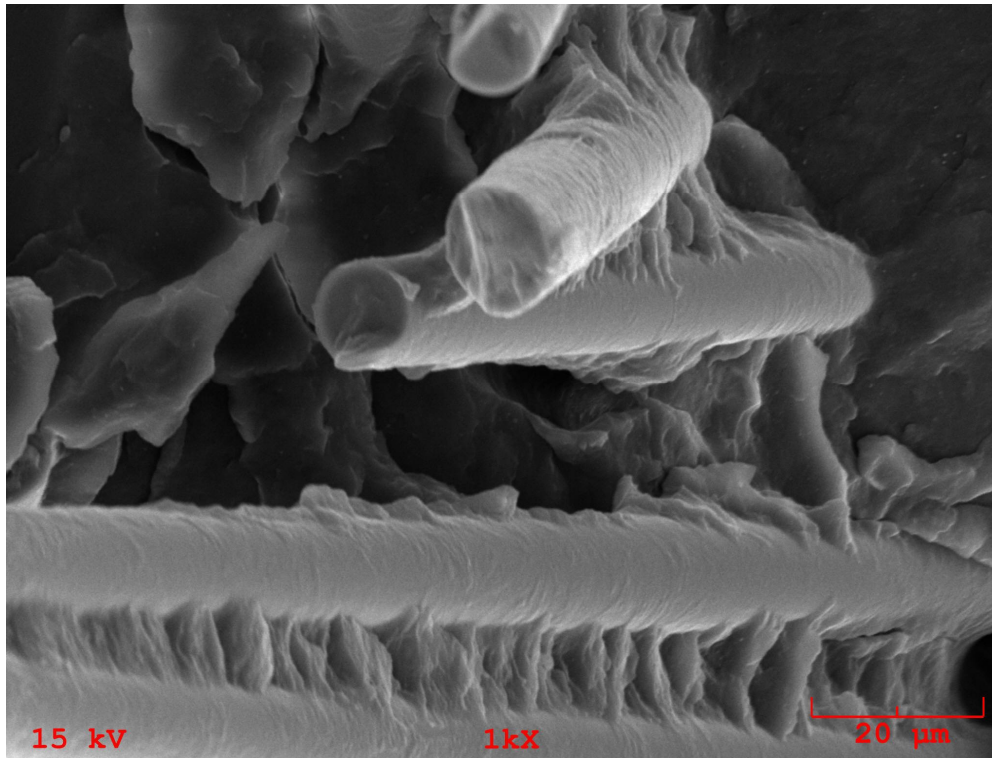


**Figure 8.26:** SEM micrograph of 6% plastomer + 2% Mah-g-PP compatibilized 30% GFR-PP

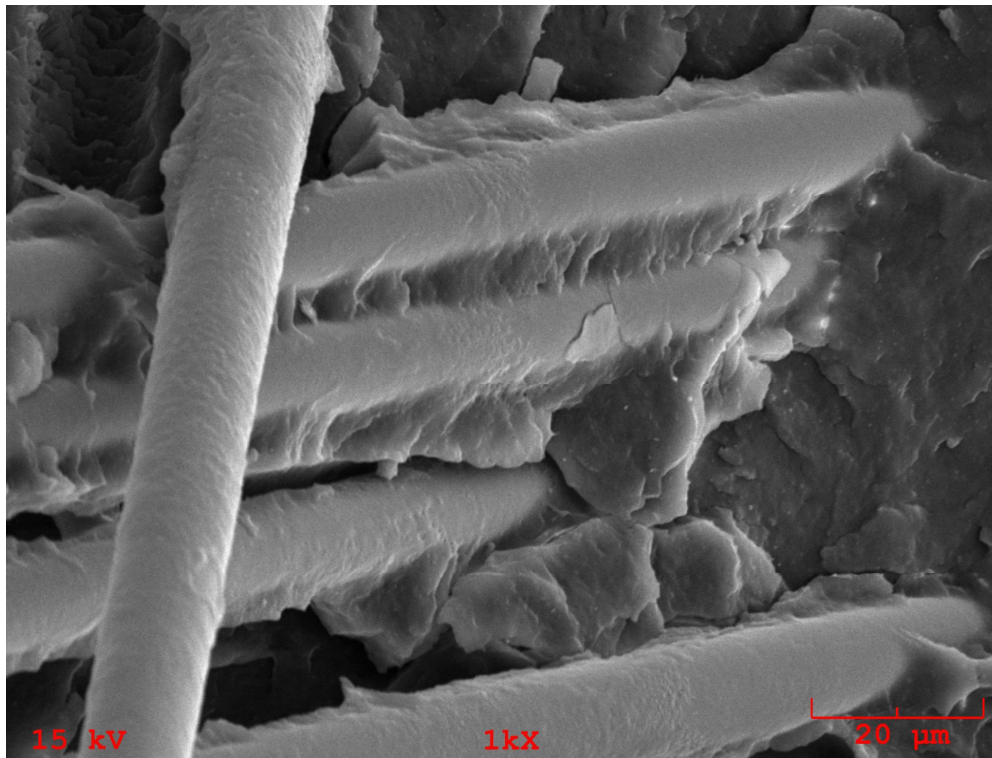


**Figure 8.27:** SEM micrograph of 8% plastomer + 2% Mah-g-PP compatibilized 30% GFR-PP



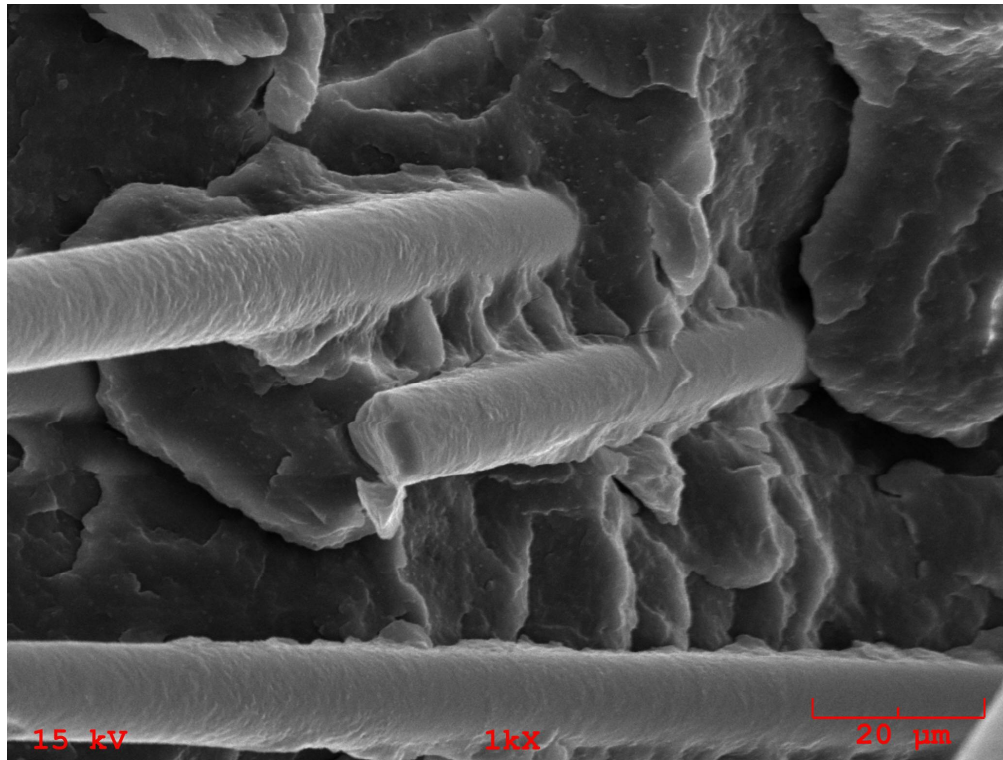


**Figure 8.28:** SEM micrograph of 10% plastomer + 2% Mah-g-PP compatibilized 30% GFR-PP

Generally, glass fibers are broken during processing because of the screw and cutters. This means fiber size is reduced after processing. Strength of the material decreases with the reduced in fiber size (explain in Section 3). After injection process, material has been kept in oven 3 hours at 600 °C to remove polymer. The length and diameter distribution of fibers was determined with SEM micrograph after extrusion and injection process as shown in Figure 8.29 and 8.30. Fiber length and diameter before process are given Figure 7.2.

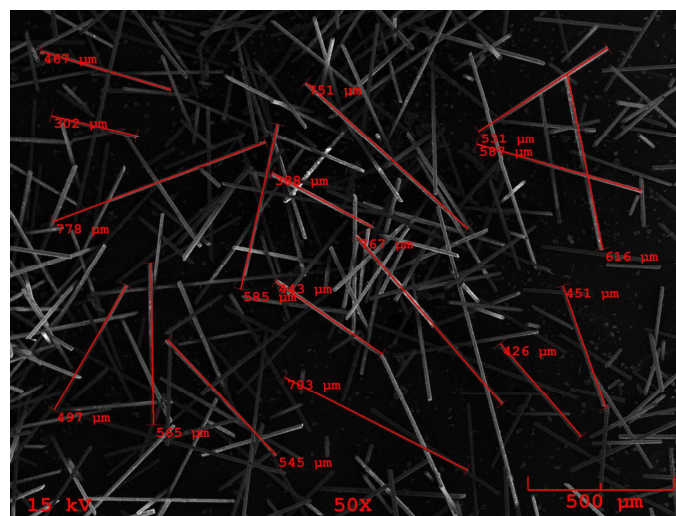


**Figure 8.29:** Lengths of some selected fibers

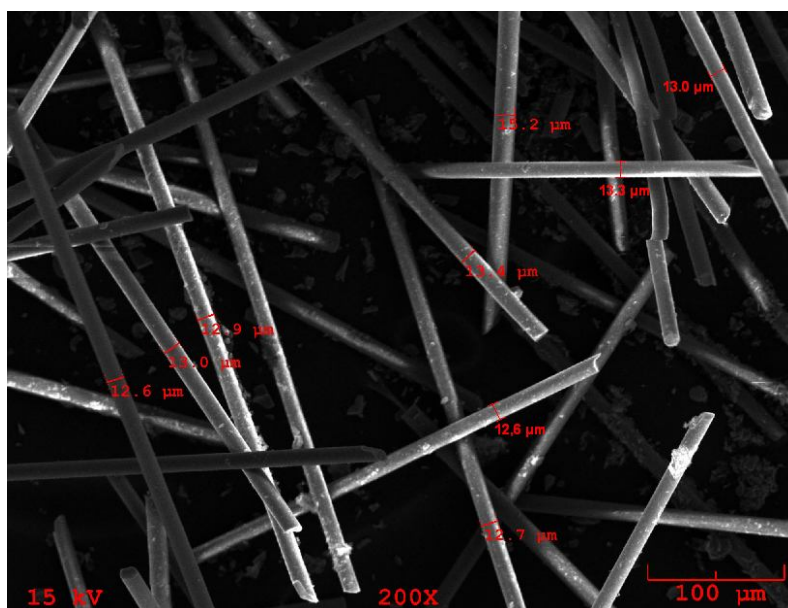


**Figure 8.30:** Diameters of some selected fibers

**Table 8.23:** Lengths of some selected fibers

Selected fiber	micron meter
1	467
2	302
3	751
4	531
5	587
6	388
7	778
8	767
9	616
10	451
11	443
12	585
13	426
14	703
15	497
16	565
17	545
Average	553
Min.	302
Max.	778
STD	137,92

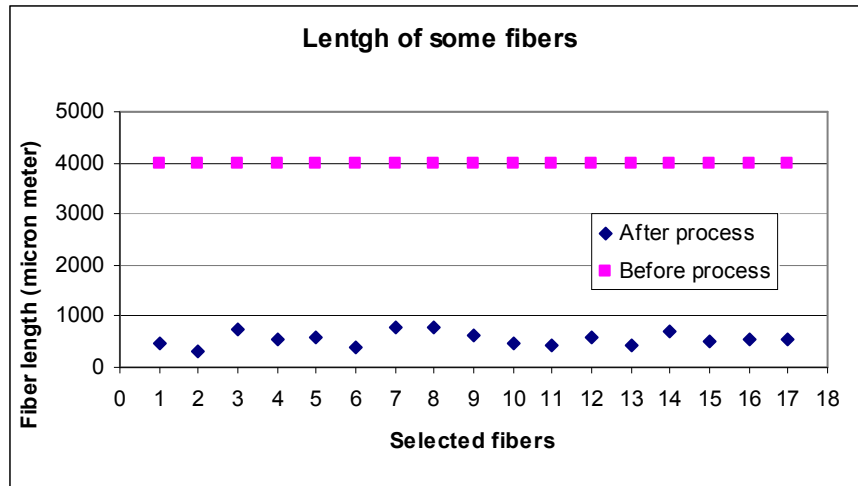


**Figure 8.31:** Lengths of some selected fibers

**Table 8.24:** Diameters of some selected fibers

Selected fiber	micron meter
1	13,00
2	15,20
3	13,30
4	13,40
5	12,60
6	12,70
7	12,90
8	13,00
9	12,60
Average	13,19
Min.	12,60
Max.	15,20
STD	0,81

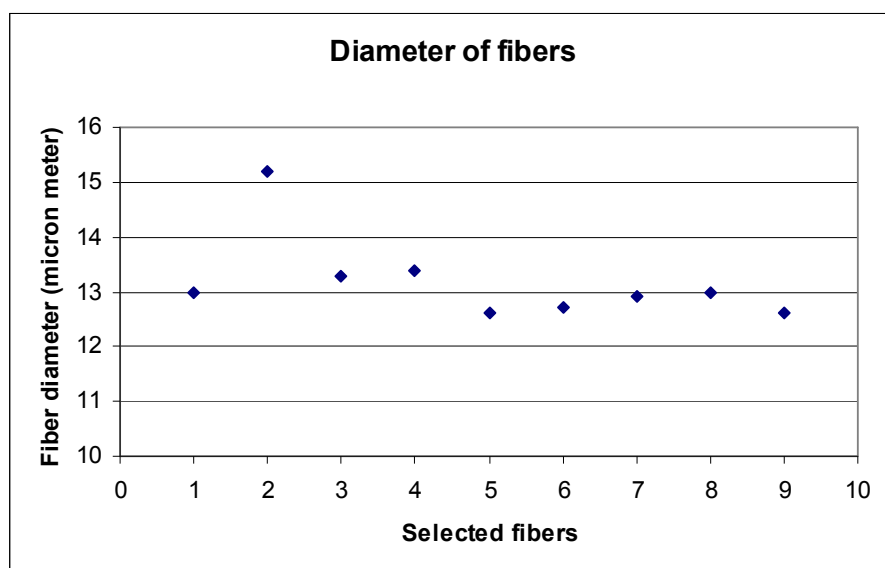


**Figure 8.32:** Diameters of some selected fibers

After measurement of fiber length, 86 % reduction in average fiber length was observed.

### 8.3.5 Tensile properties

Measurement of tensile properties of composites was done as described in section 7.8. Normal and weld-line test specimens are used for tensile properties. Each test specimen results are given table 8.25 and 8.26. Tensile yield strength also decreased linearly with increasing elastomer content.

The relationship between yield strength and elongation is given in the Hooke's rule (eq. 8.1).

$$\sigma_y = \varepsilon_y \cdot E \quad (8.1)$$

Due to Hooke's rule, yield elongation increases with the decrease yield strength. Strain at yield values increased linearly with the increasing elastomer content. Strain at yield was not affected with the addition of elastomer effectively for weld line test specimen.

**Table 8.25:** Tensile properties of 2% Mah-g-PP + 30% GFR-PP according to elastomer content (Normal test specimen)

Elastomer %	Tensile Stress		Strain at yield		E-Modul	
	MPa	STD	%	STD	MPa	STD
0	87,93	0,30	3,50	0,03	6960	144,62
2	82,74	0,39	3,52	0,03	6543	159,80
4	80,95	0,39	3,69	0,07	6296	117,37
6	79,32	0,53	3,86	0,08	6318	99,53
8	79,08	0,30	4,00	0,06	6206	113,88
10	77,03	0,20	4,27	0,06	5992	150,18

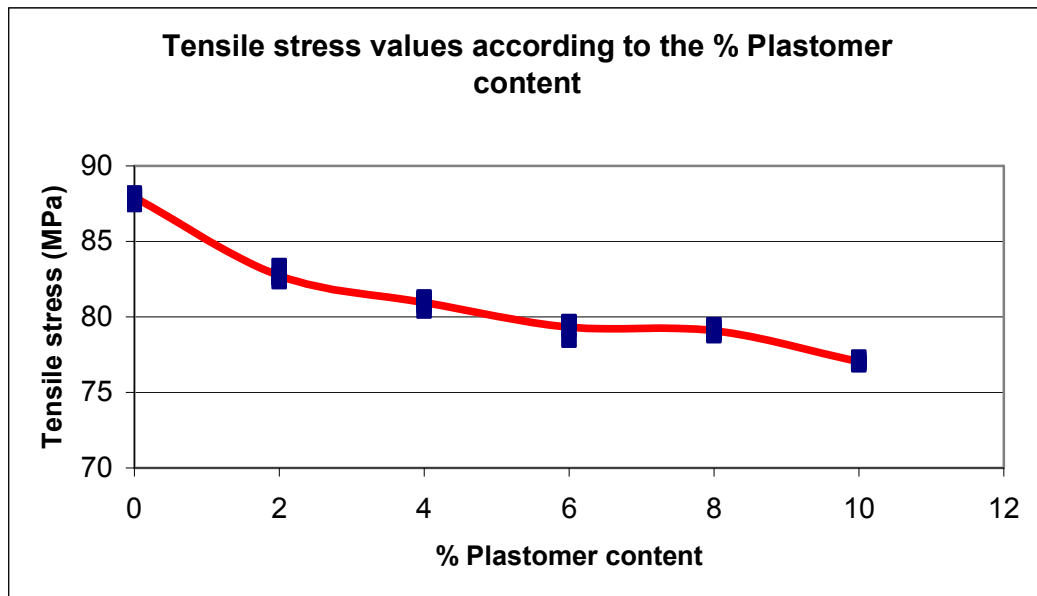


**Figure 8.33:** Tensile stress properties of 2% Mah-g-PP + 30% GFR-PP according to plastomer content (Normal test specimen)

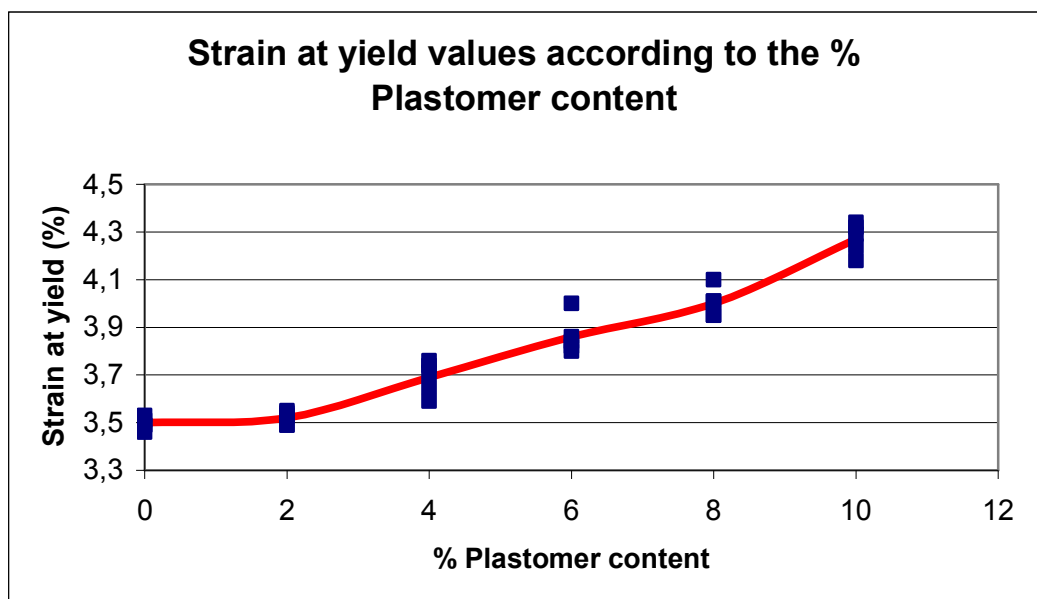


**Figure 8.34:** Strain values of 2% Mah-g-PP + 30% GFR-PP according to plastomer content (Normal test specimen)

**Table 8.26:** Tensile properties of 2% Mah-g-PP + 30% GFR-PP according to plastomer content (Weld line test specimen)

Plastomer %	Tensile Stress		Strain at yield		E-Modul	
	MPa	STD	%	STD	MPa	STD
0	35,83	0,89	0,91	0,02	4768	231,14
2	34,13	0,48	0,92	0,02	4845	97,75
4	33,03	0,31	0,92	0,01	4743	115,25
6	32,97	0,32	0,92	0,01	4591	111,31
8	31,46	0,45	0,88	0,01	4449	136,17
10	30,10	0,18	0,86	0,02	4274	69,28

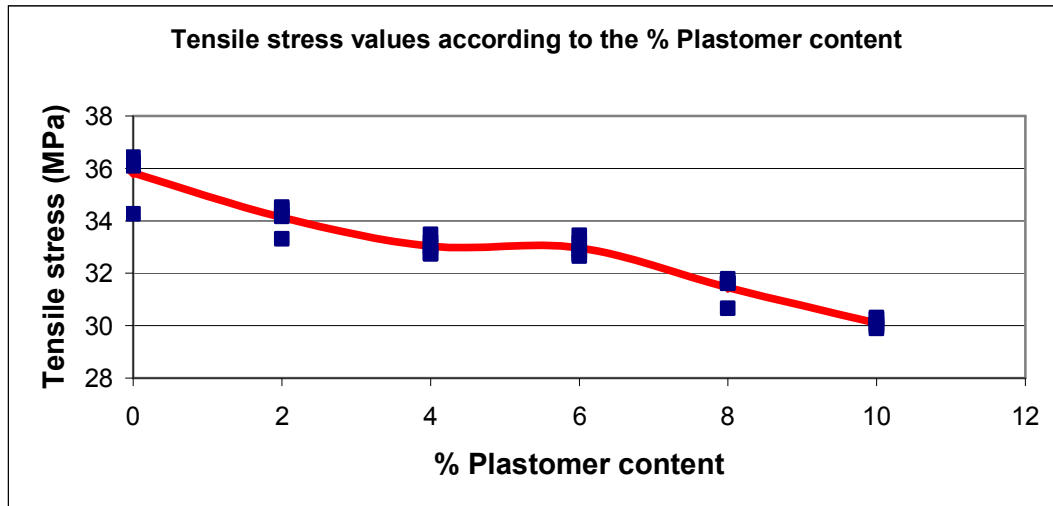


**Figure 8.35:** Tensile stress of 2% Mah-g-PP + 30% GFR-PP according to plastomer content (Weld line test specimen)

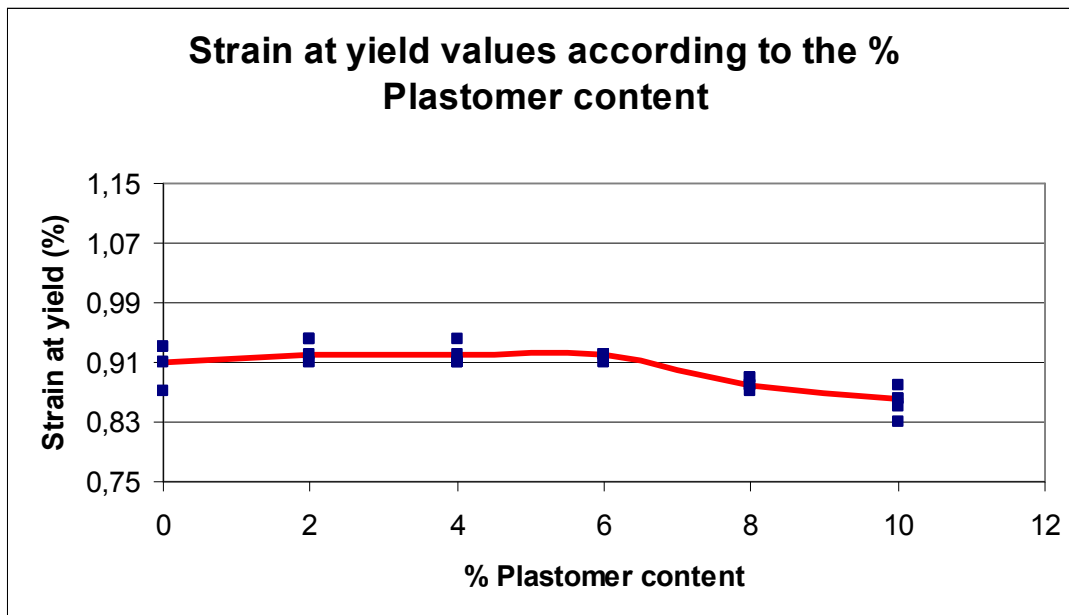


**Figure 8.36:** Strain values of 2% Mah-g-PP + 30% GFR-PP according to plastomer content (Weld line test specimen)

### 8.3.6 Flexural properties

In section 7.9 followed flexural test procedure is given and the test results are in Table 8.26. Figure 8.37 and 8.38 shows the plot of the flexural stress and modulus as a function of the plastomer concentration in the 2% Mah-g-PP compatibilized 30% GFR-PP. As seen from the plot, for all blends, the modulus and stress values decreased linearly with increasing plastomer content. Flexural modulus, like tensile modulus, is a function of the rigidity of the matrix and stiffness and size of the domains. Plastomer has a higher modulus compared to the 2% Mah-g-PP compatibilized GFR Polypropylene. The longer side chain in the ethylene octane polymer made the blend more flexible compared to the shorter side chain. As the rubber content increased, the rubber may have become larger in size and distributed the crystallinity and, hence, the resultant blend become more flexible so that the flexural modulus and stress decreased.

**Table 8.27:** Flexural values of 2% Mah-g-PP + 30% GFR-PP according to plastomer content

Plastomer %	Stress		Displacement		E-Modul	
	MPa	STD	mm	STD	MPa	STD
0	119,92	0,975	6,476	0,158	5065	40,80
2	114,25	0,247	7,158	0,199	4694	20,76
4	113,83	2,168	6,810	0,197	4710	49,51
6	110,39	0,963	7,199	0,200	4620	54,27
8	108,49	0,754	7,598	0,185	4497	26,16
10	105,48	0,964	8,196	0,160	4373	59,77

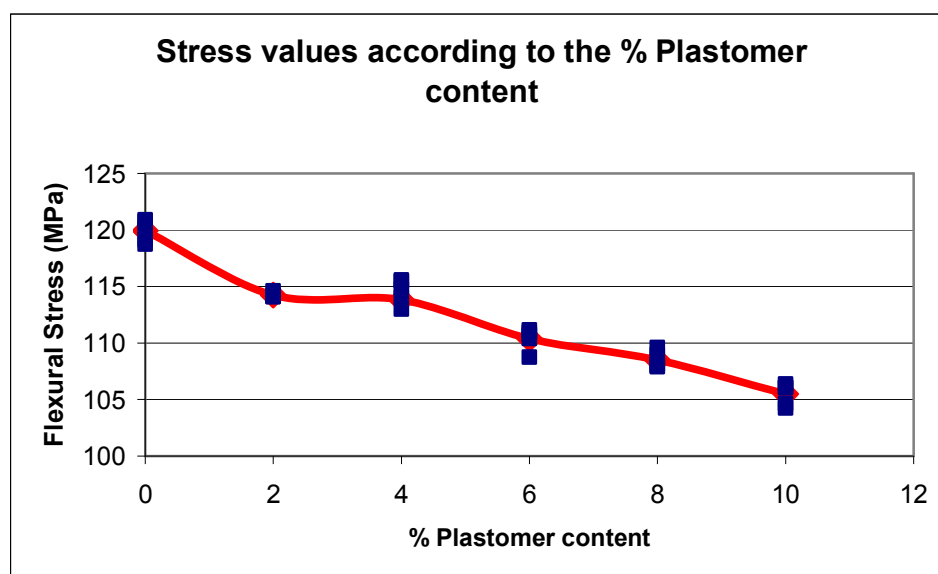


**Figure 8.37:** Flexural stress of 2% Mah-g-PP + 30% GFR-PP according to plastomer content

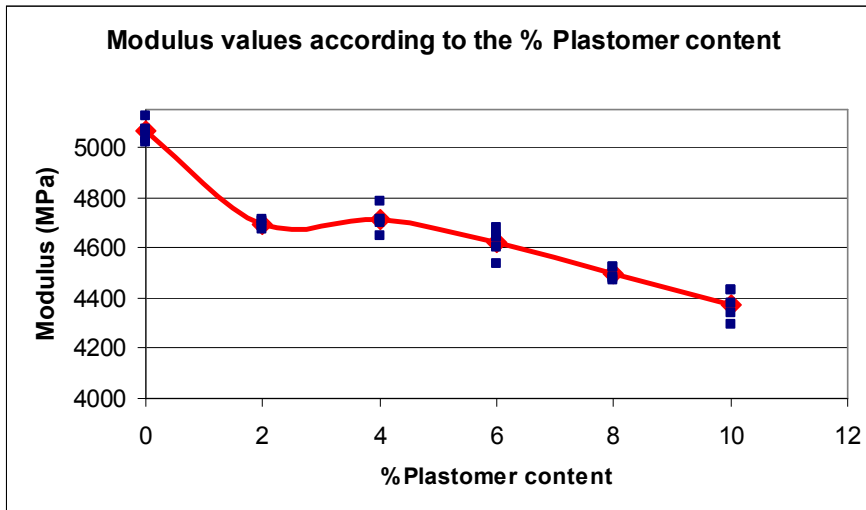


**Figure 8.38:** Modulus values of 2% Mah-g-PP + 30% GFR-PP according to plastomer content

### 8.3.7 Impact properties

Izod notched impact test applied according to the procedure explained in section 7.11 and test results are given in Table 8.27. Impact energy was absorbed during fracture when a propagating crack meets a plastomer domain and fracture energy was dispersed by deformation of the plastomeric material. Due to this situation, Impact properties of compound were increased by adding plastomer. Izod impact values increased linearly with increasing plastomer content as shown in Figure 8.39.

**Table 8.28:** Notched Izod impact propeties of 2% Mah-g-PP + 30% GFR-PP according to plastomer content

% Plastomer	0	2	4	6	8	10
	Izod Impact					
	kJ/m <sup>2</sup>	kJ/m <sup>2</sup>	kJ/m <sup>2</sup>	kJ/m <sup>2</sup>	kJ/m <sup>2</sup>	kJ/m <sup>2</sup>
	10,93	12,10	12,14	12,41	12,93	12,55
	9,84	11,30	11,51	12,02	11,96	12,59
	11,65	11,76	11,64	12,09	12,17	12,47
	9,95	11,36	12,07	12,41	11,63	12,91
	10,21	11,33	12,31	12,29	11,96	12,44
	10,89	12,23	12,04	12,07	12,88	12,39
	10,93	12,14	12,61	11,98	12,39	12,90
	9,84	12,12	11,22	12,17	12,14	13,07
	11,65	12,56	11,88	11,49	12,75	12,55
	9,95	11,33	12,44	11,68	12,21	12,29
Avr.	10,58	11,82	11,98	12,06	12,30	12,61
Max.	11,65	12,56	12,61	12,41	12,93	13,07
Min.	9,84	11,30	11,22	11,49	11,63	12,29
SD	0,72	0,47	0,43	0,29	0,43	0,26



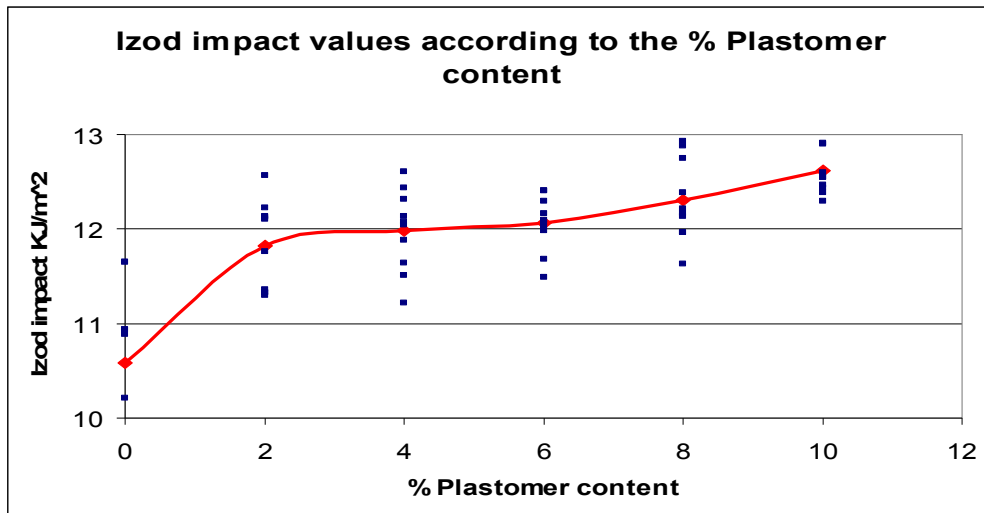


**Figure 8.39:** Notched Izod impact properties of 2% Mah-g-PP + 30% GFR-PP according to plastomer content

### 8.3.8 Heat distortion temperature - Vicat softening temperature

The Vicat and HDT test results of 2% Mah-g-PP compatibilized 30% glass fiber reinforced PP according to the plastomer concentrations are given in Table 8.28 - 8.31. HDT A temperature was increased up to 4% with the addition of plastomer. HDT B and Vicat A-B temperature were slightly decreased.

**Table 8.29:** HDT A values of 2% Mah-g-PP + 30% GFR-PP according to plastomer content

% Plastomer	HDT A (C°) (1,8MPa)					
	0	2	4	6	8	10
	143,90	158,50	160,20	158,10	156,30	158,20
	142,10	155,10	160,00	153,60	156,00	154,00
Avr.	143,00	156,80	160,10	155,85	156,15	156,10
Max.	143,90	158,50	160,20	158,10	156,30	158,20
Min.	142,10	155,10	160,00	153,60	156,00	154,00
SD	1,27	2,40	0,14	3,18	0,21	2,97

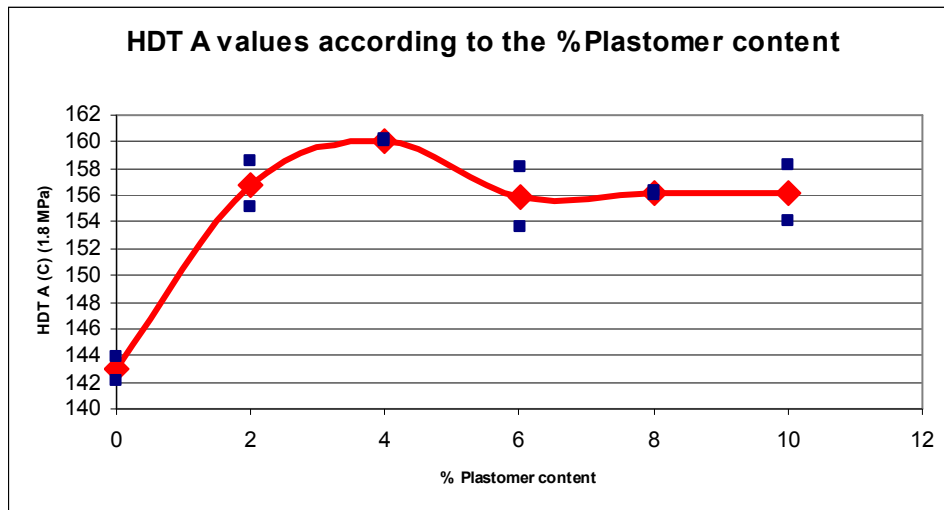


**Figure 8.40:** HDT A values of 2% Mah-g-PP + 30% GFR-PP according to plastomer content

**Table 8.30:** HDT B values of 2% Mah-g-PP + 30% GFR-PP according to plastomer content

% Plastomer	HDT B (C°) (0,45MPa)					
	0	2	4	6	8	10
	159,90	143,70	140,20	137,10	139,40	138,10
	157,00	136,10	138,60	134,90	129,80	129,50
Avr.	158,45	139,90	139,40	136,00	134,60	133,80
Max.	159,90	143,70	140,20	137,10	139,40	138,10
Min.	157,00	136,10	138,60	134,90	129,80	129,50
SD	2,05	5,37	1,13	1,56	6,79	6,08

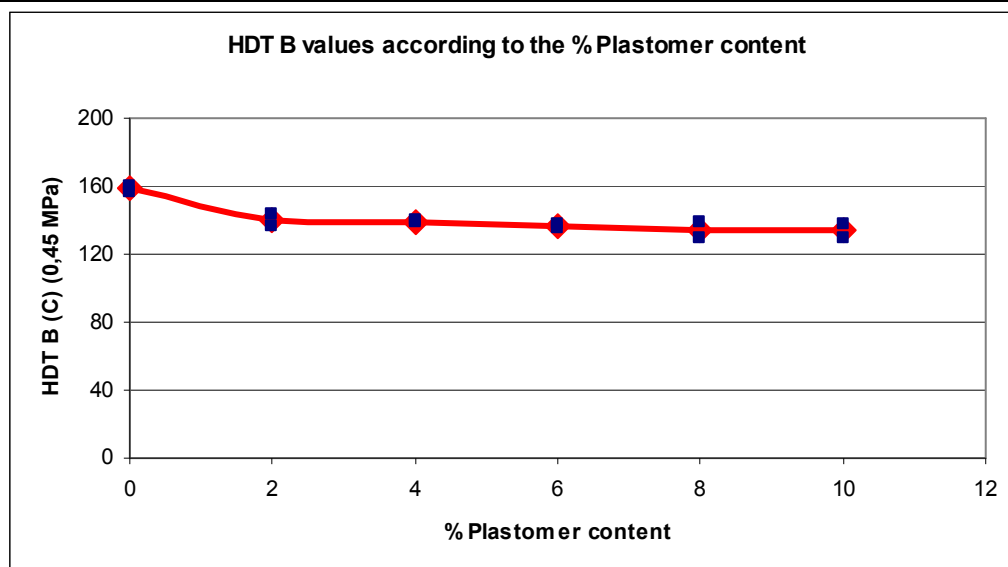


**Figure 8.41:** HDT B values of 2% Mah-g-PP + 30% GFR-PP according to plastomer content

**Table 8.31:** Vicat A values of 2% Mah-g-PP + 30% GFR-PP according to plastomer content

	Vicat A (C°) (10N)					
% Plastomer	0	2	4	6	8	10
	164,50	165,10	160,80	164,90	159,80	163,80
	164,20	164,20	167,30	165,20	165,90	163,80
Avr.	164,35	164,65	164,05	165,05	162,85	163,80
Max.	164,50	165,10	167,30	165,20	165,90	163,80
Min.	164,20	164,20	160,80	164,90	159,80	163,80
SD	0,21	0,64	4,60	0,21	4,31	0,00

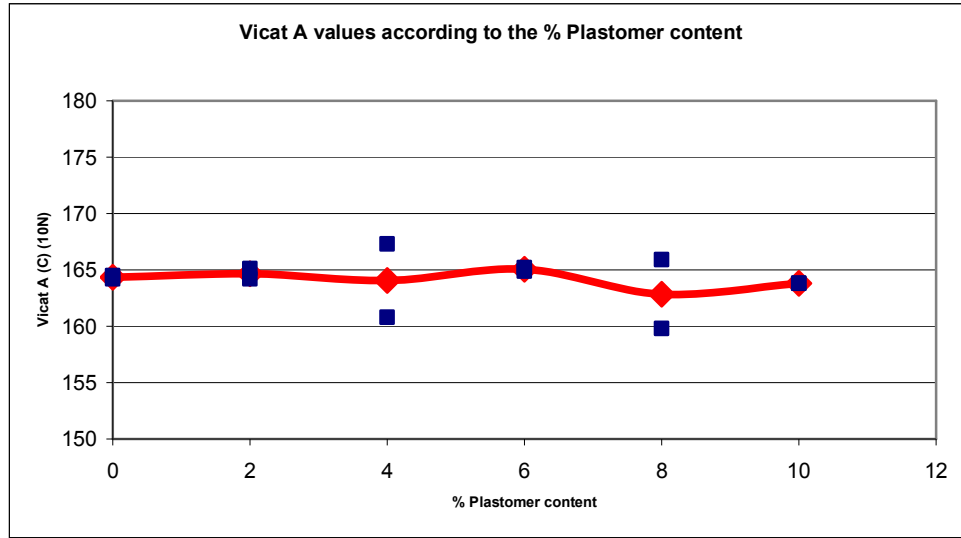


**Figure 8.42:** Vicat A values of 2% Mah-g-PP + 30% GFR-PP according to plastomer content

**Table 8.32:** Vicat B values of 2% Mah-g-PP + 30% GFR-PP according to plastomer content

	Vicat B (C°) (50N)					
% Plastomer	0	2	4	6	8	10
	135,30	135,50	123,80	129,90	126,70	113,10
	142,60	136,80	131,80	120,70	118,20	123,10
Avr.	138,95	136,15	127,80	125,30	122,45	118,10
Max.	142,60	136,80	131,80	129,90	126,70	123,10
Min.	135,30	135,50	123,80	120,70	118,20	113,10
SD	5,16	0,92	5,66	6,51	6,01	7,07

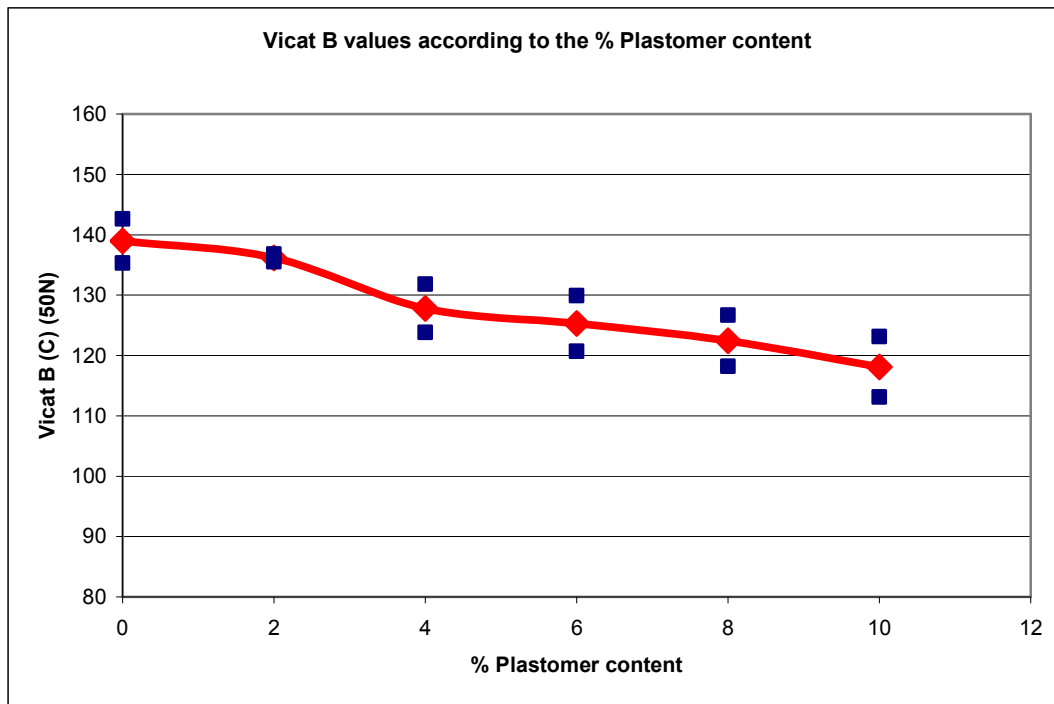


**Figure 8.43:** Vicat B values of 2% Mah-g-PP + 30% GFR-PP according to plastomer content

## 9. CONCLUSION

In this study, the effects of glass fiber on polypropylene and the effects of plastomer addition compound on physical and mechanical properties by modifying the interface interaction were investigated.

Firstly, glass fiber reinforced polypropylene composite's physical and mechanical properties were investigated and compared with neat polypropylene. It was observed that glass fiber reinforced material physical and mechanical properties were increased in accordance with neat polypropylene.

Secondly, the selected glass fiber ratio was kept constant as 30 % wt/wt to investigate effects of interface improvements on physical and mechanical properties by adding in different ratio (1-6) of maleic anhydride grafted polypropylene into the matrix. Tensile strength, impact strength, flexural strength, HDT – vicat values and elastic modulus values were significantly increased in accordance with uncompatibilized glass fiber reinforced polypropylene.

Thirdly, 2% Mah-g-PP compatibilized 30% glass fiber reinforced polypropylene that has the best strength of compatibilized formulas have been selected for improve impact properties by adding in different ratio (2-10) of plastomer. It is observed that izod impact values increased linearly with increasing plastomer content but it drastically reduced the tensile and flexural strength caused by adding of plastomer.



## REFERENCES

- Ahagon A. and Gent N.**, 1975. Effect of interfacial bonding on the strength of adhesion, *Journal of Polymer Science, Polymer Physics*, **13**, 7, 1285, quoted in ref 43.
- ASM Handbook**, 2001, *Composites*, Volume 21, p.49
- ASTM C 177-D 1600**, 1990. *Plastics (I)*, Volume 08.01, p.332
- Bhowmick, K. Anil**, 2008, Concepts of e-plastomers, *Current topics in elastomer research*, p.165, Taylor & Francis Group, LLC
- Brooks/Cole**, 2003, a division of Thomson Learning, Inc. Thomson Learning™ is a trademark used herein under license.
- Chanda M., Roy S.K.**, 2009. *Plastics Fundamentals, Properties, and Testing*, P. 1-1, CRC Press LLC
- Dani K.Amit (1.a)**, 2000, Metallocene plastomers, *Impact modification of automotive polypropylene with metallocene plastomer*, p.6, University of Massachusetts Lowell
- Dani K.Amit (1.b)**, 2000, Metallocene catalyst, *Impact modification of automotive polypropylene with metallocene plastomer*, p.7, University of Massachusetts Lowell
- Dani K.Amit (1.c)**, 2000, Toughening Mechanism of PP, *Impact modification of automotive polypropylene with metallocene plastomer*, p.3, University of Massachusetts Lowell
- Ersoy.O.G**, 2003, *Effect of inorganic filler phase on final performance of binary immiscible polypropylene/polyamide-6 blend*, PhD Thesis, Bogaziçi University
- Fu S.-Y., B. Laukeb, E. Mader, C.-Y. Yue, X. Hu**, 2000. Tensile properties of Short-glass-fiber and short-carbon-fiber-reinforced polypropylene composites, *Composites, Part A* 31 (2000) 1117–1125, Elsevier
- H.Krenchel**, 1964, *Fibre Reinforcement*, Copenhagen: Akademisk Forlag, .
- Harris B.**, 1986, Crack extension in composites, *Engineering composite materials* p. 61
- ISO 1133**, 2005. Determination of the melt flow rate of thermoplastics, *International Standard Organization*.
- ISO 1133**, 2005. Determination of the melt flow rate of thermoplastics, *International Standard Organization*.
- ISO 1183**, 1999. Methods for determining density of non-cellular plastics, *International Standard Organization*.
- ISO 178**, 2001. Plastics, Determination of flexural properties of rigid plastics, *International Standard Organization*.
- ISO 180**, 2000. Plastics, Determination of Izod impact strength of rigid materials, *International Standard Organization*
- ISO 3451 Method A**, 1981. Plastics, Determination of Ash Content, *International Standard Organization*.
- ISO R 527**, 1993. Determination of tensile properties, *ISO*.

- Kotans F.**, 2008. Mechanical adhesion, Effects of calcium carbonate ( $\text{CaCO}_3$ ) and maleic anhydride addition on fatigue properties of polypropylene, *MSc Thesis*, ITU Polymer Science and Technology, p.14
- Kulhestra A.K., C.Vasile**, 2002. Handbook of Polymer Blends and Composites, Rapra, Shawbury
- L. Tong, A.P. Mouritz and M.K. Bannister**, 2002 Preface, *3D Fibre Reinforced Polymer Composites*, p.10, Elsevier Science Ltd.
- Malguarnera, S.C. and Manisali, A.**, 1981. The Effects of Processing Parameters on the Tensile Properties of Weld Lines in Injection Molded Thermoplastics, *Polymer Engineering and Science*, 21, 10, pp. 586-593
- Mazumdar S.K. (1.a)**, 2002. What are the composites, *Composites Manufacturing Materials, Product, and Process Engineering*, p. 4, CRC Press LLC
- Mazumdar S.K.(1.b)**, 2002. Functions of fiber and matrix, *Composites Manufacturing Materials, Product, and Process Engineering*, p. 6, CRC Press LLC
- Murpy j.** 2001, Fibres: The Basic Properties, *Additives for Plastics Handbook (Second Edition)* P.40, Elsevier Science & Technology Books
- Oral M. A. (1.a)**, 2007. The interface in polymeric composites, *Effects of polymer filler interface improvements on mechanical and physical properties of  $\text{CaCO}_3$  filled polypropylene*, p.15, *MSc Thesis*, ITU Polymer Science and Technology
- Oral M. A.(1.b)**, 2007. Injection molding machine and process parameters, *Effects of polymer filler interface improvements on mechanical and physical properties of  $\text{CaCO}_3$  filled polypropylene*, p.33, *MSc Thesis*, ITU Polymer Science and Technology
- Robert H. Todd**, 1994, *Manufacturing processes reference guide*, p.240
- William D.C. (1.a)**, 1985. The matrix phase, *Materials Science and Engineering an Introduction* p.395, John wiley & sons
- William D.C. (1.b)**, 1985. Influence of fiber length, *Materials Science and Engineering an Introduction* p.397, John wiley & sons
- William D.C. (1.c)** 2003, Principles of fracture mechanics, *Materials Science and Engineering an Introduction* p.200, John wiley & sons



## **CURRICULUM VITA**

**Candidate's full name:** Deniz ERDİNÇ

**Place and date of birth:** UŞAK, 18.09.1984

**Permanent Address:** Merdivenköy mah. çavuşkuşu sok. n:4 d:5 Kadıköy/Istanbul

**Universities and Colleges attended:** Dokuz Eylül University, Metallurgical and Material Engineer, 2008

**Publications:** Erdinç D., Vural L.: Şekil hafızalı alaşımların üretimi ve mikroyapı incelemesi, Dokuz Eylül University, Engineering department, 2008, İzmir, Turkey